

**NANYANG
TECHNOLOGICAL
UNIVERSITY**

SINGAPORE

**DEVELOPMENT OF DURABLE MEMBRANES FOR
CHALLENGING WASTEWATER TREATMENT VIA
MEMBRANE DISTILLATION**

ZHANG YUJUN
Interdisciplinary Graduate Programme
Nanyang Environment and Water Research Institute
Singapore Membrane Technology Centre

2022

**DEVELOPMENT OF DURABLE MEMBRANES FOR
CHALLENGING WASTEWATER TREATMENT VIA
MEMBRANE DISTILLATION**

ZHANG YUJUN

Interdisciplinary Graduate Programme
Nanyang Environment and Water Research Institute
Singapore Membrane Technology Centre

A thesis submitted to the Nanyang Technological University in partial fulfilment of the
requirement for the degree of
Doctor of Philosophy

2022

Supervisor Declaration Statement

I have reviewed the content and presentation style of this thesis and declare it is free of plagiarism and of sufficient grammatical clarity to be examined. To the best of my knowledge, the research and writing are those of the candidate except as acknowledged in the Author Attribution Statement. I confirm that the investigations were conducted in accord with the ethics policies and integrity standards of Nanyang Technological University and that the research data are presented honestly and without prejudice.

10/08/2022

.....
Date

NTU NTU NTU NTU NTU NTU NTU NTU
NTU NTU NTU NTU NTU NTU NTU NTU
NTU NTU NTU NTU NTU NTU NTU NTU
NTU NTU NTU NTU NTU NTU NTU NTU



.....
Prof. WANG RONG

Authorship Attribution Statement

This thesis contains materials from two papers published in the following peer-reviewed journals in which I am listed as the first author, and one manuscript to be submitted to a journal for possible publication.

Chapter 3 is in preparation to be published as Facile hydrophobic modification of hydrophilic membranes by fluoropolymer coating for direct contact membrane distillation.

Chapter 4 is published as Y. Zhang, J.Y. Chong, R. Xu, R. Wang, Effective separation of water-DMSO through solvent resistant membrane distillation (SR-MD), *Water Research*. 197 (2021) 117103.

<https://doi.org/https://doi.org/10.1016/j.watres.2021.117103>.

The contributions of the co-authors are as follows:

- Prof. Wang Rong and Prof. Xu Rong provided research funding and provided the initial project direction.
- I prepared the manuscript. The manuscript was revised by Dr. Chong Jeng Yi.
- I designed the experiment in this study and performed all the laboratory work at the Singapore Membrane Technology Centre. I also analyzed the experiment data.
- All sample characterisation, including sample preparation, was conducted by me in the Nanyang Environment and Water Research Institute.
- Ms. Janelle Ng Ru Ying and Ms. Lam Mei Shan assisted in the collection of the XPS data.

Chapter 5 is published as Y. Zhang, J.Y. Chong, R. Xu, R. Wang, Hydrophobic ceramic membranes fabricated via fatty acid chloride modification for solvent resistant membrane distillation (SR-MD), *Journal of Membrane Science* (2022): 120715. <https://doi.org/10.1016/j.memsci.2022.120715>

The contributions of the co-authors are as follows:

- Prof. Wang Rong and Prof. Xu Rong provided research funding.

- Dr. Chong Jeng Yi provided the initial project direction.
- I wrote the manuscript and revised together with Dr. Chong Jeng Yi.
- I designed experiment and performed all the membrane preparation steps, separation performance tests, characterized under several equipment and conducted data evaluation at the Singapore Membrane Technology Centre.
- All sample characterisation, including sample preparation, was conducted by me in the Nanyang Environment and Water Research Institute.
- Ms. Janelle Ng Ru Ying and Ms. Lam Mei Shan assisted in the collection of the XPS data.

15/07/2022

.....
Date

NTU NTU NTU NTU NTU NTU NTU NTU NTU
NTU NTU NTU NTU NTU NTU NTU NTU NTU
NTU NTU NTU NTU NTU NTU NTU NTU NTU
NTU NTU NTU NTU NTU NTU NTU NTU NTU
ZHANG YUJUN

This page is intentionally left blank

ACKNOWLEDGEMENTS

My deepest gratitude goes first and foremost to Prof. Wang Rong and Prof. Xu Rong, my supervisors, for their constant encouragement and guidance throughout my research journey. They were always willing to share their expertise and gave a helping hand to me. I am also grateful to my mentor, Assoc. Prof. Chong Tzyy Haur, for sharing his own research experiences with me.

I am indebted to Dr. Chew Guan Pin, who led me into the field of membrane technology and helped me get started quickly. I would also like to express my heartfelt gratitude to Dr. Chong Jeng Yi and Dr. Zhao Yali for their valuable insights and contributions, which greatly enhanced the quality of my work.

I am truly grateful for the help from the other members in Singapore Membrane Technology Centre (SMTTC). Special thanks to Dr. Yang Yang, Mr. You Xiaofei, Dr. Xu Yilin, Dr. Lai Gwo Sung, Dr. Goh Kunli, Dr. Ho Jia Shin who have taught me valuable research skills or shared their experiences with me. Appreciation was also given to Mr. Lim Yu Jie, Mr. Nguyen Anh Pham, Mr. Chen Ning Yuan, Mr. Lim HuaiXun, Dr. Ng Yee Fan, Dr. Li Xin, Dr. Jiang Xu, Ms. Liu Hong, Mr. Li Can and other members of our lab for their generous help and support.

This page is intentionally left blank

I want to express my sincere appreciation to the administrative staff at the Nanyang Environment & Water Research Institute (NEWRI), especially Ms. Chan Wai Yee, Ms. Hera Catharina Adam, Ms. Zan Ong Chin Chin, and Mr. Kwan Zheng Xin Joseph. Their kind assistance in laboratory safety training and chemical purchase greatly facilitated the progress of my experiments. I would also like to thank Ms. Janelle Ng Ru Ying, Ms. Lam Mei Shan, Ms. Koh Danyu, and other members of the analytics cluster staff for their support in equipment training and characterisations.

My acknowledgement also goes to the Interdisciplinary Graduate Programme (IGP) for providing me with a research scholarship, and to SMTC for providing a safe workplace equipped with necessary facilities.

Last but not least, I am eternally grateful to my family, who are the most valuable people in my life. Their emotional support and encouragement have been invaluable during these past four years. They have provided me with love and warmth during times of setbacks, confusion, and disappointment.

Yujun

This page is intentionally left blank

LIST OF PUBLICATIONS

➤ *Journals:*

1. Chew, N. G. P., **Zhang, Y.**, Goh, K., Ho, J. S., Xu, R., & Wang, R. (2019). Hierarchically structured Janus membrane surfaces for enhanced membrane distillation performance. *ACS Applied Materials & Interfaces*, 11(28), 25524-25534.
2. **Zhang, Y.**, Chong, J. Y., Xu, R., & Wang, R. (2021). Effective separation of water-DMSO through solvent resistant membrane distillation (SR-MD). *Water Research*, 197, 117103.
3. **Zhang, Y.**, Chong, J. Y., Xu, R., & Wang, R. (2022). Hydrophobic ceramic membranes fabricated via fatty acid chloride modification for solvent resistant membrane distillation (SR-MD). *Journal of Membrane Science*, 120715.
4. **Zhang, Y.**, Chong, J. Y., Zhao, Y., Xu, R., Asakawa A., & Wang, R. (2022). Facile hydrophobic modification of hydrophilic membranes by fluoropolymer coating for direct contact membrane distillation. *Journal of Membrane Science*, 121432.

➤ *Conferences:*

1. **Zhang, Y.**, Chong, J. Y., Zhao Y., Xu, R., Asakawa, A. & Wang, R.. Facile hydrophobic modification of hydrophilic membranes by fluoropolymer coating for direct contact membrane distillation. Conference of the Aseanian Membrane Society, July 4-6 2022. Oral Presentation.
2. **Zhang, Y.**, Chong, J. Y., Xu, R., & Wang, R.. Effective separation of water-DMSO through solvent resistant membrane distillation (SR-MD). **International**

Congress on Membranes and Membrane Processes, Dec 7-11, 2020. Oral Presentation.

3. Chew, N. G. P.*, **Zhang, Y.***, Goh, K., Ho, J. S., Xu, R., & Wang, R.. Hierarchically structured Janus membrane surfaces for enhanced membrane distillation performance. **International Conference on Membrane Science and Technology**, June 13-14, 2019, Singapore. Oral Presentation.

TABLE OF CONTENTS

ACKNOWLEDGEMENTS	i
LIST OF PUBLICATIONS	v
TABLE OF CONTENTS	vii
LIST OF TABLES	ix
LIST OF FIGURES	xi
LIST OF ABBREVIATIONS	xiii
LIST OF SYMBOLS	xv
SUMMARY	xvii
Chapter 1 Introduction	1
1.1 Research background	1
1.2 Problem statement	6
1.3 Research objectives	7
1.4. Thesis outline	8
Chapter 2 Literature Review	11
2.1 MD fundamentals	11
2.1.1 MD mechanisms and configurations	11
2.1.2 MD compared with other separation methods	14
2.1.3 Essentials of MD membranes	16
2.1.3.1 Micro-structure and morphology	17
2.1.3.2 Hydrophobicity	20
2.1.3.3 Membrane thermal conductivity	21
2.1.4 MD membrane materials	21
2.1.4.1 Conventional hydrophobic polymers	21
2.1.4.2 Novel hydrophobic copolymers	23
2.1.4.3 Hydrophilic polymers	24
2.1.4.4 Ceramic membranes	24
2.2. Studied MD applications and their challenges	25
2.2.1 MD in treating high-salinity water	25
2.2.2 Separation of water-solvent mixture	27
2.2.3 Other studied MD applications	29
2.3. Hydrophobicity enhancement methods for hydrophilic membranes	30
2.3.1. Adding hydrophobic additives during fabrication	30
2.3.2. Polymerization	31
2.3.3. Surface grafting with hydrophobic compounds	32
2.3.4. Surface coating/deposition	34
2.4. Summary	34
Chapter 3 Facile Hydrophobic Modification of Hydrophilic Membranes by Fluoropolymer Coating for Direct Contact Membrane Distillation	37
3.1 Introduction	37
3.2 Experimental	38

3.2.1 Materials.....	38
3.2.2 Membrane modification	38
3.2.3 Membrane characterisations.....	40
3.2.4 DCMD performance tests in saline solution	41
3.3 Results and discussion.....	42
3.3.1 Hydrophobic modification of LF-200	42
3.3.2 Membrane Performance in DCMD Tests.....	50
3.4 Conclusions	55
Chapter 4 Effective Separation of Water-DMSO through Solvent Resistant Membrane Distillation	57
4.1 Introduction	57
4.2 Experimental	59
4.2.1 Materials.....	59
4.2.2 Hydrophobic grafting of ceramic membranes.....	60
4.2.3 Membrane characterisations.....	61
4.2.4 VMD performance tests in water/DMSO solution.....	61
4.2.5 Separation mechanism of water/DMSO solution.....	63
4.3 Results and discussion.....	65
4.3.1 Surface hydrophobic modification of ceramic membranes.....	65
4.3.2 VMD performance in water-DMSO system	69
4.3.3 Separation performance of other types of membranes.....	76
4.4 Conclusions	78
Chapter 5 Hydrophobic Ceramic Membranes Fabricated via Fatty Acid Chloride Modification for Solvent Resistant Membrane Distillation.....	81
5.1 Introduction	81
5.2 Experimental	83
5.2.1 Materials.....	83
5.2.2 Hydrophobic grafting of ceramic membranes.....	83
5.2.3 Membrane characterisations.....	85
5.2.4 VMD test and separation performance tests in water/DMSO solution	85
5.3. Results and discussion.....	86
5.3.1 Hydrophobic modification of ceramic membranes by grafting of FAC	86
5.3.2 Characterisations of hydrophobic ceramic membranes.....	91
5.3.3 SR-MD performance for water-DMSO separation	93
5.4 Conclusions	98
Chapter 6 Conclusions and Recommendations	99
6.1 Overall conclusions	99
6.2 Recommendations for future research.....	102
References	105

LIST OF TABLES

Table 2.1 MD compared with other membrane processes.....	15
Table 2.2 MD compared with traditional thermal distillation.	16
Table 2.3 Properties of conventional materials widely used in MD (Alkudhiri et al. 2012a).....	22
Table 3.1 Summary of properties of the NC and nylon membranes before and after LF-200 modification.....	48
Table 3.2 Hydrophobic coating method of hydrophilic polymeric membranes in recent literatures.	50
Table 3.3 The DCMD performance of modified membranes in this work compared with other membranes in recent literatures.	54
Table 4.1 Contact angles and liquid entry pressures of grafted membranes.....	69
Table 5.1 Ceramic membranes grafted with different modifier and their water contact angles.....	90
Table 5.2 Properties of pristine and modified membranes.	92

This page is intentionally left blank

LIST OF FIGURES

Figure 1.1 Membrane processes classified by driving force and application size range. Adapted from (Shon et al. 2013).	2
Figure 1.2 The applications of membrane technologies (Baker 2004).	3
Figure 2.1 Schematic diagram of MD mechanism.	11
Figure 2.2 Sketch of four MD configurations (Kebria and Rahimpour 2020).	12
Figure 2.3 Schematic diagram illustrating SMMs migration (Solid circles represent SMM molecule which has lower surface free energy; hollow circles represent base polymer) (Suk et al. 2002).	31
Figure 3.1 Synthesis process and polymer structure of LF-200.	39
Figure 3.2 Schematic of LF-200 crosslinking mechanism and dip coating procedure.	40
Figure 3.3 WCAs of NC membranes modified by different concentrations of LF-200.	43
Figure 3.4 (a1, b1, c1) FESEM images of the surface morphologies and (a2, b2, c2) the EDX spectra of fluorine of cross-sections of the pristine NC, 9LF-NC and 12LF-NC membranes, respectively.	44
Figure 3.5 (a) XPS wide spectra of pristine NC and modified NC membranes. N1s spectra of (b) pristine NC membrane and (c) modified NC membrane.	45
Figure 3.6 (a1, b1) FESEM images of the surface morphologies and (a2, b2) the EDX spectra of fluorine of cross-sections of the pristine nylon and 12LF-nylon membranes, respectively. The matrix near the embedded supporting fibres were very difficult to detect so it looks blank in graph (b2).	46
Figure 3.7 AFM 3D profile images of the (a1) pristine NC, (a2) 9LF-NC, (a3) 12LF-NC, (b1) pristine nylon and (b2) 12LF-nylon membranes, respectively.	47
Figure 3.8 DCMD performances of the 9LF-NC, 12LF-NC, 12LF-nylon and commercial PVDF membranes in 3.5 wt% NaCl solution Filled symbols represent permeate flux and hollow symbols represent conductivity. ($T_f=60\text{ }^\circ\text{C}$, $T_p=20\text{ }^\circ\text{C}$, $Q_f=220\text{ ml min}^{-1}$, $Q_p=120\text{ ml min}^{-1}$).	51
Figure 3.9 Long-term DCMD performances of 9LF-NC, 12LF-NC and commercial PVDF membranes with 10 wt% NaCl feed solution. Filled symbols represent permeate flux and hollow symbols represent conductivity. ($T_f=60\text{ }^\circ\text{C}$, $T_p=20\text{ }^\circ\text{C}$, $Q_f=220\text{ ml min}^{-1}$, $Q_p=120\text{ ml min}^{-1}$).	52
Figure 3.10 WCAs of 12LF-NC and PVDF membranes measured before and after test, respectively.	53
Figure 4.1 Schematic of three membrane substrates.	60
Figure 4.2 Schematic of grafting reaction.	61
Figure 4.3 Schematic of SR-MD experimental setup.	62
Figure 4.4 Schematic of transport mechanisms.	63
Figure 4.5 (a) PSD of the 200-ASY and 200-SYM membranes obtained using the gas-liquid porometry. (b) MWCO of the 20-ASY membranes. (c) FESEM images of the cross-section and inner surface morphologies of three ceramic substrates.	66

Figure 4.6 FESEM images of the inner surface morphologies of the (a) 200-mSYM, (b) 200-mASY, and (c) 20-mASY membranes.....	66
Figure 4.7 (a) XPS spectra of the 20-ASY membranes, 20-mASY and 20-mSYM-30d membranes. (b) O signal of 20-mASY membranes, (c) O signal of 20-mASY-30d membranes.....	67
Figure 4.8 (a) WCA and (b) SCA of the 20-mASY, 200-mASY and 200-mSYM membranes submerging in DMSO for 0, 14 and 30 days.....	68
Figure 4.9 VMD performances of the 200-mSYM membranes ($T_f=60\text{ }^\circ\text{C}$, $P_p=5\text{ kPa}$, $Q_f=170\text{ ml min}^{-1}$): (a) Flux and DMSO rejection vs. different feed DMSO concentrations. (b) Permeate DMSO concentration and separation factors vs. different feed DMSO concentrations.....	70
Figure 4.10 Vapour pressure difference across membrane vs. different feed DMSO concentrations.....	70
Figure 4.11 Effect of feed solution temperature on the VMD permeate flux of the 200-mASY, 200-mSYM and 20-mASY membranes ($C_f=50\text{ wt}\%$, $P=5\text{ kPa}$, $Q_f=170\text{ ml min}^{-1}$).	72
Figure 4.12 Surface porosity of the inner surface of 200-ASY, 200-SYM and 20-ASY membranes (pore area is indicated in red colour).....	74
Figure 4.13 (a) Permeate flux and (b) DMSO rejection of the 200-mSYM membranes in 20-75 wt% DMSO/water feed stream ($T_f=60\text{ }^\circ\text{C}$, $P=5\text{ kPa}$, $Q_f=170\text{ ml min}^{-1}$).	75
Figure 4.14 (a) Comparison of the separation performance of 20-mASY, 200-mSYM and other membranes. (b) Surface morphology of PTFE membrane.....	77
Figure 5.1 Mechanism of FAC modification on the surface of ceramic membranes. .	84
Figure 5.2 WCA and SCA of the hydrophobic ceramic membranes prepared under different conditions.....	87
Figure 5.3 (a) Contact angles of SC, PC, SA and OTMS modified membranes; (b) Bonds formed between different modifiers and ceramic membranes.....	88
Figure 5.4 (a) XPS spectra of pristine, SC and SA-modified membranes, (b) O signal of SC modified membrane and (c) O signal of SA membrane.....	89
Figure 5.5 FESEM images of the inner surface morphologies of the (a) pristine, (b) PC-modified and (c) SC-modified membranes.....	91
Figure 5.6 (a) Contact angles of 1.5 mM SDS (61 mN m^{-1}), 4 mM SDS (50 mN m^{-1}), 20 wt% ethanol (43.7 mN m^{-1}) and DMF (37.1 mN m^{-1}) on the surface of the PC-modified membrane. (b) Modified Zisman plot: cosine of contact angles of different liquids (1.5 mM SDS, 4 mM SDS, 20 wt% ethanol, DMF and water) versus the inverse of surface tension of the corresponding liquid. (c) WCA and SCA of the PC-modified membrane after immersing in pure DMSO for 7 and 30 days.....	93
Figure 5.7 SR-MD performance of the PC-modified and SC-modified membranes in the 20 and 50 wt% DMSO feed solution at $60\text{ }^\circ\text{C}$ ($T_f=60\text{ }^\circ\text{C}$, $P_p=5\text{ kPa}$, $Q_f=170\text{ ml min}^{-1}$).....	94
Figure 5.8 Effect of feed solution temperature on the SR-MD permeate flux and DMSO rejection of the PC-modified and SC-modified membranes. ($C_f=50\text{ wt}\%$, $P=5\text{ kPa}$, $Q_f=170\text{ ml min}^{-1}$).	96

Figure 5.9 (a) Permeate flux and (b) DMSO rejection of the pristine, PC-modified and SC-modified membranes in 50 wt% DMSO/water feed stream ($T_f=60\text{ }^\circ\text{C}$, $P=5\text{ kPa}$, $Q_f=170\text{ ml min}^{-1}$). 97

LIST OF ABBREVIATIONS

Abbreviation	Description
AFM	Atomic force microscope
AGMD	Air gap membrane distillation
DCMD	Direct contact membrane distillation
DMF	N,N-dimethylformamide
DMSO	Dimethyl sulfoxide
ECTFE	Poly (ethylene chlorotrifluoroethylene)
EDX	Energy-dispersive X-ray
FAC	Fatty acid chloride
FAS	Fluoroalkylsilane
FAS-F17	1H,1H,2H,2H-perfluorodecyltriethoxysilane
FESEM	Field emission scanning electron microscope
IPA	Isopropyl alcohol
LEP	Liquid entry pressure
LEP _w	Liquid entry pressure of water
LEP _s	Liquid entry pressure of solvent
MD	Membrane distillation
MWCO	Molecular weight cut-off
NC	Nitrocellulose
NMP	N-methyl-2-pyrrolidone
NPs	Nanoparticles
OTMS	Octadecyltrimethoxysilane
PA	Polyamide
PAI	Poly(amide–imide)
PAN	Polyacrylonitrile
PC	Palmitoyl chloride
PEI	Poly(etherimide)
PES	Polyethersulfone
PP	Polypropylene

PSD	Pore size distribution
PSf	Polysulfone
PTFE	Polytetrafluoroethylene
PV	Pervaporation
PVA	Polyvinyl alcohol
PVC	Polyvinyl chloride
PVDF	Polyvinylidene fluoride
PVDF-HFP	Polyvinylidene fluoride-co-hexafluoropropylene
RO	Reverse osmosis
SC	Stearic acid
SCA	Solvent contact angle
SDS	Sodium dodecyl sulfate
SGMD	Sweeping gas membrane distillation
SMMs	Surface modifying macromolecules
SR-MD	Solvent-resistant membrane distillation
TIPS	Thermal-induced phase separation
VLE	Vapour-liquid equilibrium
VMD	Vacuum membrane distillation
VIPS	Vapour-induced phase separation
WCA	Water contact angle
XPS	X-ray photoelectron spectrometer

LIST OF SYMBOLS

Nomenclature	Description
$\rho_{membrane}$	Membrane density
$\rho_{polymer}$	Material density
ε	Porosity
R_a	Roughness
ε_s	Surface porosity
ε_b	Bulk porosity
τ	Tortuosity
θ_W	Apparent contact angle
θ_Y	Intrinsic contact angle
r	Roughness ratio
A_m	Projection area of membrane surface in the main direction
A_n	Measured surface area by experiment technique
B	Geometric coefficient
Γ	Liquid surface tension
Θ	Contact angle
r_{max}	Biggest membrane pore size

This page is intentionally left blank

SUMMARY

Wastewater treatment and reclamation are critical in addressing global water scarcity issues. However, the large volume of wastewater containing high concentration of salinity or organic solvents poses significant challenges to conventional sewage plants. The high salinity water feeds with elevated osmotic pressure poses a problem to the most popular desalination process, reverse osmosis. Meanwhile, the presence of toxic organic solvents makes biological treatment ineffective. In order to reduce the volume of these challenging waste streams, membrane distillation (MD) is a promising solution. As a thermal-driven process, MD utilizes the partial vapour pressure difference to separate non-volatile solutes and water. It has unique strength in treating highly concentrated solutions due to its insensibility to osmotic pressure and high rejection of all non-volatile matters, including salt and organic solvents with high boiling points. Moreover, it is operated under mild conditions allowing the use of waste heat or new energy.

A porous hydrophobic membrane is essential for MD process to allow water vapour to permeate through the membranes and to produce clean water. Currently, most commercial MD membranes are made of conventional hydrophobic polymers, such as polyvinylidene fluoride (PVDF), polytetrafluoroethylene (PTFE) and polypropylene (PP). Nevertheless, these membranes have limitations such as limited hydrophobicity (PVDF), difficulties in manufacturing (PP and PTFE), or relatively high cost (PVDF and PTFE). In order to expand the range of available MD membranes, substantial efforts have been made to obtain hydrophobic membranes from materials with limited hydrophobicity. It is usually achieved by conducting hydrophobic modification to the nascent membranes. The modified membranes have been reported with benefits such as reducing membrane cost and improving MD performance. However, these hydrophobic

modification methods are often complex and expensive, impeding the large-scale use in industry, and the modified-membranes have not been examined in a challenging environment containing high concentration of pollutants. Furthermore, MD's potential in dealing with challenging waste streams has not been fully investigated, especially for the separation of water-solvent mixtures, namely solvent resistance MD (SR-MD).

To tackle these challenges, this research first aims to develop a facile, scalable and cost-effective hydrophobic modification method to tune the wettability of hydrophilic substrates to hydrophobic for the MD process. Porous commercial membranes including nitrocellulose (NC) and nylon were modified with a cost-effective fluoroethylene vinyl ether resin via dip coating method. The modified-NC membranes showed good hydrophobicity and outstanding performance in desalination of 3.5-10 wt% NaCl for over 120 hours. The results revealed that using a modified-hydrophilic membrane in MD is practicable and even can outperform the commercial polyvinylidene fluoride membrane.

Besides, the potential of SR-MD in separating water and organic solvent with a high boiling point was comprehensively studied. In order to avoid membrane swelling in the harsh solvent environment, ceramic membrane substrates were used because of their excellent solvent resistance. Solvent-resistant porous ceramic membranes were modified by fluoroalkylsilane to acquire hydrophobicity and applied to separate 3.5-85 wt% dimethyl sulfoxide (DMSO) solution via vacuum MD. Influences of membrane pore size, membrane structure, feed temperature, and feed concentration were studied to fully understand the process. SR-MD has shown superior flux compared with the other membrane process and the modified ceramic membranes were proved to be more effective and stable in the highly concentrated DMSO solution than commercial PTFE

membranes. Moreover, rejection of the SR-MD process was distinctly 105% better than the theoretical rejection estimated from vapour-liquid equilibrium at a DMSO concentration of 85 wt%.

On the basis of this research, another membrane suitable for SR-MD was prepared by fatty acid chloride grafting for the first time. This new modification method used widely much cheaper and greener than the previous method and the modified membranes showed comparable SR-MD performance with the commonly silane-grafted membranes. The excellent separation performance in treating water-DMSO mixture again demonstrated the potential of SR-MD in dealing with this kind of wastewater.

In summary, this thesis highlights the potential of membrane distillation for treating challenging waste streams, particularly those with high salinity or organic solvents with high boiling points. Moreover, this research also develops effective and straightforward hydrophobic modification methods, which have great potential to scale up. This work can guide the development of future MD processes for industrial applications and lead to more effective solutions for wastewater treatment.

This page is intentionally left blank

Chapter 1 Introduction

1.1 Research background

With the fast-growing population and economy, the global water demand has been increasing dramatically and it is forecasted that more than half of the world population will be saddled with clean water scarcity by 2050 (Boretti and Rosa 2019, Water 2020). As water availability around the world has been significantly impacted by the decline in clean water resources and water quality, wastewater treatment and reclamation are crucial in solving the pressing water scarcity problem. Wastewater has been considered as a kind of ‘new’ resource that can increase the water supply for different purposes (Tortajada 2020). Besides that, there is a growing demand for more efficient water processing technologies, driven by the increasingly stricter environmental protection regulations. Zero liquid discharge, which means complete elimination of liquid waste, has also become an ambitious target for wastewater treatment (Tong and Elimelech 2016).

In the field of water treatment, membrane separation plays a critical role. It is a process that can selectively separate one component and reject the others in the gas or liquid streams. After more than 60 years of unremitting development, membrane-based processes with different driving forces have been invented to focus on the separation of different size of solutes (Javier et al. 2022). They can be categorized as Figure 1.1 depending on the driving force. For example, pressure-driven processes, including microfiltration, ultrafiltration, nanofiltration and reverse osmosis (RO), are able to reject substances of different sizes, from suspended particles ($>0.2 \mu\text{m}$) to monovalent ions ($<1 \text{ nm}$), with different applied pressure (Van der Bruggen et al. 2003). With such a high adaptivity to different substances, membrane technology can be adopted in extensive industrial uses

(Figure 1.2) and produce high-quality products. Compared to other traditional separation processes, membrane technology has its merits. To be specific, it is more energy-saving and land-saving than the conventional physical treatment (e.g., adsorption, distillation, and crystallization); more cost-effective than the chemical treatment (e.g., oxidation, photocatalysis, chemical precipitation); and demonstrates wider applicability than the biological treatment, such as bioreactors which are constrained by effluent toxicity. Generally, membrane separation processes have merits of low footprint, high energy efficiency, easy operation, high flexibility and high scalability (Le and Nunes 2016).

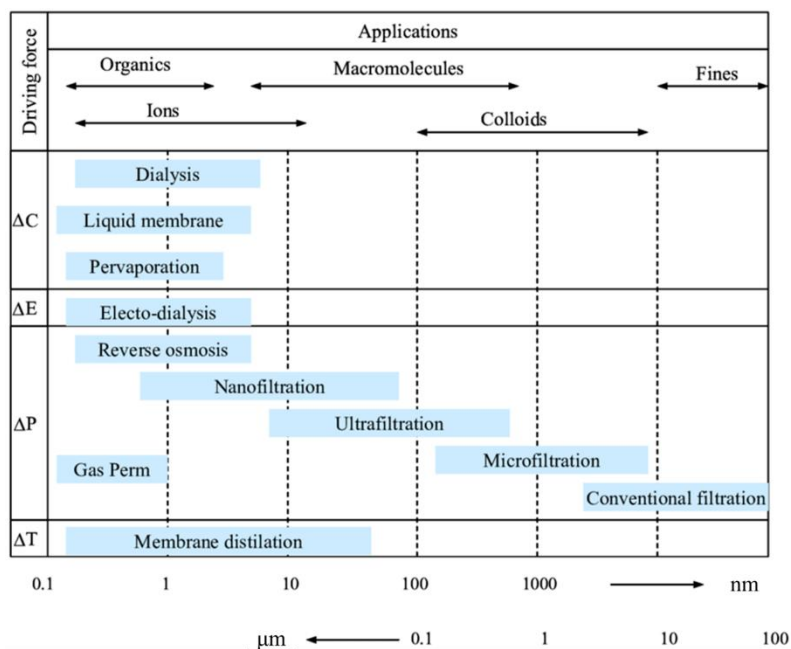


Figure 1.1 Membrane processes classified by driving force and application size range. Adapted from (Shon et al. 2013).

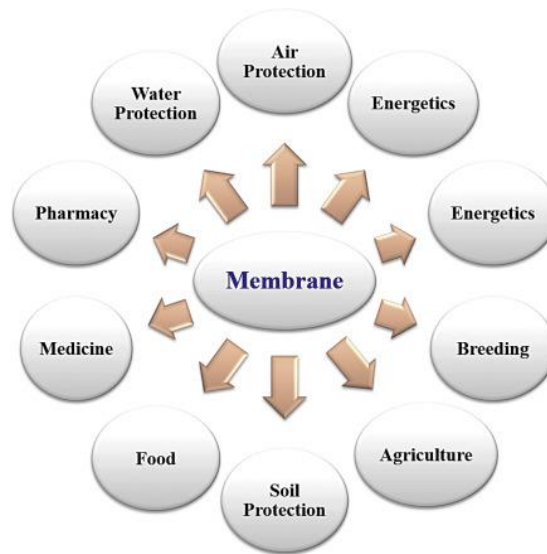


Figure 1.2 The applications of membrane technologies (Baker 2004).

Today, wastewater treatment is still accompanied by many difficulties. The first problem is the large volume of wastewater. It was reported that the worldwide wastewater production reached 360 billion m³ yearly, coming from domestic, commerce, and industry (Jones et al. 2021). Secondly, the wastewater from different sources has very different compositions, and especially the industrial waste streams may contain numerous pollutants. Thus, it is impossible to handle different waste streams with a similar set of solutions. Moreover, some waste streams can be a big challenge to wastewater management, such as those containing a high concentration of salts or organic solvents.

Highly salty water is a type of challenging waste stream that is difficult to handle. The main source is brine from desalination plants, which produce 141.5 million m³/day globally (Jones et al. 2019) and the rest comes from the oil, textile, mining, and leather industries (Shah et al. 2022). From the economic perspective, it is necessary to use membrane technology to concentrate the brine as much as possible. However, the most prevailing desalination technique, RO, typically has a salt concentration limit of 7 wt% with a high operating pressure in the range of 5500 to 7000 kPa (Lim et al. 2021). Above

this concentration, the high operating pressure required could damage the normal RO membranes and ultimately results in diminished performance.

In terms of organic solvents, they are heavily used for synthesis and cleaning in paint, chemical, petrochemical, paper, electronics, pharmaceutical industries, etc. (You et al. 2021). A typical example is dimethyl sulfoxide (DMSO), which is widely used as solvent for drug formulation or reaction solvent and cleaning agent for semiconductor manufacturing. According to an industry report, the global market for DMSO was estimated to have reached approximately US\$ 253 million in 2022 while pharmaceutical and electronics industries are the largest consumer segments of DMSO (Global Industry Analysts. 2023). The widespread use of DMSO can generate large volume of organic wastewater and pose a challenge to conventional water treatment plant. The chemical, biological processes degrade the valuable solvent while the thermal distillation processes require high temperature and large footprint. In addition, the commonly used pressure-driven membrane processes, they could not separate water-solvent mixtures effectively due to the similar size between water and solvents, as well as the high osmotic pressure when feed solution is concentrated (Fane et al. 2011).

Membrane distillation (MD) is an emerging thermal-driven membrane process that is promising in treating those challenging wastewater (Roy and Ragunath 2018). During the MD process, water or volatile substances from the hot feed side can transport in vapour phase through the membrane pores to the cold permeate side under the driven of vapour pressure gradient (Chew et al. 2019a). A hydrophobic porous membrane acts a barrier to the liquid feed streams (Khayet 2011). MD has theoretically 100% rejection to the nonvolatile pollutants and other advantages of low energy consumption, moderate operating conditions and potential to use small-scale waste heat from factories or new

energy resources like solar energy, geothermal energy (Camacho et al. 2013). For salts and organic solvents with high boiling points, which have significant difference in vapour pressure from water, MD is able to separate them from water based on partial vapour pressure difference, regardless of the solute size. In addition, MD is different from pressure-driven membrane processes (e.g., RO) that it is less affected by the salinity and is able to treat high-salinity water under moderate operating conditions. Compared to the commonly employed pervaporation (PV) method, which utilizes dense membranes to separate solvent mixtures (Li et al. 2020c), MD has potential to obtain higher flux due to the use of porous membranes in treating mixtures of water and organic solvents with high boiling points.

The successful operation of MD relies on the good membrane hydrophobicity to repel the percolation of liquid water. At present, most of the MD membranes are confined to hydrophobic polymers such as polyvinylidene fluoride (PVDF), polytetrafluoroethylene (PTFE) and polypropylene (PP) (Yao et al. 2020). However, the PVDF usually has limited intrinsic hydrophobicity, while the fabrication of PTFE and PP membranes with appropriate pore size distribution (PSD) is difficult. Moreover, the price of PTFE and PVDF are relatively expensive. Commercial membranes custom-made for MD are limited compared to other membrane processes. Therefore, it is beneficial to expand the range of materials suitable for MD application. Efforts have been made to enhance the hydrophobicity of materials with less hydrophobic or hydrophilic nature, such as some hydrophilic polymers and ceramics. People have investigated novel modification methods to engineer MD membranes with high performance from hydrophilic materials. The use of new materials not only provides more available MD membranes, but also contributes to simplifying membrane fabrication, reducing membrane cost and improving membrane performance.

1.2 Problem statement

Despite the potential in treating challenging wastewater, MD is still a growing technology that hasn't been commercialized and even the related pilot-scale applications are few (Francis et al. 2022b, Hussain et al. 2022). In order to promote MD in the treatment of wastewater containing high salinity or organic solvents and advance its potential for large-scale applications, the following problems should be addressed.

As mentioned in section 1.1, many previous studies have tried to explore new materials to engineer MD membranes and one possible solution is by tuning the wettability of hydrophilic membranes through hydrophobic modification. However, plenty of modification methods are often involved with time-consuming process, special handling or expensive equipment and chemicals, such as plasma polymerization or UV irradiation, which are difficult for large-scale membrane fabrication/modification (Liu et al. 2016a, Yang et al. 2017). Also, the adaptation of those complicated methods to different substrates are limited, hindering the actual promotion of novel materials for MD membranes. It is crucial to find a cost-effective hydrophobic coating materials that can eliminate the need for multiple modification steps and complex processing, which is capable of improving the hydrophobicity of a broad range of hydrophilic materials, such as nylon and nitrocellulose. Moreover, the modified membranes should be able to work effectively in challenging waste streams with compositions closer to real feed. Additionally, the viability of hydrophobic membranes made from hydrophilic materials in treating challenging waste streams remains unknown, as most associated studies have only tested them with low-concentration saline water.

Regarding the recovery of organic solvents from wastewater, MD can offer a viable solution when the organic solvents have distinct boiling points with water. However, the

MD studies related to separating organic solvents from water are limited, while the majority of previous studies focusing on the non-volatile compounds like inorganic salts and metals with relatively low concentrations (Chen et al. 2019, Dao et al. 2016, Jia et al. 2018, Twibi et al. 2021, Wang et al. 2021). There is a need to fully explore the potential of solvent-resistant MD (SR-MD) for this type of application, as well as to design MD membranes specifically for SR-MD. In addition to hydrophobicity, chemical resistance is another critical property must be considered to avoid the deformation of membrane structure by organic solvents. Among the conventional hydrophobic MD membranes, only PP and PTFE membranes are solvent-resistant, but both of them with appropriate pore sizes are difficult to fabricate using common membrane fabrication techniques (Feng et al. 2018, Tan and Rodrigue 2019b). An alternative solution is the use of ceramic membranes, which have gained attention because of their great chemical and thermal stability. Nevertheless, the hydrophilic ceramic membranes need appropriate hydrophobic modification and their potential in SR-MD has not been fully explored.

1.3 Research objectives

This thesis focuses on the applications of MD in treating challenging wastewater streams containing a high concentration of organic solvents or salts. The project aims to develop robust and cost-effective MD membranes from hydrophilic materials and explore the broader applications of MD, demonstrating the versatility and potential of MD technology in industrial water treatment. The specific objectives include:

- Developing a facile, cost-effective, and scalable hydrophobic modification method to modify hydrophilic membranes, making them available for MD application in treating high-salinity water.

- Exploring the potential of MD in treating wastewater with a high concentration of organic solvent such as DMSO through SR-MD.
- Developing a simple, green and cheap method to prepare hydrophobic ceramic membranes available for SR-MD.
- Elucidating the separation and transport mechanism and understanding the roles of MD membrane play in the SR-MD process.
- Comparing MD performance in treating challenging wastewater with other approaches to highlight the superiority.

1.4. Thesis outline

This thesis comprises six chapters. The main contents are briefly summarized below.

Chapter 1: Introduction – This chapter introduces the background of MD, its advantages, challenges in treating challenging wastewater and research objectives.

Chapter 2: Literature review – This chapter first introduces basic MD information, including the mechanisms, configurations, membrane selection, and requirements. After that, the studied MD applications related to the topic and membrane hydrophobic modification methods applied on hydrophilic membranes are reviewed.

Chapter 3: Facile hydrophobic modification of hydrophilic membranes by fluoropolymer coating for direct contact membrane distillation – This chapter

develops a simple coating method using LUMIFLON™ to produce viable MD membranes to treat highly salty water. This method is time-saving and simple to handle. It imparts the hydrophilic nitrocellulose (NC) and nylon membranes with considerable hydrophobicity of $\sim 130^\circ$. Also, the modified NC membrane performs better than the commercial PVDF membrane.

Chapter 4: Effective separation of water-DMSO through solvent resistant membrane distillation (SR-MD) – This chapter elucidates the potential of MD in separating water-solvent mixtures over a wide range of organic solvent concentrations. Hydrophobic ceramic membranes modified by fluoroalkylsilanes were used in separating water and DMSO via SR-MD. The separation and transport mechanisms were demonstrated. The results show that SR-MD has superiority over the PV process. This study facilitates SR-MD applications for other water-solvent systems associated with high boiling point solvents.

Chapter 5: Hydrophobic ceramic membranes fabricated via fatty acid chloride modification for solvent resistant membrane distillation (SR-MD) – This chapter develops a simple surface modification method to prepare hydrophobic ceramic membranes using fatty acid chloride (FAC). The performance of the FAC-modified membranes is comparable to hydrophobic membranes modified with a common silane agent. It is the first study to demonstrate that FAC can be grafted on ceramic membranes. Compared with the hydrophobic modification method in Chapter 4, this modification method is cheaper and more environmental-friendly.

Chapter 6: Conclusions and recommendations – The critical findings of Chapters 3, 4, 5, and recommendations for future work are presented in this chapter.

This page is intentionally left blank

Chapter 2 Literature Review

This literature review first provides the basic information about MD, including the mechanisms, advantages, and requirements. Then, the MD applications in treating challenging waste streams and the shortages of existing membranes are discussed. The last part focuses on the hydrophobic modification methods conducted on hydrophilic polymeric or ceramic membranes to extend the scope of MD membranes with high performance.

2.1 MD fundamentals

2.1.1 MD mechanisms and configurations

In a typical MD process, a hydrophobic porous membrane is used to repel aqueous feed solution while providing interfaces for water evaporation (Khayet 2011). By heating the feed solution to a temperature greater than that of the permeate side, vapour pressure difference is generated across the membrane. As a result, the water vapour diffuses through membrane pores and condenses on the cold permeate side, while nonvolatile substances with very low partial vapour pressure are remained in the feed solution and rejected by the membrane barrier (Srisurichan et al. 2006). The mechanism is shown in Figure 2.1.

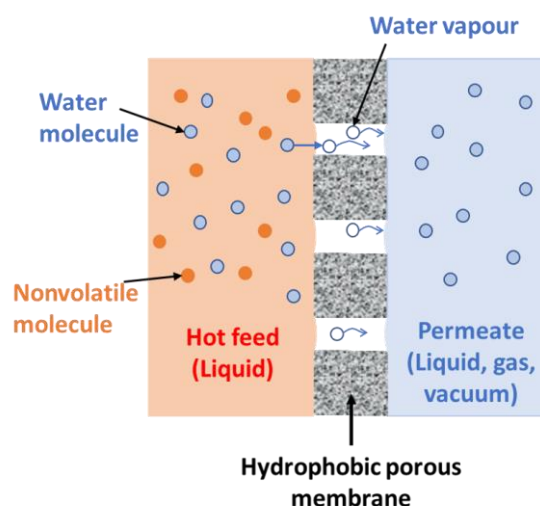


Figure 2.1 Schematic diagram of MD mechanism.

MD can be categorized into four major configuration types based on the medium on the permeate side: the vapour passed through the membrane can be condensed by cool water, air, sweeping gas, or an external condenser (Wang and Chung 2015). The schematic diagrams of the four configurations are shown in Figure 2.2.

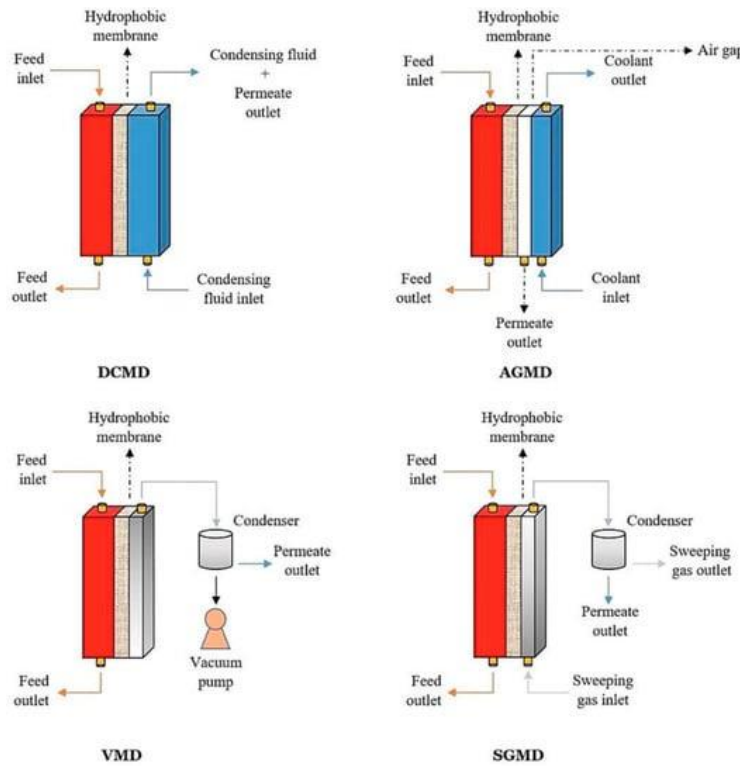


Figure 2.2 Sketch of four MD configurations (Kebria and Rahimpour 2020).

In direct contact membrane distillation (DCMD), cooling water circulates on the permeate side and provides a lower vapour pressure than the feed stream. The water vapour can pass through the membrane pores and condense once it contacts the cold water stream inside the module. DCMD is the most widely studied mode because it is easy to use and does not need external condensers or vacuum pumps. However, it has the problem of high heat loss due to the greater thermal conductivity of liquid water relative to the gas phase. In addition, the temperature polarization effect in DCMD may be more severe than in other configurations, which refers to the phenomenon where there is a temperature gradient near the membrane surface. The severe temperature polarization can significantly reduce the

driving force and permeate flux in MD, especially when the used membranes have high thermal conductivity (Alkhudhiri et al. 2012a, Tai et al. 2020).

In air gap membrane distillation (AGMD), vapour needs to travel across the membrane pores and an air layer to condense on a cool condensation surface inside the module (Kalla et al. 2019). Compared with cold water, the air layer (typically 2-10 mm) is beneficial in reducing conductive heat loss and increasing thermal efficiency (Kalla et al. 2019). However, the air barrier brings additional mass transfer resistance to permeate condensation, and the flux decreases with an increasing air gap (Janajreh et al. 2017).

In sweeping gas membrane distillation (SGMD), the vapour that passes through the hydrophobic membranes is continuously swept by inert gas and carried to an external condenser. Compared with the stagnant air gap in AGMD, the flowing gas in SGMD enhances the mass transfer coefficient and reduces conductive heat loss at the same time (Nagy 2019). However, this model requires a large condenser to collect the small portion of permeate in the sweeping gas (Said et al. 2020). SGMD is less studied compared with the other configurations, and most applications are reported in the treatment of salt (Lee et al. 2022, Thakur et al. 2020), dye (Mousavi et al. 2021), organic matters (Ajdar et al. 2020, Chandra Bhoumick et al. 2021) and solution concentration (A Shirazi et al. 2020).

In vacuum membrane distillation (VMD), a vacuum pump is utilized on the permeate side to produce a vacuum condition and condensation happens outside the membrane module (Choudhury et al. 2019). The pressure at the permeate side is reduced to lower than the vapour pressure of the volatile constituent, so the vapour molecules tend to diffuse across the membranes (Eykens et al. 2016a). Because of this design, conductive heat loss and mass transfer resistance are negligible, and VMD has the highest driving force

compared with other modes. In addition, VMD requires a smaller condenser compared with SGMD because it involves less gas volume. VMD system is more complex and expensive than DCMD, and it has a higher risk of membrane wetting when the partial pressure gradient exceeds the liquid entry pressure (LEP) (Eykens et al. 2016b).

Besides the four main configurations, there are other various configurations that are modified from the four major modes, such as permeate gap MD (Cheng et al. 2018), conductive gap MD (Swaminathan et al. 2016), material gap MD (Francis et al. 2013), vacuum assisted air gap MD (Bindels and Nelemans 2021, Eryildiz et al. 2020), vacuum-multi effect MD (Chen et al. 2020a, Mohamed et al. 2017, Zhao et al. 2013), thermostatic sweeping gap MD (Souhaimi and Matsuura 2011), submerged MD (Francis et al. 2015, Meng et al. 2015, Ryu et al. 2019) and flashed-feed vacuum MD (Alsaadi et al. 2018). Most of them are designed to improve wetting resistance, increase thermal energy efficiency or decrease specific energy consumption (Francis et al. 2022a). However, MD studies using these configurations are still very limited, and they are limited to commercialized MF membranes made of PTFE, PVDF, PP. Some of these membranes may have large PSD which can lead to poor separation efficiency and low permeate flux in MD. Additionally, their hydrophobicity might not be sufficient to prevent wetting by challenging feed solutions with low surface tension. There is a lack of integrated considerations combining the advanced MD membranes and the improved MD configurations to further optimize MD performance.

2.1.2 MD compared with other separation methods

MD can be seen as a combination of membrane technology and thermal distillation, and it has unique strengths compared to other separation technologies. For example, compared with RO, MD is more viable to treat concentrated brine water with salinity >7

wt%, because it is not very sensitive to osmotic pressure (Chen et al. 2020b). However, it still has some unsettled issues and its large-scale use in industries is relatively rare compared with other separation processes (Ravi et al. 2020). Table 2.1 and Table 2.2 list the main pros and cons of MD compared with other membrane processes and traditional thermal distillation, respectively.

Table 2.1 MD compared with other membrane processes.

Pros	Cons
<ul style="list-style-type: none"> • MD is effective to separate a wide range of non-volatile pollutants regardless of their sizes, ranging from macromolecules to small ions. • MD displays theoretically 100% rejection to particulates and nonvolatile solutes (Hendren et al. 2009, Tai et al. 2019, Tan et al. 2016). • MD is a thermal-driven process that is viable to deal with highly saline water with a higher allowable salt concentration than the pressure-driven process, such as RO (Chen et al. 2020b). • MD has less demand for membrane mechanical strength, and fewer problems in operating safety because of the moderate operating conditions. • MD can use low-graded heat such as waste heat from industries, or renewable energy resources such as solar and geothermal energy (Camacho et al. 2013, Chew et al. 2017). 	<ul style="list-style-type: none"> • MD has a relatively lower permeate flux because the trapped air in membrane pores increases mass transfer resistance. • MD performance may deteriorate due to membrane wetting, and temperature polarization (Ghaffour et al. 2019). • Without covering the energy demand with low-grade thermal energy, MD is not as cost-effective and energy-saving as RO (González et al. 2017). • Limited suppliers of suitable hydrophobic membranes.

Table 2.2 MD compared with traditional thermal distillation.

Pros	Cons
<ul style="list-style-type: none">• MD is suitable to be applied to off-grid regions on a small scale, as it eliminates the need for large vapour space like the large-scale thermal distillation methods of multi-stage flash distillation and multi-effect distillation (Basile and Napporn 2020, Zaragoza et al. 2018, Zhani et al. 2016).• Evaporation can happen under the boiling point and it is unnecessary to heat the feed solution to the boiling point (Ashoor et al. 2016). This feature allows MD to be applied to liquid food or biological solutions whose quality becomes erratic under high temperature (Khayet and Matsuura 2011).	<ul style="list-style-type: none">• MD has complex module design and need hydrophobic membranes to separate feed and product.• MD still suffers from common issues of membrane processes: membrane fouling and scaling caused by the accumulation of foulants on membrane surface (Yang et al. 2022).

2.1.3 Essentials of MD membranes

MD membrane, as the key component in the MD process, provides the interfaces for phase change and channels for permeate to pass through, while not directly engaging in the vapour-liquid equilibrium (VLE) (El-Bourawi et al. 2006). Its characteristics greatly affect mass and heat transfer as well as the repellency to feed solution, deciding MD capacity to ensure good separation performance.

LEP, the pressure at which the feed stream is able to penetrate membrane pores to the permeate side, decides whether a membrane is viable in MD. It is determined by several factors, including pore size and structure, surface wettability and membrane thickness. It can be calculated by Laplace (Cantor) equation as shown below (Chen et al. 2017, Servi et al. 2016).

$$LEP = -\frac{2B\gamma}{r_{max}} \cos \theta \quad (2-1)$$

where B is a geometric coefficient (1 means ideal circular shape), γ is liquid surface tension, θ is the contact angle, and r_{max} is the biggest membrane pore size. Higher LEP endows the membrane with a better resistance to pore wetting and ensures the stability of

the MD process. Moreover, the pore structure and porosity of membranes also determine the mass and heat transfer. Therefore, the following properties for an MD process with excellent separation performance and practical application are essential: (1) high hydrophobicity or low surface energy to prevent liquid water from passing through membranes pores; (2) porous structure to decrease the resistance of vapour transport; (3) small thickness and low tortuosity to reduce mass transfer resistance; (4) high porosity to enhance flux and improve heat efficiency; (5) narrow PSD to prevent wetting, (6) low thermal conductivity to alleviate conductive heat loss (Zare and Kargari 2018). In addition, good chemical stability is very important when MD is applied in harsh environments, such as corrosive water (Fan et al. 2018), strong organic solvent (Shao et al. 2014), strongly acidic and alkaline solution (Ji et al. 2021). We will introduce the influences of membrane properties in detail in the following section.

2.1.3.1 Micro-structure and morphology

Membrane structural properties greatly affect their performance in MD. To begin with, the membrane thickness will pose mass resistance to permeation flux, so a thin membrane wall is beneficial to increase permeation flux. However, a thin membrane is detrimental to heat efficiency because more conductive heat is lost through the solid membranes, resulting in decreased driving force. Thus, optimizing the membrane thickness to balance the tradeoff between mass transfer and heat loss is necessary. It has been noted that membranes with a hydrophilic skin layer usually have a higher flux than the homogenous hydrophobic membranes when they have the same thickness because they decrease the mass transfer resistance while maintaining a similar heat resistance (Bonyadi and Chung 2007, Zhao et al. 2020, Zou et al. 2020). A lot of studies have investigated the effect of thickness on MD performance. For instance, Lagana et al. described the ideal

polymeric membrane thickness should be in the range of 30-60 μm based on the assumptions that (1). The thermal conductivity, tortuosity and porosity of the membrane are 0.1-0.3 $\text{W m}^{-1} \text{K}^{-1}$, 1.3 and 75%, respectively (Laganà et al. 2000). It is worth mentioning that in AGMD configuration, the mass resistance of membrane thickness can be ignored as the stagnant air gap is the dominant hindrance to mass transport (Alkudhiri et al. 2012a).

More importantly, membranes with high porosity are paramount to improving heat efficiency as well as mass transfer. Porosity (ϵ) is determined as the ratio of pores volume to bulk membrane volume. To be specific, the air/vapour trapped in pores plays the role of an excellent thermal insulation layer to reduce the heat loss across the membranes because gas has lower thermal conductivity than solid (Capizzano et al. 2022, Shahu and Thombre 2019). In addition, high surface porosity provides large liquid-vapour interfacial areas to increase vapour transport. Nonetheless, highly porous membranes are more possible to crack during long-term operations (Camacho et al. 2013). In MD, porosity ranging from 70-80% is recommended, though ceramic membranes with porosity low to ~35% are often reported (Cong et al. 2019). The porosity is defined as:

$$\epsilon = 1 - \frac{\rho_{\text{membrane}}}{\rho_{\text{material}}} \quad (2-2)$$

where ρ_{membrane} and ρ_{material} are the membrane density and the material density, respectively.

In terms of pore size, membranes with small pore sizes have advantages in the separation of feed water with lower surface tension, owing to the fact that smaller pores are more difficult to penetrate by feed streams. But it is likely that membranes with small pore sizes have lower flux than membranes with larger pore sizes. Thus, pore size should be optimized regarding the feed stream characteristics. It is noteworthy that when pore size

increases to a certain level, the flux enhancement can be neglectable. In DCMD, it is reported that membrane pore size ranging from 0.2 to 1.0 μm has very little effect on flux compared with membrane porosity and thickness (Adnan et al. 2012). In VMD, a pore size smaller than 0.2 μm is considered suitable to prevent wetting (Eykens et al. 2016a). In the case of ceramic membranes, a review paper points out that pore size even has no connection to flux (Camacho et al. 2013).

PSD, which is the deviation of membrane pore size to the mean pore size also plays a positive role in MD. As mentioned above, the maximum pore size decides the LEP of membranes, while the average pore size determines the mass transfer. Thus, a narrow PSD is always preferred in MD.

Another membrane structural characteristic is pore tortuosity, which means the discrepancy of the pore structure from the ideal cylinder structure, affecting MD performance by vapour transport. A lower degree of pore tortuosity is postulated to be correlated with a higher permeate flux (Alkhudhiri et al. 2012a). The tortuosity (τ) is determined by:

$$\tau = \frac{(2-\varepsilon)^2}{\varepsilon} \quad (2-3)$$

Besides, membrane surface roughness has an impact on MD performance as well because it affects the contact angle and membrane fouling. The influence of roughness on surface wettability can be depicted by Wenzel's theory, which can be written as:

$$\cos \theta_W = r \cos \theta_Y \quad (2-4)$$

where θ_W is the apparent contact angle on a surface with single-level roughness, θ_Y is the intrinsic contact angle (Chew et al. 2019b), r is the roughness ratio of the actual

membrane surface area to the projected area of the membrane surface (r is always >1), which can be calculated by:

$$r = \frac{A_m}{A_n} \quad (2-5)$$

where A_m and A_n are the projection area of membrane surface in the main direction and the measured surface area by experiment technique (Camacho et al. 2013).

2.1.3.2 Hydrophobicity

Hydrophobicity is a critical characteristic of MD membranes. It is often evaluated by the water contact angle (WCA), which is the angle formed between a water droplet and the membrane surface. Based on the degree of WCA, there are three common classifications of membrane hydrophobicity: (1) hydrophobic membranes with WCA between 90 and 150° , (2) superhydrophobic membranes with $WCA >150^\circ$, and (3) omniphobic membranes, which repel virtually all liquids, including water, oils, and organic solvents with liquid contact angles $>90^\circ$ (Law 2014, Wang et al. 2019a). Membranes with high WCAs are generally favored because they allow a higher LEP, which is essential factor in deciding whether the MD process can work successfully. In recent years, researchers have great enthusiasm in engineering omniphobic membranes to repel liquid with low surface tension that may exist in wastewater. These membranes are constructed using a variety of strategies, such as the use of surface patterning, incorporation of nanoparticles, fluorinated materials and silicone-based materials (Fang et al. 2023, Li et al. 2019, Wang et al. 2019a).

2.1.3.3 Membrane thermal conductivity

The heat transfer in MD process mainly consists of two paths: (1) the latent heat of vapour across the membrane related to the permeate flux, and (2) the conduction heat transfer through the membrane which is considered as heat loss (Fane et al. 1987). Specifically, membrane materials with low thermal conductivity are preferred as they avoid high conduction heat flux and present higher thermal efficiency. In addition, membranes with low thermal conductivity are also considered an advantage in reducing temperature polarization in MD (Anvari et al. 2020). In this sense, polymeric materials are more suitable for MD membranes as they usually have lower thermal conductivity ($0.2\text{-}0.5 \text{ W m}^{-1} \text{ K}^{-1}$) than some inorganic materials made of alumina, zirconia, silica, titania ($\sim 30 \text{ W m}^{-1} \cdot \text{K}^{-1}$). (Hendren et al. 2009, Ravi et al. 2020).

2.1.4 MD membrane materials

2.1.4.1 Conventional hydrophobic polymers

Different materials have been reported to fabricate MD membranes. Hydrophobic polymers, including PVDF, PTFE, and PP are the most conventional and extensively used membrane materials because of their good hydrophobicity, thermal and chemical stability (Shi et al. 2022). As shown in Table 2.3, PTFE has the highest hydrophobicity (WCA of pure film $\sim 108^\circ$) and best stability, while PP has the lowest heat conductivity (Zhang et al. 2015). However, due to the resistance to regular solvents, they are challenging to fabricate via the normal non-solvent induced phase inversion method. The commercial PP and PTFE membranes fabricated by traditional stretching technology often have a symmetric structure with a relatively large pore size (typically from $0.2\text{-}20 \mu\text{m}$) and wide PSD, which may result in an adverse effect on the separation performance and wetting resistance (Camacho et al. 2013). Besides stretching, some studies report electrospinning PTFE membranes which are fabricated by blending additives like poly(vinyl alcohol) and

polyethylene oxide into PTFE emulsion to make a spinnable solution (Feng et al. 2018, Huang et al. 2017, Su et al. 2019, Zhou et al. 2014). The membranes formed have a high WCA and high porosity, but the pore size is still relatively large, and the method needs a high sintering temperature of up to 400 °C. Similarly, PP membranes fabricated by thermal-induced phase separation (TIPS) also require a high temperature to dissolve the polymer (Tang et al. 2010).

Table 2.3 Properties of conventional materials widely used in MD (Alkhudhiri et al. 2012a).

Material	Structures	WCA of pure film (°)	Surface energy (dynes cm ⁻¹)	Thermal conductivity (W m ⁻¹ K ⁻¹)	Melting point (°C)
PTFE	-(CF ₂ CF ₂) _n -	~108	19.1	0.25	327
PP	-CH ₂ CH(CH ₃) _n -	~104	30	0.17	151-166
PVDF	-(CH ₂ CF ₂) _n -	~86	30.3	0.19	140-170

In comparison, the PVDF membrane can be manufactured by the non-solvent induced phase inversion (NIPS) method, so it is more controllable in pore size and has the versatility to form asymmetric structures (Wang and Lai 2013). Moreover, it has a lower cost per unit membrane area than the PTFE membrane (Khaisri et al. 2009), so it attracts great interest from scientists and industries. However, PVDF has relatively lower hydrophobicity (pure film ~86°) and most commercial PVDF membranes are customized for conventional membrane filtration processes with hydrophilic modification. The common PVDF membranes usually have a WCA of 75-95°. Hydrophobicity enhancement is often needed to obtain a PVDF MD membrane with the good anti-wetting property. For example, some studies modified the NIPS process to improve PVDF membranes' hydrophobicity, such as replacing the coagulation bath with alcohols (Ahmad et al. 2012, Munirasu et al. 2017) or saturated salt aqueous solution (Zhang et al. 2021a). But the PVDF membranes fabricated by these methods have larger pore sizes, which may result in a lower LEP.

Besides, other methods such as vapour-induced phase separation (VIPS) (AlMarzooqi et al. 2016, Peng et al. 2012), blending hydrophobic additives (Li et al. 2020b) and surface coating (Cui et al. 2020) also contribute to improving PVDF membranes' hydrophobicity.

2.1.4.2 Novel hydrophobic copolymers

Since PTFE, PP and PVDF membranes have their drawbacks, some studies invented some novel hydrophobic copolymers in order to get more suitable MD membranes. Copolymers of PVDF such as PVDF-co-hexafluoropropylene (PVDF-HFP) and PVDF-co-chlorotrifluoroethylene are used to fabricate MD membranes. They not only have good processing flexibility but also provide better hydrophobicity, mechanical strength and chemical resistance than conventional PVDF membranes because of the higher fluorine content in the polymer compounds (Lalia et al. 2013, Wang et al. 2016, Wang et al. 2018). Besides, poly (ethylene chlorotrifluoroethylene) (ECTFE) is a new MD membrane material with excellent chemical and temperature stability. Xu et al. fabricated hydrophobic ECTFE membranes via TIPS and applied them in VMD for treating 3.5 wt% NaCl solution. The membrane had a high WCA $\sim 140^\circ$ and presented a flux of $22.3 \text{ L m}^{-2} \text{ h}^{-1}$ at 80°C (Xu et al. 2019). However, most of the ECTFE membranes are fabricated via the TIPS method because they cannot dissolve in organic solvents under room temperature. The related studies are still limited (Gryta 2016, Pan et al. 2015). Moreover, it is worth noting that fluorinated membranes are more costly than non-fluorinated ones (Giannetti 2001), and their fabrication process is not environmental-friendly (Nguyen et al. 2022). It is suggested that environmentally friendly membranes with less fluorine content should be used.

2.1.4.3 Hydrophilic polymers

The restricted availability of hydrophobic polymers has compelled researchers to explore alternative options such as hydrophilic polymers, which offer a more diverse and extensive range of choices. Although they are unsuitable for MD in terms of natural wettability, they may be more cost-effective and flexible in processing compared with conventional hydrophobic membranes. It is easier to obtain membranes with favourable microstructures like high porosity and suitable pore structure via NIPS. Until now, the availability of MD membranes has been expanded to a wide range of hydrophilic materials, including polysulfone (PSf) (Fahmey et al. 2019, Peng et al. 2013), polyimide (Ju et al. 2020), poly(amide-imide) (PAI), poly(etherimide) (PEI) (Zhang et al. 2012), polyacrylonitrile (PAN) (Liu et al. 2016a), polyvinyl alcohol (PVA), polyvinyl chloride (PVC) (Hussein et al. 2020), polyethersulfone (PES) (Wei et al. 2012), polyamide (PA) (Figoli et al. 2017), cellulose acetate (CA) and NC (Wu et al. 1992). Usually, it is necessary to enhance the hydrophobic of these membranes before MD application, which will be discussed in section 2.3.

2.1.4.4 Ceramic membranes

Ceramic membranes are a class of inorganic membrane materials, including alumina, titania, silicon dioxide, kaolin, zirconia, etc. Recently, ceramic membranes gained increasing attention in the industrial fields because of the following properties: (1) excellent thermal and chemical stability, which means they resist acids, alkalis and organic solvents; (2) long using period without degradation; (3) good resistance to the abrasive environment to withstand high shear rate of liquid containing particles; (4) good anti-fouling properties and high competence in treating wastewater under harsh conditions, including high temperature, extreme pH, high pressure and solvent-containing environments (Ciora and

Liu 2003). Unlike the uncrosslinked polymeric membrane substrates, ceramic membranes hardly swell or dissolve in organic solvents (Chong and Wang 2019, Marchetti et al. 2014), so they are good at handling challenging waste streams containing a high concentration of organic solvents. However, the hydrophilic nature of ceramic surface does not meet MD requirements, so hydrophobic modification is necessary. Other disadvantages include the low packing density and expensive manufacturing cost due to the high sintering temperature (Hubadillah et al. 2019a). The hydrophobic modification of ceramic membranes will be discussed in section 2.3.

2.2. Studied MD applications and their challenges

Recently, there has been a surge of interest in MD's potentiality in dealing with challenging waste streams, such as high-salinity water (Anvari et al. 2019, Farid et al. 2022) and wastewater containing organic solvents (Chandra Bhoumick et al. 2023). They are difficult and expensive to purify because of the characteristics of high organic content, high toxicity and high salt content. The poor biodegradability and high salt content also restrict other membrane treatment methods such as MBR and RO. On the contrary, MD has shown potential to treat the challenging feed and provide a high-quality product.

2.2.1 MD in treating high-salinity water

Desalination of high-salinity water is an important application of the MD process. Commercial PVDF and PTFE membranes have been applied to treat high-salinity water. Alkudhiri et al. studied the impact of highly salty water on the performance of AGMD and reported that the energy consumption (3.5-4.0 kWh) had very little relation to the membrane pore size, salt types and concentration (Alkudhiri et al. 2012b). The PTFE membrane with a pore size of 0.2 μm had a stable salt rejection when the feed concentration

increased, while the PTFE membrane with a 0.45 μm pore size was wetted in feed solution containing 4.2 wt% of Na_2CO_3 (Alkhudhiri et al. 2012b). It may indicate that small pore size is relatively more durable in treating high-salinity water. Another study explored the potential of DCMD in treating hypersaline water with a commercial PVDF membrane whose WCA was 120° and pore size was 0.22 μm . It was found that the permeate flux decreased a lot with the increasing salinity, from the original 8.43 to 4.06 $\text{kg m}^{-2} \text{h}^{-1}$ when the feed NaCl concentration increased from 0.5 to 5 M (2.93-29.3 wt%) (Bouchrit et al. 2015). This is a common observation, which is ascribed to the decrease of water activity and vapour pressure and the concentration polarization can exacerbate this phenomenon. The study also mentioned a sudden increase in permeate conductivity after the WCA of PVDF membranes decreased to 90° under the effect of the scaling (Bouchrit et al. 2015). It emphasized the importance of hydrophobicity of MD membranes, which can reduce the tendency of salt crystal attachment. To improve the permeate flux, a study laminated two superhydrophobic PTFE membranes with WCA of 151.7° and compared its performance with a single-layer membrane. In the treatment of 3.26 M (19.05 wt%) NaCl solution, the laminated membrane obtained a high flux of 30 $\text{kg m}^{-2} \text{h}^{-1}$, while the original PTFE membrane had a much lower flux of 14 $\text{kg m}^{-2} \text{h}^{-1}$.

In addition, many researchers modify superhydrophobic or omniphobic membrane surfaces for this application. Du et al. prepared electrospun with polyphenylene oxide membrane with WCA of 138° for desalination, with water recovery of 80% and the concentrate has a concentration of $\sim 21.9\%$ (Du et al. 2019). Zhu et al. modified an electrospun PP membrane with a superhydrophobic-omniphobic feature and applied it to treat 20 wt% NaCl solution (Zhu et al. 2021). Although the membrane had a high flux $\sim 25 \text{ L m}^{-2} \text{h}^{-1}$ as well as stable rejection, the modification process was complicated and involved coating polydopamine, silica nanoparticles (NPs), fluorination and

polydimethylsiloxane (PDMS) crosslinking. Similarly, Zhang. et al. sprayed coated silica NPs and PDMS on the surface of PVDF membrane to improve WCA to 156°. The modified membrane presented flux of 8 and 5 L m⁻² h⁻¹ in 3.5 and 25 wt% NaCl, respectively. In another study, Dong et al. prepared a superhydrophobic ceramic membrane coated with carbon nanotubes with a high WCA of 170°. The membrane showed a flux of 11.2 L m⁻² h⁻¹ in electrochemically assisted DCMD fed with 10.5 wt% NaCl solution (Dong et al. 2018).

These previous studies have demonstrated MD as a promising technology in treating high-salinity feeds with a high rejection of salts. However, the commercial hydrophobic membranes usually have limited performance, with relatively low flux. Meanwhile, the modification methods to enhance the hydrophobicity often have multi-steps with time-consuming processing. Also, the sophisticated structures of some modified membranes in the actual application may deteriorate (e.g. loss of NPs, abrasive environment), and whether they can maintain the special wettability can be a problem. In order to advance the practical implementation of MD for large-scale application, it is necessary to fabricate durable MD membranes using cheap materials and simple modification techniques that can be readily scaled up.

2.2.2 Separation of water-solvent mixture

The separation of water and organic solvents with high water miscibility is typically achieved through distillation in industry, which involves heating the feed to a temperature close to its boiling point (Kolesnichenko et al. 2019, Ravikumar et al. 2013, Smallwood 2002). For instance, the reboiler temperature of distillation column used to separate water-DMSO mixtures was reported to be around 120-150 °C even when operating under vacuum (Horváth et al. 2017). The high temperature in conventional distillation not only means a

huge energy consumption, but also has potential for accelerated hydrolysis of certain solvents such as dimethyl formamide (DMF) and dimethylacetamide (DMAc) (Smallwood 2002). The hydrolysed products can lead to azeotrope formation and affect the separation performance (Smallwood 2002). Moreover, the conventional distillation has drawbacks of high capital costs and large space requirement as indicated in Table 2.1. Therefore, there is a need for efficient separation processes enabling low operating temperature and flexible operation to treat organic waste streams.

In this regard, thermally driven membrane-based processes such as PV and MD offer a promising solution. PV has been widely adopted in industry because of its strength in separating azeotrope or mixtures with close boiling points (Li et al. 2020c). Generally, organophilic PV membranes favour the permeation of organic solvents, enabling the extraction of solvents, while hydrophilic PV membranes are suitable for reclaiming water from water-solvent mixtures. Though PV has excellent separation ability, it often has low permeation flux because the mass transfer is restricted by the diffuse rate in dense membrane. In the case of DMSO removal from water solution, Hosseini and Ameri reported a separation factor of 57 and DMSO flux was $0.5 \text{ kg m}^{-2} \text{ h}^{-1}$ at $70 \text{ }^\circ\text{C}$ for feed organic concentration of 10 wt% (Hosseini and Ameri 2017). Likewise, Tang and Sirkar used perfluoropolymer-based membranes to dehydrate 90 wt% DMSO at $30 \text{ }^\circ\text{C}$ and achieved a separation factor over 1000 (Tang and Sirkar 2012).. However, the water permeation flux was only $0.0098 \text{ kg m}^{-2} \text{ h}^{-1}$ (Tang and Sirkar 2012).

In comparison to PV, the potential of MD in treating water-solvent mixtures is often overlooked and there are relatively fewer publications concerning separating water-solvent mixtures via MD. Actually, MD process is able to separate water and organic solvent as long as there is a difference between the partial vapour pressure of two components.

Moreover, MD can separate the small organic molecules with a porous membrane (as shown in Figure 1.1). Thus, it is reasonable to expect a higher flux in MD than in the PV process. Gupta et al. developed carbon nanotube immobilized PTFE membranes for the separation of 5-15 vol% isopropyl alcohol (IPA) from an aqueous solution via sweeping gas MD. IPA with a higher vapour pressure permeated through the membranes faster, but the separation factor was fairly low, below 13 due to the small difference in the vapour pressure for IPA and water (Gupta et al. 2018). Besides that, another study uses PP membranes in the dehydration of n-methyl-2-pyrrolidone (NMP) through VMD. The membranes exhibited a high water permeation flux of $9.5 \text{ L m}^{-2} \text{ h}^{-1}$ and a rejection of 98% when the feed contained 10 wt% NMP at 80 °C (Shao et al. 2014). It could be seen MD give a considerable flux when treating solvents with a distinct boiling point to water. Nevertheless, the solvent concentration range tested by far was relatively narrow and only PTFE and PP membranes were involved in these studies. There is a need for further investigation to expand the range of solvents concentration and to explore the long-term stability of MD membranes exposed to organic solvents.

2.2.3 Other studied MD applications

Besides wastewater with high salinity and organic solvents, MD has been reported to be applied in different fields, including but not limited to: desalination (Camacho et al. 2013, Hou et al. 2009, Jafari et al. 2018, Marni Sandid et al. 2021); concentration of juice in food industry (Gunka et al. 2006); enrichment of protein in pharmaceutical industry; elimination of radioactive compounds in low-level radioactive waste (Zakrzewska-Trznadel et al. 1999), ammonia from agricultural wastes (Zarebska et al. 2014), and boron from geothermal water (Ozbey-Unal et al. 2018); treatment of textile wastewater (Leaper et al. 2019, Villalobos Garcia et al. 2018), oily wastewater (Aloulou et al. 2021) and produced water (Chew et al. 2019a, Chew et al. 2017, Chul Woo et al. 2017).

2.3. Hydrophobicity enhancement methods for hydrophilic membranes

As mentioned, MD membranes are still very limited because only a narrow range of polymers are intrinsically hydrophobic, and their fabrication is not easy. To reduce the cost and expand the availability of MD membranes, it is useful to enhance the hydrophobicity of the hydrophilic polymeric or ceramic membranes. Some modification methods have been invented, which are carried out on the membranes either during membrane fabrication or carried out to nascent membranes as post-treatment.

2.3.1. Adding hydrophobic additives during fabrication

The blending of hydrophobic compounds in the polymer dope is the most direct method to decrease the surface energy of polymer dope. Surface modifying macromolecules (SMMs) are oligomeric fluoropolymers with fluorinated end groups, which will shift to the membrane surface layer in the phase inversion process (Figure 2.3) and impart hydrophobic property to the surface (Khayet et al. 2003). As the SMMs are concentrated near the membrane surface, this method is often used to produce dual-layer hydrophobic/hydrophilic membranes. Different types of SMMs have been blended with hydrophilic polymers like PES (Khayet 2013, Qtaishat et al. 2009b, Suk et al. 2010), PS (Khayet 2013), PSf (Qtaishat et al. 2009a) and PEI (Qtaishat et al. 2009b) for MD application. However, it should be noted that these reported membranes have a WCA of 90° - 114° , which might not be satisfactory in the application related to low surface tension pollutants. Besides SMMs, other hydrophobic additives can also be blended with a hydrophilic polymer solution. Gholamzadeh used oleic acid-modified cobalt oxide (Co_3O_4) NPs to prepare PES membrane and the blended membranes had a higher WCA of 106° compared to the original 75° (Gholamzadeh et al. 2017). The membrane has flux of $11.6 \text{ kg m}^{-2} \text{ h}^{-1}$ and rejection $>99.8\%$ in treating 3.5% NaCl solution. Besides blending,

hydrophobic components can be added in by other methods, such as co-electrospinning, co-extrusion, etc. However, attention should be paid to the possible surface delamination caused by the incompatibility of hydrophobic and hydrophilic components.

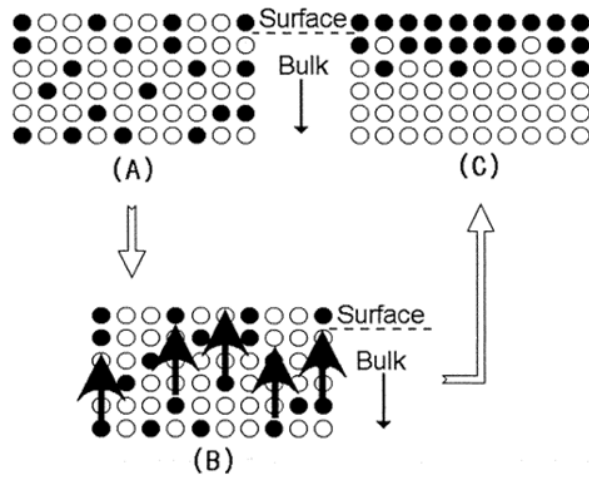


Figure 2.3 Schematic diagram illustrating SMMs migration (Solid circles represent SMM molecule which has lower surface free energy; hollow circles represent base polymer) (Suk et al. 2002).

When these methods are conducted on electrospun membranes, the hydrophilic membranes' wettability can be much increased to superhydrophobic or even omniphobic. This is because the intrinsic roughness provided by the overlapping nanofibres can enhance hydrophobicity. For example, Khayet et al. synthesized fluorinated polyurethane additive and fabricated superhydrophobic PSf nanofibrous membranes with WCA $>150^\circ$ (Khayet et al. 2019, Khayet and Wang 2018). Ju et al. developed a hydrophobic/hydrophilic bi-component membrane by co-electrospinning of PTFE and PI. They formed a rough structure with PTFE microclusters on polyimide nanofibres and increased WCA from 77 to 150° (Ju et al. 2020).

2.3.2. Polymerization

Polymerization means combing monomers into polymers. It can be used to modify hydrophilic polymers and improve their hydrophobicity. Hussein et al. prepared DHPVC-

g-PEA copolymer by free radical graft copolymerization and used to fabricate membranes via NIPS, which showed a WCA of 95.5° (Hussein et al. 2020). Liu et al. fabricated PES-g-PFMA-C8 copolymer by γ -ray simultaneous irradiation and used the copolymer to modify PES membrane by spray-coating (Liu et al. 2016b). They increased the membrane WCA from 82.3° to 114.3° . The spray coating method decreased the amount of copolymer needed to fabricate a membrane, but the hydrophobicity improvement is still limited. Besides, in situ polymerization, which is loading monomer onto hydrophilic membranes followed by polymerization, was also reported. Wu et al. modified NC membranes by plasma polymerization in a vinyltrimethylsilicon/ CF_4 system and improved the WCA to 115° (Wu et al. 1992). In another study, a PA membrane was coated with UV-curable perfluoropolyether by immersing in the oligomer solution followed by a UV treatment (Figoli et al. 2017). It increased the WCA from 40° to 140° . However, these methods have drawbacks of limited or need for special expensive irradiation equipment.

2.3.3. Surface grafting with hydrophobic compounds

Grafting can modify membrane' surface functional groups and form covalent bonds with the membranes so it has good durability. Grafting has been used to transform hydrophilic polymeric membranes into hydrophobic ones. For example, the WCA of PAI and PEI membranes grafted with octadecylamine increased from 75.6° to 108° (Zhang et al. 2012); PES membranes grafted with tetraethylorthosilicate and trimethylchlorosilane increased from 75° to 149° (Rastegarpanah and Mortaheb 2016); electrospun PVA grafted with (Heptadecafluoro-1,1,2,2-tetradecyl) trimethoxysilane increased from 5.6° to 158° (Dong et al. 2015). Sometimes, plasma treatment is needed to induce the grafting and improve the modification. It was reported that plasma etching and plasma grafting with 1H, 1H, 2H, 2H-perfluorodecyl methacrylate was carried out on PAN membranes, which greatly improved the WCA from 45.5° to 132.2° (Liu et al. 2016a). Except for inducing

polymerization, grafting and etching, plasma treatment with fluorinated gas can also increase the WCA of hydrophilic PES (Wei et al. 2012) and PSf membranes (Tian et al. 2015) to 120° and 144°, respectively. However, plasma modification needs expensive equipment and may decrease the membrane mechanical strength by breaking C-C bonds in substrates (Ravi et al. 2020).

Moreover, grafting is the most popular method in the production of hydrophobic ceramic membranes and many compounds have been previously studied. Among them, fluoroalkylsilane (FAS) is widely used because of the low surface energy of fluoroalkyl compounds (Lu et al. 2019). The FAS compound consists of three hydrolysable groups, which can react with hydroxyl groups on ceramic membranes to form strong covalent bonds and a fluoroalkane chain that can provide hydrophobic character to the membranes (Wei and Li 2009). Hendren et al. studied ceramic membranes modified by FAS, trichloromethylsilane and trimethylchlorosilane, and they found that FAS-modified ceramic membranes had a higher water permeability and better chlorine resistance compared with PTFE membranes (Hendren et al. 2009). Compared to other silane agents without fluorocarbon chain or with a short fluoroalkyl chain, a FAS agent with a longer fluoroalkyl chain imparts a better wetting-resistance to the anodized aluminium oxide membranes (Li et al. 2020a). The WCA of FAS modified-ceramic membranes are often >135° (Ko et al. 2018). The contact angle of the ceramic membrane can also be further enhanced by UV irradiation grafting, but the improvement is not obvious (~5° compared to without irradiation) (Yang et al. 2017). Besides, omniphobic ceramic membranes with 167° can be constructed accompanied by adding NPs (Alftessi et al. 2022). Although fluorinated compounds are the most effective in hydrophobic modification, it should be noted that they are much more expensive than the other modifiers (Nguyen et al. 2022).

2.3.4. Surface coating/deposition

Coating is a commonly used surface modification and there is a wide range of choices of coated material, such as fluorinated NPs and fluoropolymers. Guo et al. prepared a modified electrospun PA membrane via initiated chemical vapour deposition of poly(1H,1H,2H,2H-perfluorodecyl acrylate), resulted increasing WCA from $<90^\circ$ to 151° (Guo et al. 2015). Ghorabi et al. introduced fluorinated Ag NPs to the PES membrane surface to improve roughness, and the WCA significantly improved from 66° to 115° (Ghorabi et al. 2021). Wu et al. prepared PAN membrane with a WCA of 148.3° by plasma treatment and PDMS coating (Wu et al. 2018). Ceramic membranes prepared by dip-coating with polymethylhydrosiloxane/tetraethylorthosilicate hybrid solution followed by post-coating spinning were reported a WCA of 108.2 - 124.1° (Tai et al. 2021). Recently, a ceramic membrane with robust hydrophobicity was prepared with SiO₂@PDMS layer together with FAS grafting (Dai et al. 2022). The superhydrophobic membrane showed stable flux for >300 hours in desalination of 3.5 wt% NaCl via VMD. Another study fabricated superhydrophobic ceramic by spray coating of a mixture of PVDF-HFP, 1H, 1H, 2H, 2H-perfluorooctyltriethoxysilane, and ZnO nanoparticles (Abd Aziz et al. 2022). However, these coating methods are often laborious and involve multi-steps. In addition, the addition of NPs may cause leakage problems and reduce the membrane pore size.

2.4. Summary

From the literature review, it is seen that MD is a promising technique with unique advantages in wastewater treatment. To expand the range of MD membranes, a significant progress has been made to develop hydrophobic modification methods to fabricate desirable MD from hydrophilic materials. However, there is still room for improvement as the existing methods often require multi-steps and special handlings, with limited

scalability and adaptability on different substrates. Thus, this thesis is dedicated to the exploration of simple, scalable and cost-effective post-treatment modification methods to engineer durable MD membranes utilizing new hydrophobic modifiers. Furthermore, this thesis focuses on the treatment of highly saline water or water organic solvent mixture to fully exploit the unique advantages of MD applications. At present, there is a lack of a comprehensive MD study for the separation of aqueous solution with high organic solvent concentration.

This page is intentionally left blank

Chapter 3 Facile Hydrophobic Modification of Hydrophilic Membranes by Fluoropolymer Coating for Direct Contact Membrane Distillation¹

3.1 Introduction

MD has unique strength in dealing with high-salinity wastewater. However, the existing studies used conventional hydrophobic membranes, which have low permeability. The other modified membranes have complicated processing, which hampered the use for extended applications.

In this study, a simple and time-saving hydrophobic modification method was developed with the use of a fluoroethylene vinyl ether (FEVE) resin. The modification was conducted via direct and convenient dip coating of the FEVE polymer and followed by a crosslinking step carried out at low temperature or even room temperature to ensure the stability of coating layer. In this work, two types of hydrophilic membranes were used for the hydrophobic modification. First, NC membranes with a high porosity and low price were first studied and the optimum coating conditions were developed. Then, the FEVE polymer was coated on nylon membranes to evaluate the versatility of this modification method. A series of characterisations were carried out to investigate the membranes' hydrophobicity, morphologies and chemistry. Following that, DCMD experiments were conducted to explore the potential of the modified NC and nylon membranes in the desalination of salty water with different salt concentrations of up to 10 wt%. The permeate flux and product quality were compared with commercial PVDF membrane. This work

¹ This chapter has been published Zhang, Y., Chong, J.Y., Zhao, Y., Xu, R., Asakawa, A. and Wang, R. (2023) Facile hydrophobic modification of hydrophilic membranes by fluoropolymer coating for direct contact membrane distillation. *Journal of Membrane Science* 672, 121432. Permission has been granted by the licensed content publisher "Elsevier" to use the published content as a chapter in this thesis.

demonstrated a facile and widely applicable hydrophobic modification method to produce MD membranes with high performance for the desalination of highly salty water.

3.2 Experimental

3.2.1 Materials

A FEVE resin product, LUMIFLON™ LF-200, was supplied by AGC company and its crosslinker, Desmodur® N3300 was supplied by Covestro AG. Xylene (C₈H₁₀, ≥ 98.5% xylenes + ethylbenzene basis) and sodium chloride (NaCl, ≥ 99.0%) were bought from Sigma-Aldrich (Singapore). All chemicals were used as received. Commercial flat-sheet nylon membranes (mean pore size = 0.2 μm) and NC membranes (mixed cellulose esters, mean pore size = 0.22 μm) used as the substrates were purchased from Sterlitech (USA) and Merck Millipore (USA), respectively. PVDF membranes (mean pore size = 0.2 μm) were obtained from Merck Millipore for a comparative study. Deionized water was produced by a Milli-Q® system of Merck Millipore.

3.2.2 Membrane modification

LUMIFLON is a type of FEVE copolymer, which is synthesized by chlorotrifluoroethylene and alkyl vinyl ether through solution polymerization in xylene. Different vinyl ethers, such as ethyl vinyl ether, cyclohexyl vinyl ether and hydroxy butyl vinyl ether can be used in synthesis to introduce different properties to LUMIFLON. Specifically, LUMIFLON LF-200 has a hydroxyl value of 52 mg (KOH)/g polymer, and its structure can be illustrated as Figure 3.1. The rich -OH functional groups in LF-200 allow its crosslinking with polyisocyanate groups in N3300 to form strong urethane bonds, imparting the coating good chemical stability and durability (Štirn et al. 2022). Besides, the use of nonpolar solvent, xylene can prevent the damage of the membrane substrates.

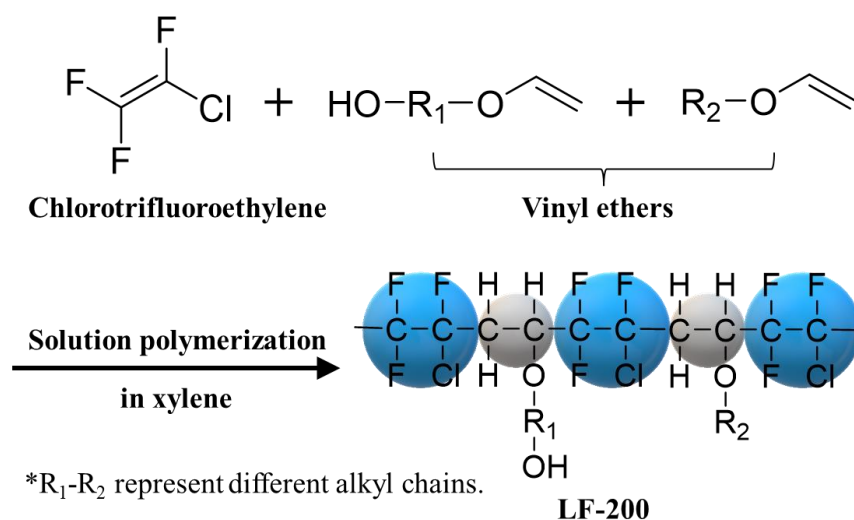


Figure 3.1 Synthesis process and polymer structure of LF-200.

To conduct the modification, a coating solution with certain amount of LF-200 and N3300 in xylene was first prepared followed by a vigorous stirring for 15 min at 60 °C. The concentration of LF-200 was designed as 6, 9, 12, 15 wt% in order to optimize the coating effectiveness, and the amount of N3300 was fixed as 17.8 wt% of LF-200 according to the stoichiometric number of functional groups. After getting a homogenous solution, the pristine nylon or NC membrane was dipped in the coating solution for 10 min to ensure the penetration of the coating solution into the membrane substrates and the complete wetting of membrane pores. After that, the membrane was quickly taken out and air-purged for 3 min to remove the residual coating solution as well as accelerating the xylene evaporation. Lastly, the coated membrane was cured at 70 °C in an oven overnight. The coated membrane was named as nLF-NC/nylon, in which n represents the LF-200 concentration (6, 9, 12, 15 wt%) and NC/nylon means the substrate material.

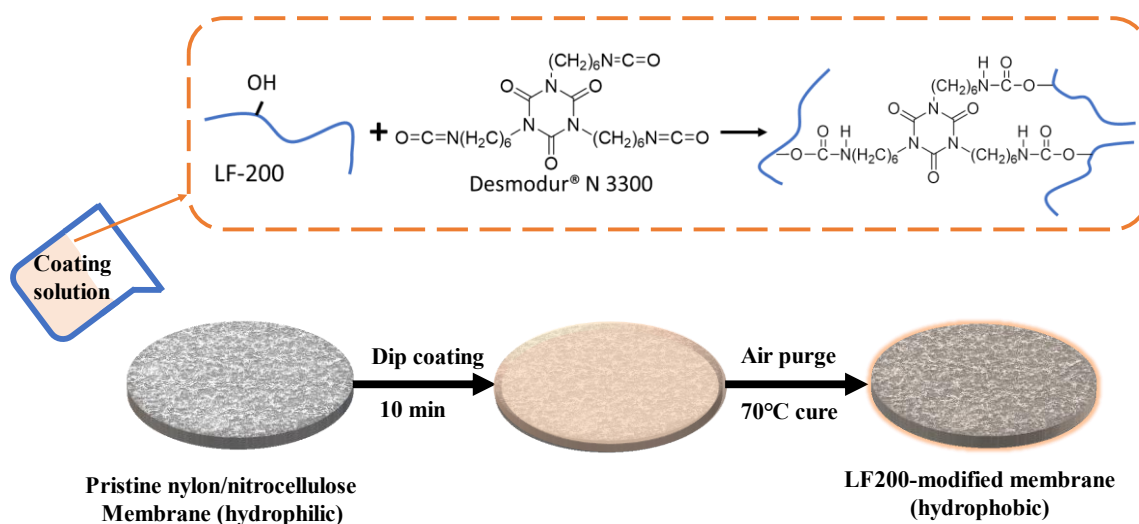


Figure 3.2 Schematic of LF-200 crosslinking mechanism and dip coating procedure.

3.2.3 Membrane characterisations

The morphologies of membrane surface were studied by field emission scanning electron microscope (FESEM, JSM-7200F, JEOL, Japan) and the fluorine scanning spectra of membrane cross-section was obtained by energy-dispersive X-ray (EDX) in low vacuum mode at 10 kV (Chew et al. 2019a). All membrane samples were sputtered by a thin layer of platinum before FESEM and EDX tests. The surface roughness and topography of the respective membranes was characterized through an atomic force microscope (AFM) (XE-100, Park Systems, Republic of Korea) (Chew et al. 2019a). The average surface roughness (R_a) illustrated the roughness of the membrane surface.

To confirm the successful modification of LF-200, the surface compositions of pristine and modified NC membranes were analysed by X-ray photoelectron spectrometer (XPS, AXIS Supra, Kratos Analytical, Japan) with monochromatic Al- $K\alpha$ X-ray source ($h\nu = 1486.6$ eV). The WCA of the pristine and modified membranes were measured using the sessile drop method by a goniometer (Contact Angle System OCA 15EC, DataPhysics, Germany) (Hebbar et al. 2017). During each test, a water droplet with volume of 3 μl was

dropped onto the membrane surface and WCA was measured after 3 min. Each sample was tested for 5 times in different positions.

The mean pore size of the pristine and modified membranes was measured by a capillary flow porometer (CFP 1500A, Porous Material. Inc., USA). Prior to the measurement, the membrane sample was wetted by Galwick[®] ($\gamma \approx 15.9 \text{ mN m}^{-1}$) and nitrogen was used as the displaced gas. Liquid entry pressure of water (LEP_w) was tested in a dead-end filtration cell, where pure water was pressurized by nitrogen with a gradually increased pressure (20 kPa). The pressure when the first droplet spilt out from the cell was recorded as LEP_w . Similar method has been reported in literature (Khayet and Matsuura 2001).

The membrane surface porosity (ε_s , %), considered as the ratio of open pore area on the surface, was calculated from the surface FESEM graph. The membrane bulk porosity (ε_b , %), defined by the ratio of pore volume to the matrix volume, was measured by weighing the pristine membrane and membrane wetted by IPA (Liao et al. 2013a). As the coating layer was extremely thin, so the effect of coating layer was eliminated, and the calculation was based on equation (3-1):

$$\varepsilon_b = 100 \times \frac{(w_w - w_d)/\rho_{ipa}}{(w_w - w_d)/\rho_{ipa} + w_d/\rho_m} \quad (3-1)$$

where w_w and w_d are the weight of dry and wet membrane, ρ_{ipa} and ρ_m are density of IPA and the membrane substrate material, respectively.

3.2.4 DCMD performance tests in saline solution

The lab-scale test rig used for DCMD performance tests has been described in the previous work of our group (Liao et al. 2013b). The tested membrane was fixed in a

stainless-steel membrane cell with an effective area of the was 12.56 cm². Feed stream with different concentration of NaCl was circulated on the feed side by a peristaltic pump (Masterflex, Cole-Parmer, USA) with a flowrate of 220 ml min⁻¹. Milli-Q[®] water was circulated on the permeate side with a flowrate of 120 ml min⁻¹. The inlet temperatures of the feed and permeate streams were kept constant at 60 ± 0.5 °C and 20 ± 0.5 °C, respectively. The overflow from permeate reservoir was collected and weight automatically by an electrical balance. In the long-term test, the collected permeate was returned to the feed tank every 24 hours in order to maintain the stable conductivity of feed solution. The water tanks and tubing were covered with insulating materials to reduce heat loss. The permeate flux (J , kg m⁻² h⁻¹) and salt rejection (R) were calculated as equations (3-2) and (3-3) (Chen et al. 2018a):

$$J = \frac{m}{A \cdot \Delta t} \quad (3-2)$$

$$R = \left(1 - \frac{C_p}{C_f}\right) \times 100\% \quad (3-3)$$

where m is the mass of the collected product (kg), Δt is the time interval (h). C_p and C_f are the concentrations of permeate and feed streams, respectively. After the long-term experiment, respective membranes were washed thoroughly in water with ultrasonication for 10 min and then fully dried in a 60 °C oven. The surface morphologies and WCAs on the feed side of the membranes were tested again to evaluate the stability of the hydrophobic coating.

3.3 Results and discussion

3.3.1 Hydrophobic modification of LF-200

Hydrophobicity is a requisite property of MD membranes to resist the penetration of feed stream into the membrane pores. In order to optimize the membrane hydrophobicity, coating solutions with a concentration of 6, 9, 12, 15 wt% LF-200 were applied to modify

the NC membranes. The WCAs of the respective coated membranes were compared, as shown in Figure 3.2(a). The LF-200 concentration of 6% was too low to obtain sufficient hydrophobicity, and the WCA of the modified membranes reached the peak at $129.0 \pm 1.3^\circ$ at the LF-200 concentration of 12 wt%. The concentrated LF-200 coating solution had a higher viscosity, enabling more polymers to attach on the membrane matrix after air-purging. However, the WCA decreased when the LF-200 concentration further increased to 15 wt%. The thicker coating at high concentration tended to decrease the surface roughness, which in turn reduced the WCA.

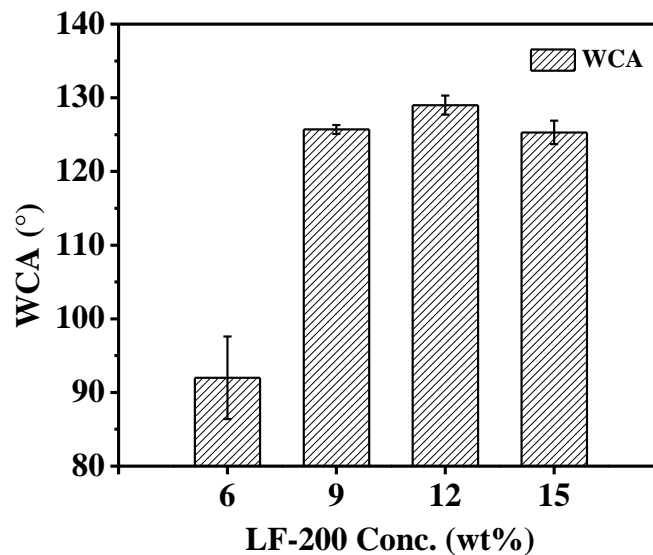


Figure 3.3 WCAs of NC membranes modified by different concentrations of LF-200.

The FESEM images of the surface morphologies and the EDX scanning of the cross-section of the pristine, 9LF-NC and 12LF-NC membranes are presented in Figure 3.4. The pristine NC membrane had a very porous and thin matrix, with no dense skin layer observed. After the modification, some of the porous structures on the surface were covered and this observation was more obvious in the 12LF-NC membrane as more LF-200 polymer was deposited on the membrane. Nevertheless, both modified membranes still preserved porous structures for vapour transport. From the EDX scanning images (Figures 3.4(b2) and (c2)), it could be observed that the fluorine exhibited in the entire cross-section of

modified membrane. It means the hydrophobic modification was not only on the surface but also throughout the whole membrane matrix, which was important to effectively prevent the pore wetting during DCMD.

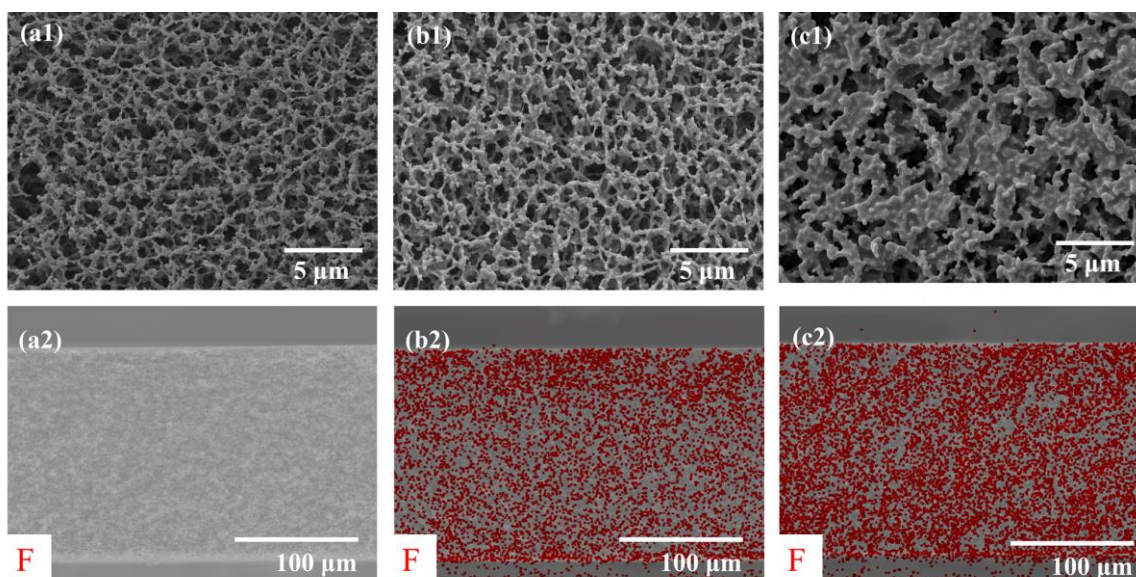


Figure 3.4 (a1, b1, c1) FESEM images of the surface morphologies and (a2, b2, c2) the EDX spectra of fluorine of cross-sections of the pristine NC, 9LF-NC and 12LF-NC membranes, respectively.

To confirm the coating of LF-200 onto membrane and the crosslinking of the coating layer, the XPS spectra of pristine NC and modified-NC membranes were compared in Figure 3.5. From the wide spectra, it was seen that the pristine NC membrane exhibited peaks at ~285, 406 and 532 eV, represented the C1s, N1s and O1s in the NC compounds (Luo et al. 2018). In the case of 12LF-NC membrane, besides the characteristic peaks of NC, it had extra peaks of F1s at 685 eV and Cl2p at 200eV because of the introduction of LF-200 onto the membrane surface. Meanwhile, most of the O and N elements existed on the NC substrate was covered by the coating layer so the O1s and N1s peaks decreased. In the N1s narrow spectra (Figures 3.5(b) and (c)), the pristine NC membrane only showed a peak of the $-(\text{ONO}_2)$ bond at 408.3 eV (Yoshihara and Tanaka 2002) while the 12LF-NC membrane had two extra deconvoluted peaks at 401 and 400 eV, corresponding to the N atoms in the N3300 compounds and polyurethane bonds, respectively (Qaiser and Hyland

2010, Vieira et al. 2019). It implied the existence of a thin layer of polyurethane coating on the membrane as the NO_2 groups of the substrate still could be found. The LF-200 coating layer on the membrane can attach on the membrane surface through physical attachment since the coating was thoroughly modified the membrane matrix. In addition, the rich carboxyl groups in the polyurethane coating allow hydrogen-bonding with the acetate groups in the NC substrate (Yılıgör et al. 2002) or amide groups in the nylon substrate (Fukuda et al. 2017).

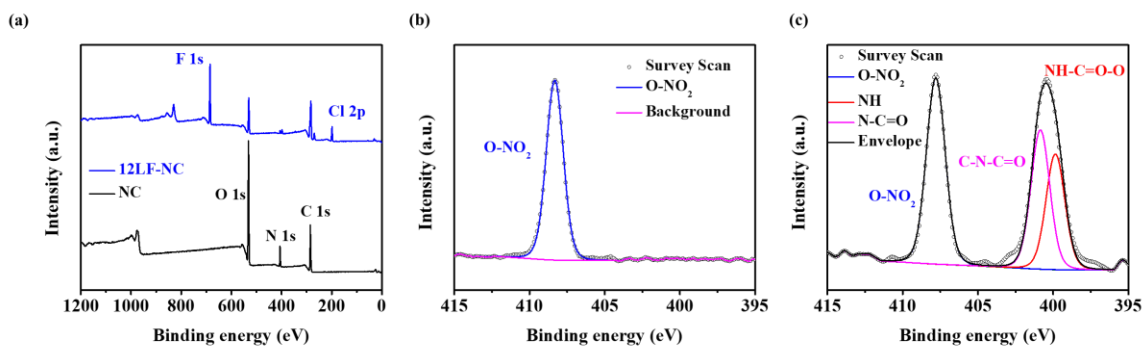


Figure 3.5 (a) XPS wide spectra of pristine NC and modified NC membranes. N1s spectra of (b) pristine NC membrane and (c) modified NC membrane.

Aside from the NC membranes, the fluoropolymer coating was also carried out on the hydrophilic nylon membrane with LF-200 concentration of 12 wt%. Figure 3.6 illustrates the surface morphologies as well as the fluorine EDX spectra of the pristine nylon and 12LF-nylon membranes. Similarly, the modified membrane was also covered by a thin layer of coating and the matrix looked thicker, but the membrane porosity was largely preserved. At the same time, the EDX spectra indicated that the modification was able to cover the entire matrix.

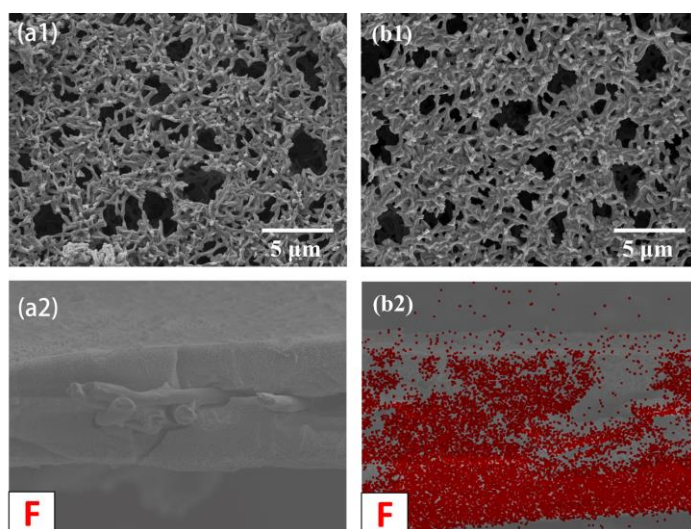


Figure 3.6 (a1, b1) FESEM images of the surface morphologies and (a2, b2) the EDX spectra of fluorine of cross-sections of the pristine nylon and 12LF-nylon membranes, respectively. The matrix near the embedded supporting fibres were very difficult to detect so it looks blank in graph (b2).

Figure 3.7 presents the AFM images and roughness parameters of the modified NC and nylon membranes. The surface roughness of the membranes decreased after the modification, and the decrease was more significant when the concentration of LF-200 solution was higher, which agreed with the observation from the SEM images. Although the reduce of roughness could have a negative effect on the WCA according to the Wenzel's theory (Wenzel 1936), the WCA of the modified membranes 12 LF-NC was still high $\sim 130^\circ$ thanked to the low surface energy of coating layer. Combined with the high LEP_w value ~ 200 kPa for all modified membranes (Table 3.1), it could be confirmed that the modification imparted excellent water repellence to NC and nylon membranes. Apart from the hydrophobicity, the pore size and porosity of membranes are also important to the performance of MD. Table 3.1 showed that the modified membranes had a smaller average pore size after modification, but the decrement was very small (<10 nm). In addition, the increment in membrane thickness is also in the range of $1.3\text{-}3\ \mu\text{m}$ after modification. It was ascribed that the air purge after dip coating removed most coating solution stuck in the pores and only left a thin layer firmly affixed to the membrane matrix. Likewise, the bulk

and surface porosity only decreased <10% after the polymer coating. When compared to the commercial PVDF membrane, the 12LF-nylon membrane generally had a smaller porosity while the modified-NC membranes had a higher surface porosity but a lower bulk porosity.

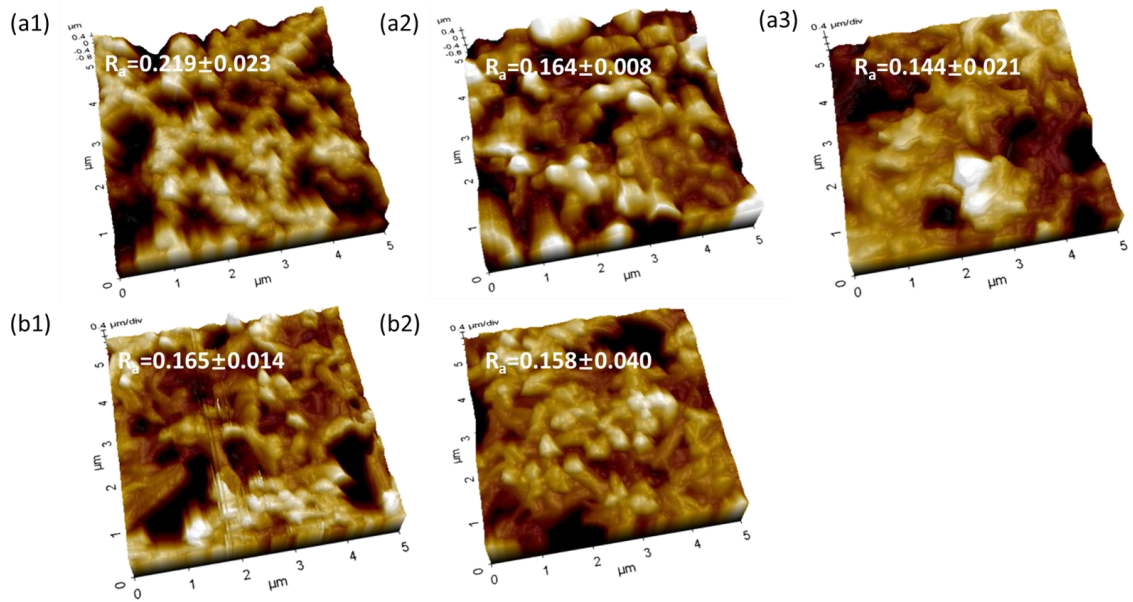


Figure 3.7 AFM 3D profile images of the (a1) pristine NC, (a2) 9LF-NC, (a3) 12LF-NC, (b1) pristine nylon and (b2) 12LF-nylon membranes, respectively.

Table 3.1 Summary of properties of the NC and nylon membranes before and after LF-200 modification.

Membrane	WCA (°)	LEP _w (kPa)	Mean pore size (nm)	Bubble point (nm)	Thickness (μm)	Bulk porosity (%)	Surface porosity (%)
Pristine NC	0.0*	/	262±2.8	540.8±3.3	173.0±1.0	72.5±1.7	51.4±0.8
9LF-NC	125.7±0.6	200±10	257±3.8	536.0±1.1	174.3±0.6	68.1±2.3	48.4±2.0
12LF-NC	129.0±1.3	220±20	256±13.3	531.4±0.4	176.0±0.1	62.0±3.4	41.5±1.5
Nylon	0.0*	/	273.3±6.2	508.2±0.5	130.3±0.6	59.7±3.5	30.3±1.8
12LF-nylon	130.0±0.2	190±10	273.7±1.5	501.1±0.1	133.0±1.7	51.7±5.4	20.6±0.9
PVDF	130.0±0.9	230±10	230.9±3.0	513.9±4.0	210.0±0.1	75.6±3.3	37.2±4.0

* The water droplet completely wicked into membranes within 20 seconds.

In summary, for all the LF-200 modified membranes, the coating layer was thin and uniform all over the membranes with only a small change in the pore size and porosity. The hydrophobicity of the membranes was greatly improved from the extremely hydrophilic state. Table 3.2 summarized the methods of transfer membrane wettability from hydrophilic to hydrophobic in literature. It can be achieved by using special techniques to improve membrane morphology or adding low surface tension modifiers into membranes. However, most of those methods require extra equipment. For instance, a gas stream with non-solvent vapour is needed when membranes are fabricated with VIPS method. Also, only a few of them are able to significantly improve WCA to $\sim 130^\circ$. In comparison, the LF-200 modification not only is simple (dip coating and crosslinking under low temperature), but also has a remarkable improvement in the WCA. The amount of LF-200 used for coating is much less than fabricating a whole membrane with fluoropolymer. Thus, it makes the membrane's more cost-effective and environmental-friendly. Moreover, the modification method works on different substrates, including but not limited NC and nylon. Its broad applicability allows to produce MD membranes with various substrates.

Table 3.2 Hydrophobic coating method of hydrophilic polymeric membranes in recent literatures.

	Membrane substrate	Method	WCA improvement	Ref.
Processing during membrane fabrication	PSf	VIPS	126.0°	(Peng et al. 2013)
	Polyimide	Electro spraying PTFE onto membrane during electrospinning	77° → 150°	(Ju et al. 2020)
	PAI or PEI	Grafting with octadecylamine	75.6° → 108°	(Zhang et al. 2012)
Post-treatment to nascent membrane	PAN	Plasma treatment with 1H, 1H, 2H, 2H-perfluorodecyl methacrylate	45.5° → 132.2°	(Liu et al. 2016a)
	PVC	Dehydrochlorination + free radical graft copolymerization with the addition of an ethyl acrylate (EA) monomer	79° → 95°	(Hussein et al. 2020)
	PES	CF ₄ Plasma treatment	0° → 120°	(Wei et al. 2012)
	PA	UV curable Fluorolink® coating	40° → 140°	(Figoli et al. 2017)
	CA	Irradiated polystyrene-grafting	96°	(Wu et al. 1992)
	NC	Plasma polymerization	115°	
	NC	LF-200 dip coating followed by thermal crosslinking	0° → 129°	This work
	Nylon		20° → 130°	

3.3.2 Membrane Performance in DCMD Tests

The modified hydrophobic membranes were applied for DCMD for desalination and their performance was first tested with 3.5 wt% NaCl feed solution for 24 h. The 9LF-NC, 12LF-NC, 12LF-nylon membranes were selected due to their high WCA and their DCMD performance was compared to the commercial PVDF membranes. Figure 3.8 showed the permeate flux and salt rejection of each membrane over time. During all the DCMD tests, the permeate conductivity was very stable, with negligible change $<1 \mu\text{S cm}^{-1}$ after 24 h. It would be conservative to say that all membranes' rejection was nearly 100%. In addition, the fluxes in all tests did not show a downward trend though there were fluctuations. The average fluxes of 9LF-NC, 12LF-NC and PVDF membranes were 14.2,

12.1 and 12.6 kg m⁻² h⁻¹, respectively. Among them, the 9LF-NC membrane presented a higher flux than the other two membranes because it had a smaller membrane thickness and low wettability (Table 3.1), which were beneficial to mass transfer. It also had a slightly larger pore size and surface porosity to provide larger area for water vapour evaporation (Zhang et al. 2021b, 2022). Meanwhile, the 12LF-NC membrane also had a similar flux with PVDF, contributed by its smaller thickness, slightly larger pore size and surface porosity. In case of the 12LF-nylon membrane, the effect of low porosity was very obvious. Even though it possessed a similar WCA and a smaller thickness compared with other membranes, it exhibited a much lower flux of 6.3 kg m⁻² h⁻¹. Considering the relatively lower flux of 12LF-nylon membrane, the following study will only put the emphasis on the modified NC membranes.

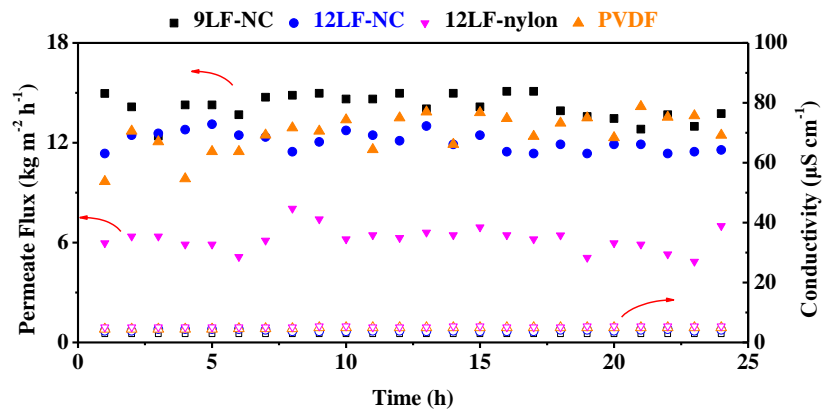


Figure 3.8 DCMD performances of the 9LF-NC, 12LF-NC, 12LF-nylon and commercial PVDF membranes in 3.5 wt% NaCl solution Filled symbols represent permeate flux and hollow symbols represent conductivity. ($T_f=60$ °C, $T_p=20$ °C, $Q_f=220$ ml min⁻¹, $Q_p=120$ ml min⁻¹).

The 9LF-NC, 12LF-NC and commercial PVDF membranes were continued in long-term DCMD experiments feeding with 10 wt% NaCl. The desalination of feed solution with such a high osmotic pressure (~8400 kPa) is a dilemma to RO process. However, the constraint can be overcome by MD process since it is insensitive to the feed's osmotic pressure. Figure 3.9 depicts the permeate flux and the permeate conductivity over time. The DCMD performance of both of PVDF and 12LF-NC membranes were stable over 120

hours, with a very slightly increment in the permeate conductivity. Their flux both decreased compared to the performance in 3.5 wt% NaCl. This was because the higher salt concentration decreased the water vapour pressure and caused more severe concentration polarization (Ameen et al. 2020). Surprisingly, the flux decrement of 12LF-NC membrane (18.5%) was lower than PVDF membrane (38.8%). It may be related with the different structure and property of membrane substrate, leading to a different driving force in DCMD. For the 9LF-NC membrane, it was not as durable as the 12LF-NC membrane though it did work well in the baseline test. The increasing permeate conductivity from 3.9 to 16.1 $\mu\text{S cm}^{-1}$ after 74 h showed a sign of salt leakage from the feed side to the permeate side. The salt leakage in MD process can be caused by either the small droplet entrained in water vapour or membrane pore wetting caused by the lower WCA and water repellence of the 9LF-NC membrane (Rezaei et al. 2017). As the feed flowrate was higher relative to the permeate, the partial wetting of membrane pores and the consequent formation of water bridges may lead to a slight increase in permeate flux, despite the reduction in evaporation areas.

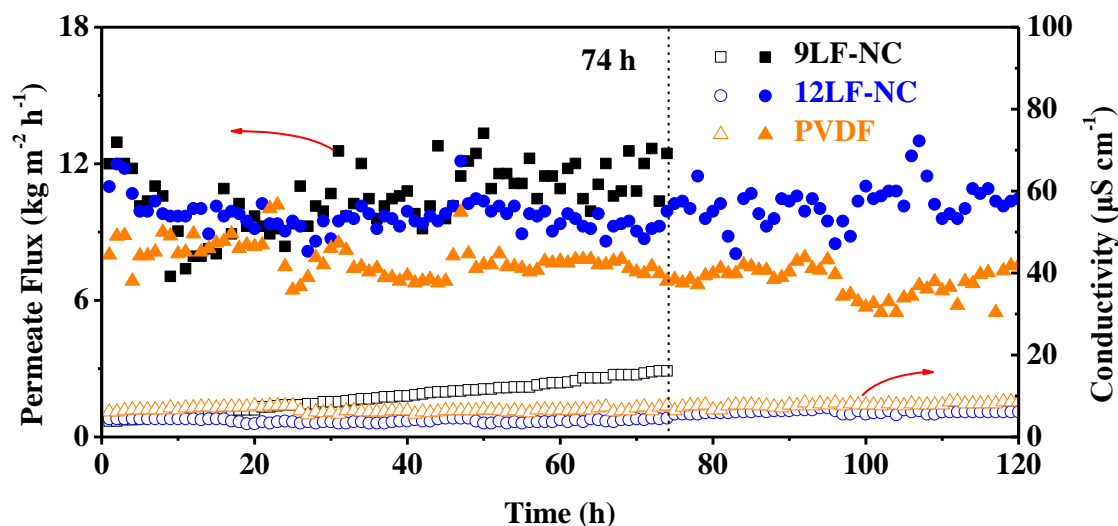


Figure 3.9 Long-term DCMD performances of 9LF-NC, 12LF-NC and commercial PVDF membranes with 10 wt% NaCl feed solution. Filled symbols represent permeate flux and hollow symbols represent conductivity. ($T_f=60\text{ }^\circ\text{C}$, $T_p=20\text{ }^\circ\text{C}$, $Q_f=220\text{ ml min}^{-1}$, $Q_p=120\text{ ml min}^{-1}$).

To study the stability of the hydrophobic coating, the WCAs of the 12LF-NC and PVDF membranes was measured again after the long-term DCMD. As shown in Figure 3.10, the WCA of the modified membrane after 144 hours DCMD run remained at a high value of $127.7 \pm 2.9^\circ$. Compared to the commercial PVDF membrane, the decrement was much smaller. This result was a good proof of the persistence of the coating layer and the sufficient adhesion between the coating and substrates.

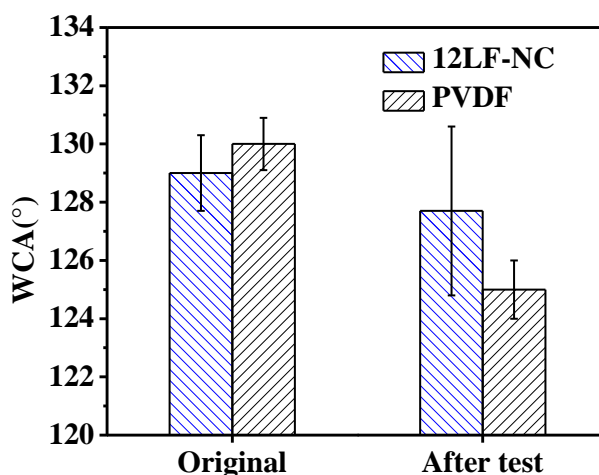


Figure 3.10 WCAs of 12LF-NC and PVDF membranes measured before and after test, respectively.

Table 3.3 compares the MD performance of the LF-200 coated NC membranes with other flat sheet membranes. Both the 9LF-NC and 12LF-NC membranes have a rejection $>99.99\%$ when treating 3.5% NaCl feed, which outperformed many commercial hydrophobic polymeric membranes. Compared to other modified membranes, the LF-200 coated NC membranes is still very competitive in permeation flux and rejection considering its facile modification process. Furthermore, in the case of 10 wt% NaCl feed solution, the 12LF-NC membrane showed an outstanding performance over 120 h while most of the other membranes were only challenged with a lower NaCl concentration for a short time. Its durability allows its application in the brine water that has high salinity and make good use of the unique character of MD.

Table 3.3 The DCMD performance of modified membranes in this work compared with other membranes in recent literatures.

	Membrane	WCA (°)	Feed/Permeate Temperature (°C)	NaCl conc. (wt%)	Flux (kg m ⁻² h ⁻¹)	Performance	Ref.
Made of hydrophobic polymer	PVDF (co-casting)	130.0	60/20	3.5	24	Conductivity increased from 7 to 10 $\mu\text{S cm}^{-1}$ in 48 h	(Tian et al. 2021)
	PVDF-HFP	89.3	60/18.5	3.5	16.1	99.3%	(Fadhil et al. 2016)
	PVDF (Millipore, GVHP)	120.0	59/20	3.5	8.4	/	(Bouchrit et al. 2015)
				10.0	3.7	/	
	PTFE (CHMLAB)	114.0	60/20	3.5	13.0	>99.97%	(Ameen et al. 2020)
10.0				10.0			
PVDF (Merck Millipore)	130.0	60/20	3.5	12.6	Stable conductivity	This work	
			10.0	7.7			
Made of hydrophilic polymer	PA modified by PFPE	140.0	50/15	3.5	11.0	99.6% for 12 h	(Figoli et al. 2017)
	DHPVC-g-PEA	90.0	65/20	3.5	19.3	99.9%, 80 h	(Hussein et al. 2020)
	Polystyrene-grafted CA	78.4	60/25	0.5 M	2.4	99.1%	(Wu et al. 1992)
	Vinyltrimethylsilicon/CF ₄ plasma-treated NC	115.0	70/25	0.5 M	30.3	99.9%	
	9LF-NC	125.0	60/20	3.5	14.0	>99.99% for 24 h	This work
	12LF-NC	129.0	60/20	3.5	12.1	>99.99% for 24 h	
				10.0	10.1	Stable conductivity over 120 h	

3.4 Conclusions

This work successfully developed a facile hydrophobic modification method that could transform the originally hydrophilic NC and nylon membranes into hydrophobic membranes. Fluoropolymer LF-200 was coated on the entire surface of the membrane matrix through a simple dip coating approach, and crosslinking of the polymers was carried out via low temperature heat treatment. The modified membranes have high WCA ($>125^\circ$) and LEP_w (~ 200 kPa), with their porous microstructure largely preserved. The membranes are applicable in DCMD, treating high-salinity feed solutions with NaCl concentration up to 10 wt%. The 12LF-NC membrane showed excellent flux of $10.1 \text{ kg m}^{-2} \text{ h}^{-1}$ in the treatment of 10 wt% salt water, which is 31% higher than the commercial PVDF membrane. Also, the conductivity was stable over 120 h, showing no sign of membrane wetting. The good MD performance is attributed by the highly porous structure of the pristine hydrophilic membrane and the uniform hydrophobic layer throughout the matrix imparted by the LF-200 coating. In comparison to other hydrophobic modification method, this method is superior in the facile operation and versatility in different hydrophilic substrates without the use of plasma or irradiation. The remarkable performance of 12LF-NC membrane also strongly elucidates the potential of the MD membranes for the treatment of high-salinity water.

This page is intentionally left blank

Chapter 4 Effective Separation of Water-DMSO through Solvent Resistant Membrane Distillation²

4.1 Introduction

Chapter 3 introduces a hydrophobic modification method viable for different substrates. The method is simple and effective in transforming hydrophilic membranes into hydrophobic membranes. However, the matrixes of the membranes and LF-200-modified layer are solvent-sensitive polymer materials for strong organic solvents, which limit MD application in solvent-containing wastewater. In this Chapter, we continue to follow the simple surface modification method and broaden MD application to another kind of challenging wastewater, which contains a high concentration of organic solvents with high boiling points, such as DMF, DMSO, and NMP. Therefore, a more suitable membrane, combining ceramic membrane and fluorinated surface modification, was used in this study. Also, the influence of membrane pore size and structure, organic solvent concentration, and the transport mechanisms are thoroughly studied.

Here, DMSO is selected as the target foulant. It is a comparatively green dipolar aprotic organic solvent because of its low toxicity and good stability (Alder et al. 2016, Xiang et al. 2017). DMSO has been frequently used as a reactant or a reaction medium in the production of pharmaceuticals and waste containing a high concentration of DMSO is often a challenge to conventional sewage plants (Mountford 2010). Both chemical and biological treatments carry their drawbacks: the advanced oxidation process, such as Fenton oxidation is costly while the biological treatment is inhibited by the toxic intermediate products and releases an unpleasant odour from dimethyl sulfide (Cheng et al.

² This chapter has been published Zhang, Y., Chong, J.Y., Xu, R. and Wang, R. (2021) Effective separation of water-DMSO through solvent resistant membrane distillation (SR-MD). *Water Research* 197, 117103. Permission has been granted by the licensed content publisher "Elsevier" to use the published content as a chapter in this thesis.

2009, He et al. 2011). In fact, wastewater with high DMSO content is difficult to be treated in bioreactors because of the biological effect caused by the invasion of DMSO into microorganisms (Smallwood 2002). The upper limit of DMSO concentration for microbial acclimation in biological processes is often reported in the range of 0.10-0.15 wt% (Cheng et al. 2019, Hwang et al. 2012, Yang and Myint 2003). Meanwhile, incineration is another common method used to treat these wastes, but it has a large carbon footprint and a risk of releasing harmful gases and particulates into the atmosphere (Chea et al., 2020, Seyler et al., 2006). For these issues, the separation of solvent-water mixtures is important to reduce the volume and improve the treatability of solvent-containing waste streams.

SR-MD is highly desirable for treating water-DMSO mixtures. With a boiling point of 189 °C, DMSO has a lower vapour pressure compared to water. For instance, the vapour pressure of pure DMSO is only 0.7 kPa, while that of water is 19.9 kPa at 60 °C (Nishimura et al. 1972). Thus, the vapour condensed subsequently on the permeate side of the MD membrane will have a low DMSO proportion. Ceramic membranes are selected in this study because of their intrinsic solvent-resistant property and good stability in harsh environments. Previously, Kujawski et al. applied modified ceramic membranes to separate dilute ethyl acetate solution, with a concentration up to 4 wt% (Kujawski et al. 2016). The performance of MD was found to be comparable with PV and the separation factor of ethyl acetate was in the range of 32-60. Besides separating light solvents, hydrophobic ceramic membranes can potentially be used to separate water from heavy solvents through SR-MD. Nevertheless, the application of SR-MD in a broader solvent concentration and for a longer operating time is still understudied.

In this work, we proposed SR-MD as a novel and effective alternative for separating water from solvents with high boiling points. DMSO was selected in this study because of

its relatively low toxicity and increasing use in the industry (Alder et al. 2016, Xiang et al. 2017). Hydrophobic ceramic membranes were modified by grafting FAS onto the substrates, and then their performance in water-DMSO separation was examined by a series of VMD experiments. The effects of feed concentration, temperature and membrane structure were studied in order to understand the separation and transport mechanisms in the SR-MD process. Moreover, a commercial PV membrane was used to separate the water-DMSO feed stream, and the results were compared with the counterparts of the SR-MD process. This study aims to demonstrate the effectiveness of SR-MD in separating water-DMSO mixtures over a wide range of DMSO concentrations and facilitate SR-MD applications for other water-solvent systems associated with high boiling point solvents.

4.2 Experimental

4.2.1 Materials

Three types of alumina ceramic tubular membranes from Coorstek B.V. (Netherlands) were used as the membrane substrates. They were named as 20-ASY, 200-ASY, 200-SYM according to their pore size (20 or 200 nm) and matrix structures (symmetric or asymmetric) as illustrated in Figure 4.1. The alumina substrates have an average outer diameter of 4.5 mm and an average inner diameter of 3 mm. Hydrophobic PTFE hollow fibre membranes with average pore size of 112 nm, bubble point pore size of 361 nm and dynamic WCA of 106° were kindly supplied by a commercial company. They were tested for MD to compare with the modified ceramic membranes. Hybrid Silica HybSi[®] AR tubular membranes were purchased from Pervatech B.V. (Netherlands) were tested for PV as a comparative study. This kind of hybrid silica PV membranes are hydrophilic, made of α -Al₂O₃ support layer and a hybrid silica selective layer with Si-C_mH_n-Si bonds (van Veen et al. 2011). They have been widely employed in the dehydration

of different water-solvent mixtures, such as NMP, n-butanol, IPA, ethanol, and butyraldehyde (Agirre et al. 2011, Klinov et al. 2017, van Veen et al. 2011).

DMSO was purchased from Merck Millipore (Singapore). 1H,1H,2H,2H-perfluorodecyltriethoxysilane ($C_{16}H_{19}F_{17}O_3Si$, 97%) (FAS-F17), methanol (CH_3OH , $\geq 99.9\%$), were bought from Sigma-Aldrich (Singapore). All chemicals were used as received. Deionized water was produced by a Milli-Q[®] system of Merck Millipore (USA).

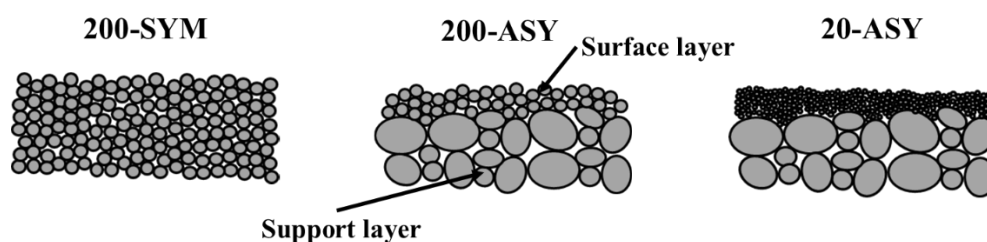


Figure 4.1 Schematic of three membrane substrates.

4.2.2 Hydrophobic grafting of ceramic membranes

The hydrophobic grafting of ceramic membranes is similar to the method reported by other research groups (Koonaphapdeelert and Li 2007, Kujawski et al. 2007). Firstly, the virgin ceramic membranes were immersed in an ultrasonic water bath for at least 10 min to remove contaminants beforehand. After drying in an oven at 60 °C for overnight, the ceramic membranes were then immersed into the grafting solution at 30 °C for 2 h, which was prepared by dissolving 2 wt% FAS-F17 in methanol. Then, the membranes were washed in an ultrasonic methanol bath followed by drying in air for 1 h and in an oven at 110 °C for 1 h. After taking out from the oven, the same grafting and drying processes were conducted once again to enhance the grafting efficiency. The modified membranes were named as 20-mASY, 200-mASY and 200-mSYM accordingly. The schematic of grafting reaction among the FAS-F17 molecules and ceramic membranes is shown in Figure 4.2.

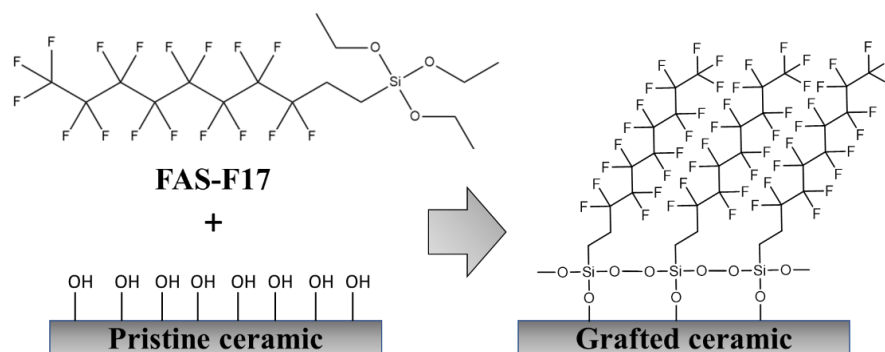


Figure 4.2 Schematic of grafting reaction.

4.2.3 Membrane characterisations

The characterisation methods of surface morphologies, porosity, average pore size, PSD, WCA, roughness, chemical bonds can refer to section 3.2.3. Solvent contact angles (SCA) and solvent entry pressure (LEP_s) were also tested with methods similar to WCA and LEP_w tests but used DMSO instead of water, respectively. In the tests of WCA and SCA, the displays of liquid droplets were captured by a camera and the degree formed by the tangent lines of the droplet and the inner circle of membranes was measured. In addition, the contact angles tests were performed after the modified membranes were immersed in pure DMSO at room temperature for 14 and 30 days, to evaluate the linkage stability of the hydrophobic chains on the membranes.

4.2.4 VMD performance tests in water/DMSO solution

A series of VMD tests were conducted on the modified ceramic membranes and the diagram of the setup used is shown in Figure 4.3. Membrane modules with an effective length of 0.18 m were used in this study. During the VMD tests, the feed solution was heated up to 60 °C unless otherwise stated, with a flow rate of 170 ml min⁻¹ through the lumen of the membranes. A vacuum condensation system was applied in the shell side of the membranes to control the vacuum level at 5 kPa. The generated permeate stream was

extracted from the system by a vacuum pump (RV3, Edwards, UK) and was condensed in a glass condenser cooled by liquid nitrogen. The 24 hours test was conducted 8 hours for three days as the experiment setup could not be left on overnight. In the interval time, the membrane module was left in air without drying.

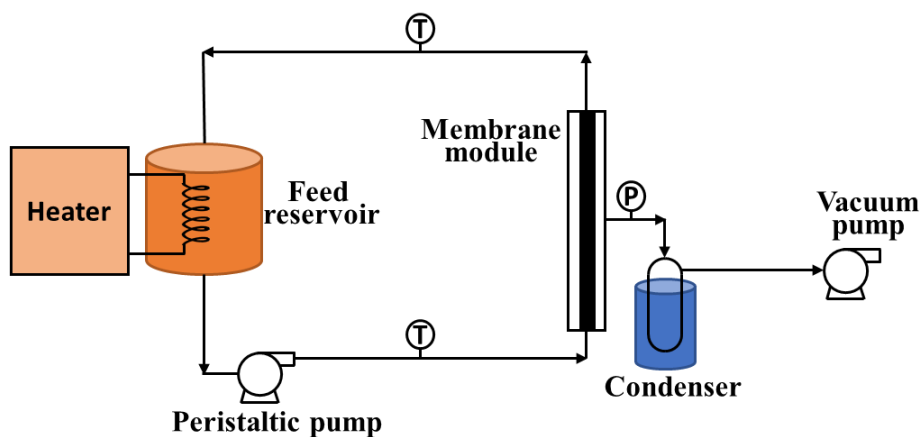


Figure 4.3 Schematic of SR-MD experimental setup.

The collected product was weighed by a mass balance and its DMSO concentration was measured by a gas chromatography equipped with a flame ionization detector (7890 GC System, Agilent Technologies, USA). The permeate flux (J) was calculated by equation (4-1):

$$J = \frac{m}{\pi \cdot d \cdot l \cdot \Delta t} \quad (4-1)$$

where m is the mass of the collected product, Δt is the time interval, d is the inner diameter of the membrane, l is the effective length of membrane contacting feed stream.

The separation performance was evaluated by DMSO rejection (R) and separation factor (α), which were presented as equations (3-3) and (4-2), respectively:

$$\alpha = \frac{c_{p,1}/c_{p,2}}{c_{f,1}/c_{f,2}} \quad (4-2)$$

where $c_{p,1}$ and $c_{p,2}$ are the weight fractions of water and DMSO in permeate, $c_{f,1}$ and $c_{f,2}$ are the weight fractions of water and DMSO in feed, respectively.

4.2.5 Separation mechanism of water/DMSO solution

To evaluate the separation performance of VMD, it is necessary to analyse the transport mechanisms of water/DMSO mixtures. During the VMD process, vapour-liquid interface is formed on the membrane surface, as illustrated in Figure 4.4. The feed solution undergo an evaporative phase change near the pore entrance and the vapour transports across the membrane driven by the pressure difference across membrane. Since there is vacuum on the permeate side, the permeate partial pressure (p_0) can be considered as zero. Different from VMD in desalination where the salt solute is non-volatile, both water and DMSO will evaporate at the vapour-liquid interface so the DMSO partial pressure also contributes to vapour pressure on the feed side (p_f). Thus, the driving force (ΔP) can be obtained by:

$$\Delta P = p_f - p_0 = p_1 + p_2 \quad (4-3)$$

where p_1 and p_2 are the partial vapour pressure of water and DMSO, respectively.

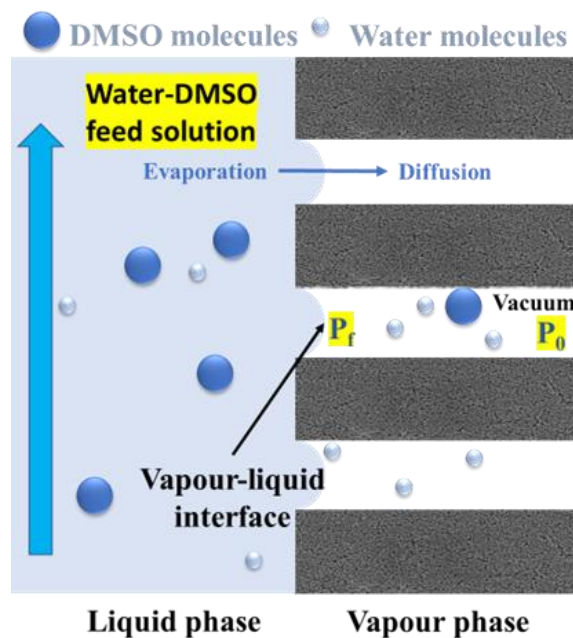


Figure 4.4 Schematic of transport mechanisms.

To obtain the proportion of components in vapour phase, it is necessary to know the VLE state of the feed solution. Wilson activity model was used because it is suitable for non-ideal liquid mixtures and only requires two parameters independent of temperature and compositions (Van Ness et al. 1996). Based on this model, the activity coefficients of water (γ_1) and DMSO (γ_2) are calculated as:

$$\ln\gamma_1 = -\ln(x_1 + \Lambda_{12}x_2) + x_2\left(\frac{\Lambda_{12}}{x_1 + \Lambda_{12}x_2} - \frac{\Lambda_{21}}{x_2 + \Lambda_{21}x_1}\right) \quad (4-4)$$

$$\ln\gamma_2 = -\ln(x_2 + \Lambda_{21}x_1) + x_1\left(\frac{\Lambda_{21}}{x_2 + \Lambda_{21}x_1} - \frac{\Lambda_{12}}{x_1 + \Lambda_{12}x_2}\right) \quad (4-5)$$

$$\Lambda_{12} = \frac{V_2}{V_1} \exp\left(-\frac{(g_{21} - g_{11})}{RT}\right) \quad (4-6)$$

$$\Lambda_{21} = \frac{V_1}{V_2} \exp\left(-\frac{(g_{12} - g_{22})}{RT}\right) \quad (4-7)$$

$$\frac{(g_{21} - g_{11})}{R} = -555.6 \quad (4-8)$$

$$\frac{(g_{12} - g_{22})}{R} = 116.8 \quad (4-9)$$

where x_1 and x_2 are mole fraction in feed solution; Λ_{12} and Λ_{21} are parameters of the equations; V_1 and V_2 are the molar volumes; $(g_{21} - g_{11})$ and $(g_{12} - g_{22})$ are interaction energy constants of water and DMSO, respectively; R is the gas constant and T is the temperature. Here, molar volumes of components at feed temperature are determined based on the density reported by Pruett et al. (Pruett and Felker 1985) and the interaction energy constants are obtained from a study of water-DMSO binary system (Li 2010). Based on the vapour composition on the feed side, the theoretical DMSO concentration in permeate ($C_{p,est}$) and DMSO rejection (R_{est}) can be estimated.

$$p_1 = \gamma_1 x_1 p_1^0 \quad (4-10)$$

$$p_2 = \gamma_2 x_2 p_2^0 \quad (4-11)$$

$$C_{p,est} = \frac{p_2 M_2}{p_1 M_1 + p_2 M_2} \quad (4-12)$$

$$R_{est} = 1 - \frac{C_{p,est}}{C_f} \quad (4-13)$$

where p_1^0 and p_2^0 are the vapour pressure of the pure water and DMSO at certain temperature calculated from Antoine empirical equation (Nishimura et al. 1972). M_1 and M_2 are the molar mass of water and DMSO, respectively.

4.3 Results and discussion

4.3.1 Surface hydrophobic modification of ceramic membranes

Three types of ceramic tubular membranes were used as the substrate: 20-ASY, 200-ASY and 200-SYM, and their pristine properties were first examined before the hydrophobic modification. Figs. 3.4a and 3.4b show the characterisation of their pore sizes. The 200-SYM and 200-ASY membranes have an average pore size of 228 and 218 nm, respectively, and a fairly narrow PSD. The 20-ASY membrane has a much smaller average pore size, which is hardly measured using the gas-liquid porometry. Instead, the molecular weight cut-off (MWCO) was evaluated by measuring the dextran rejection. The 20-ASY membrane has an MWCO of 94 kDa, and the pore size was estimated to be about 12.8 nm (Ren et al. 2006). Figure 4.5(c) shows their structure characteristics: the 200-SYM membrane has a homogeneous pore structure while the 200-ASY and 20-ASY membranes have a surface layer of about 20 and 10 μm , respectively.

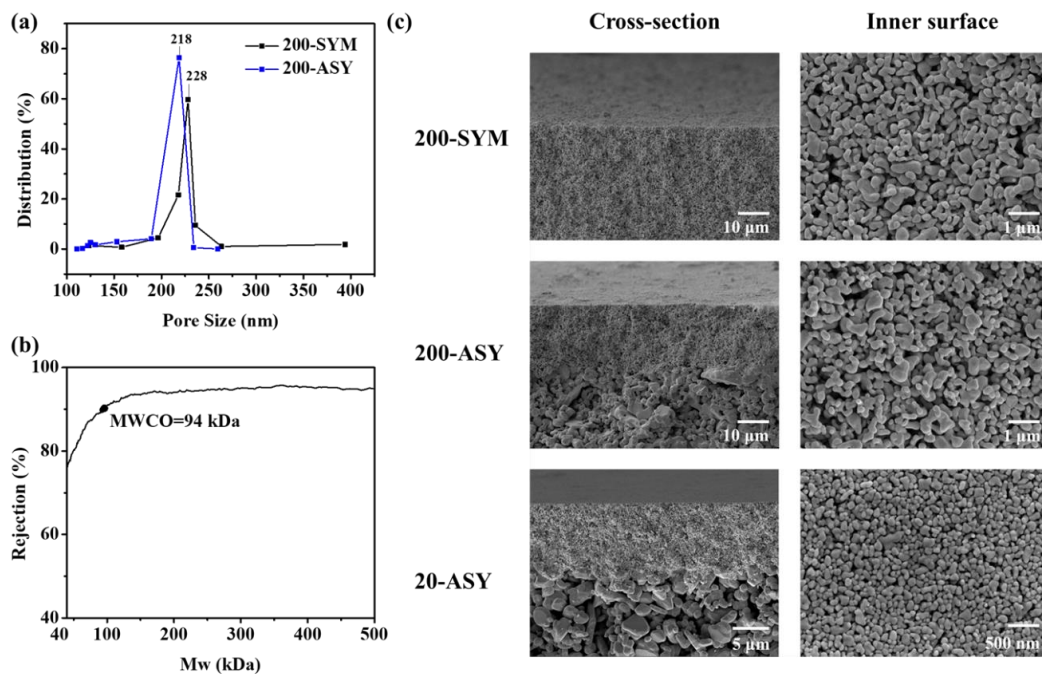


Figure 4.5 (a) PSD of the 200-ASY and 200-SYM membranes obtained using the gas-liquid porometry. (b) MWCO of the 20-ASY membranes. (c) FESEM images of the cross-section and inner surface morphologies of three ceramic substrates.

The inner surface morphologies of the modified membranes, 200-mSYM, 200-mASY and 20-mASY are shown in Figure 4.6. Compared with the pristine membranes shown in Figure 4.6(c), it can be concluded that the surface morphologies had no significant change after the chemical grafting, as the grafting step only imparted a molecular layer of perfluorinated chains to the membrane surface. Similar observations were reported in previous studies associated with FAS-F17 grafting (García-Fernández et al. 2017, Koonaphapdeelert and Li 2007, Zhong et al. 2017).

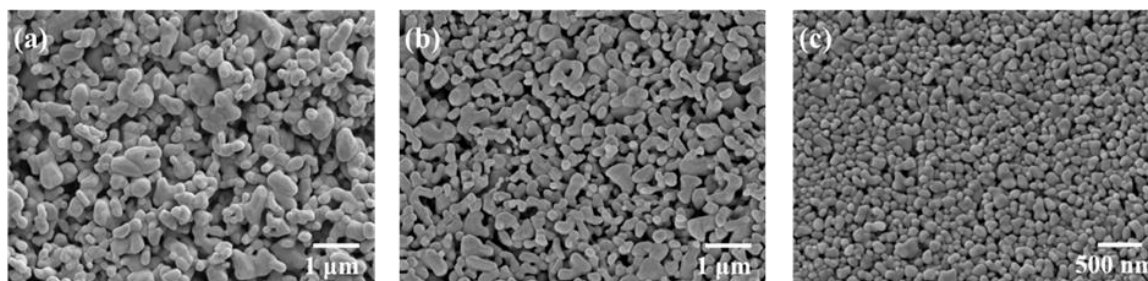


Figure 4.6 FESEM images of the inner surface morphologies of the (a) 200-mSYM, (b) 200-mASY, and (c) 20-mASY membranes.

XPS scan was carried out to analyse the elements on the surfaces of the 20-ASY, 20-mASY and 20-mASY-30d membranes. The 20-mASY-30d refers to the sample that has been immersed in pure DMSO for 30 days to evaluate the stability of the hydrophobic modification. As shown in Figure 4.7, the 20-mASY membrane spectra clearly shows the characteristic peaks of silicon (Si) and fluoride (F) in addition to carbon (C), oxygen (O) and aluminium (Al), while the 20-ASY membranes are lack of Si and F element. It suggests the successful grafting of FAS-F17 (Koonaphapdeelert and Li 2007). For the O signals, both Si-O bonds and oxygen in Al₂O₃ lattice can be detected at the range of 531.6 and 533.2 eV, respectively. Furthermore, the 20-mASY-30d membrane has similar characteristic peaks and spectrum as the 20-mASY membrane, indicating good stability of the hydrophobic grafting.

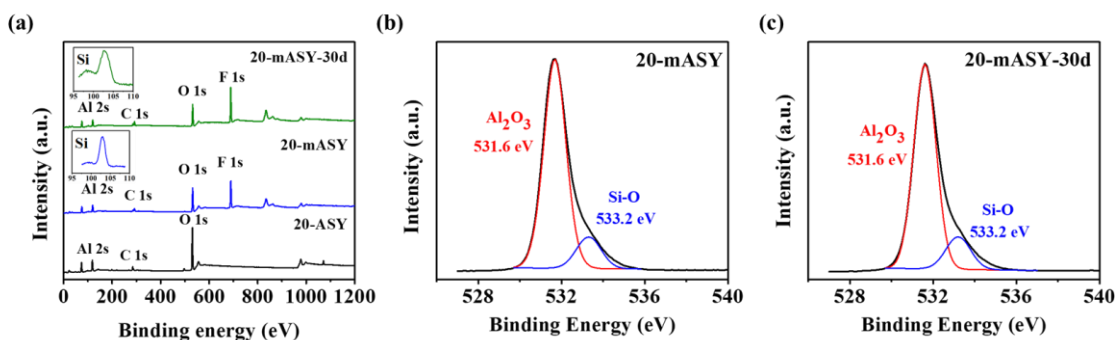


Figure 4.7 (a) XPS spectra of the 20-ASY membranes, 20-mASY and 20-mSYM-30d membranes. (b) O signal of 20-mASY membranes, (c) O signal of 20-mASY-30d membranes.

To determine the surface wettability of the grafted membranes, the contact angles of the membranes were tested and the results are depicted in Figure 4.8. It can be seen that the newly modified (0 d) 200-mASY and 200-mSYM membranes have similar WCA >150° and SCA >118°. The lower SCA was ascribed to the lower surface tension of DMSO compared to water (Lide 2004). Meanwhile, the 20-mASY membrane possesses slightly smaller contact angles than the membranes with larger pore sizes but still shows high hydrophobicity. Though the grafting method used in all three membranes was identical, the

difference in the apparent contact angles of hydrophobic surfaces could be contributed by the difference in surface roughness. Table 4.1 shows the surface roughness parameters of three modified membranes obtained from AFM. The 200-mASY and 200-mSYM membranes have much higher surface roughness, which can contribute to higher apparent contact angles than the 20-mASY membranes. Moreover, the grafted membranes also show good stability in solvent environment, evidenced by the stable contact angles after immersing in pure DMSO for 14 and 30 days. Although there were slight decrements, all modified membranes maintained good hydrophobicity, with WCA $>144^\circ$ and SCA $>110^\circ$ after 30 days.

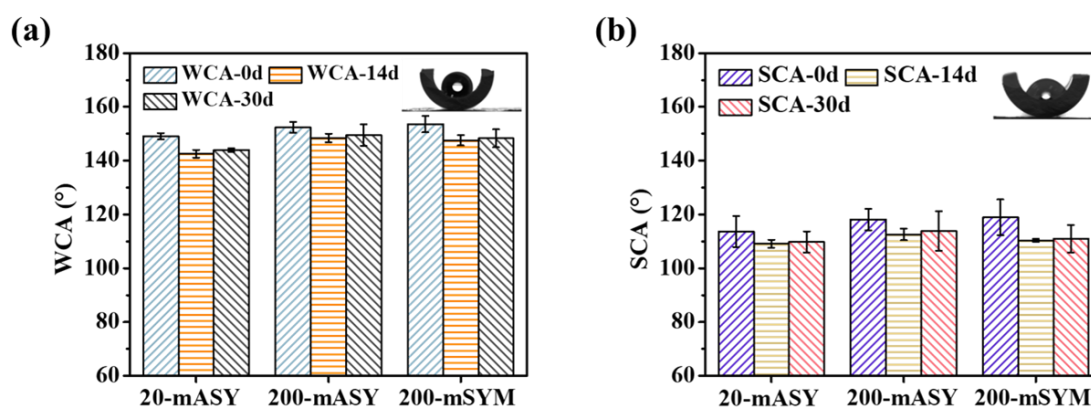


Figure 4.8 (a) WCA and (b) SCA of the 20-mASY, 200-mASY and 200-mSYM membranes submerging in DMSO for 0, 14 and 30 days.

The results of LEP_w and LEP_s in Table 4.1 are in good agreement with the contact angle tests. Before hydrophobic grafting, the ceramic membranes are extremely hydrophilic and both water and DMSO would disperse and penetrate into the pores quickly. However, after the grafting process, the modified membranes possess high $LEP_w > 220$ kPa and $LEP_s > 84$ kPa, which are much higher than the operating pressure in SR-MD. The good hydrophobicity and high liquid entry barrier can prevent the modified membranes from being wetted by the feed solution, especially when the feed contains high concentration of solvent.

Table 4.1 Contact angles and liquid entry pressures of grafted membranes.

Membranes	LEP _w (kPa)	LEP _s (kPa)	Surface roughness parameters	
			R _a ^a (nm)	R _q ^b (nm)
20-mASY	272.3±4.8	89.0±16.5	15.4	19.3
200-mASY	247.5±9.0	84.1±2.8	86.3	109.3
200-mSYM	220.0±24.1	104.8±24.1	126.8	157.9

^a Average roughness.

^b Root-mean-square roughness.

4.3.2 VMD performance in water-DMSO system

4.3.2.1 Feed stream with various DMSO concentrations

To study the feasibility of applying the modified ceramic membranes for SR-MD to separate water-DMSO mixtures, the 200-mSYM membranes were first tested with 3.5-85 wt% DMSO feed streams at 60 °C. As presented in Figure 4.9(a), the permeate flux was as high as 7.3 kg m⁻² and DMSO rejection reached 99.7 % at the DMSO concentration of 3.5 wt%. However, both the permeate flux and the solvent rejection decreased with increasing DMSO concentration in the feed. When feed DMSO concentration was 85 wt%, the permeate flux and DMSO rejection was only 1.7 kg m⁻² h⁻¹ and 88.4%, respectively. Figure 4.9(b) indicates the impact of feed DMSO concentration on the permeate purity and the separation factor. Generally, when DMSO in the feed stream became more concentrated, the DMSO concentration in the permeate increased slightly, too. This trend became more distinct when the DMSO concentration in the feed was higher than 65 wt%. As for the separation factor, it reached the best value of 284.4 at 3.5 wt% and remained fairly constant at about 170 when the feed DMSO concentration was between 20 and 65 wt%. Nevertheless, it decreased significantly when the feed concentration was higher than 65 wt%. The transport behaviours of water and DMSO permeation across the membranes was analysed to explain the experiment results. As depicted in Figure 4.4, the driving force in MD process was the vapour pressure difference across membrane ($p_f - p_0$) and highly dependent on the VLE state of the solution. Figure 4.9 shows the driving force of the system

under different DMSO concentrations. It could be seen a decrement of vapour pressure difference from 19.5 kPa to 1.9 kPa when the feed DMSO concentration went up from 3.5 to 85 wt%. The reduced driving force resulted in the decreasing permeate flux in Figure 4.9(a).

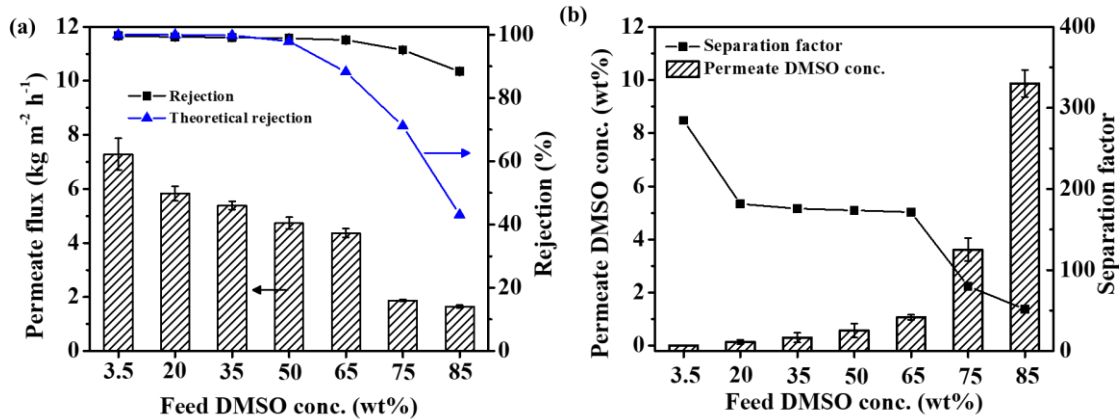


Figure 4.9 VMD performances of the 200-mSYM membranes ($T_f=60$ °C, $P_p=5$ kPa, $Q_f=170$ ml min⁻¹): (a) Flux and DMSO rejection vs. different feed DMSO concentrations. (b) Permeate DMSO concentration and separation factors vs. different feed DMSO concentrations.

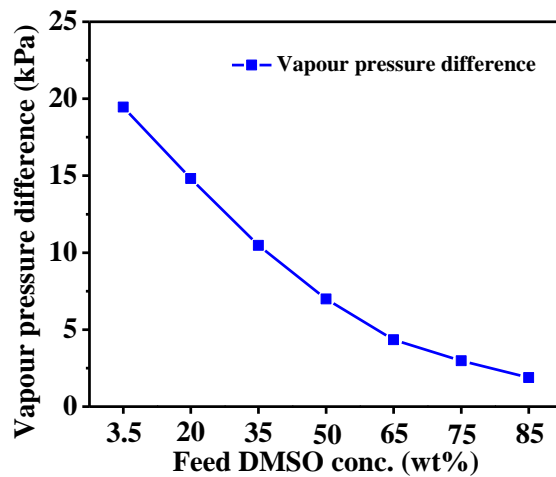


Figure 4.10 Vapour pressure difference across membrane vs. different feed DMSO concentrations.

Although SR-MD process enabled the diffusion of both DMSO and water vapour through membrane pores, it could still effectively separate water from DMSO because of

the considerably higher saturated pressure of pure water, which is 19.9 kPa compared to 0.7 kPa of pure DMSO at 60 °C (Nishimura et al. 1972). As presented as the blue line in Figure 4.9(a), the simulation of VLE indicated that the theoretical DMSO rejection was nearly 100% when the feed concentration is <20 w%, but it would decrease to 43.1% when the feed concentration is 85%. Nonetheless, the actual DMSO rejection in the experiments was much higher than estimation when the feed concentration was high (≥ 65 wt%). The DMSO rejection only reduced to 88.4 wt% at DMSO concentration of 85 wt%, showing distinctly 105% better than the estimation. To understand the reason behind, the diffusion of vapour molecules in the membrane pores should be considered, in addition to the evaporation of feed stream at the interfaces. In the case of VMD, the mean free path of transporting molecules was much higher than the membrane pore sizes. Thus, the diffusion phase was dominated by the Knudsen model which emphasizes the interactions between molecules and membrane pore walls (Schofield et al. 1990). Knudsen diffusion favours the transport of smaller molecules (water) so it has a positive effect on the transport of water. Although the hydrophobic interaction was weak in gas/vapour phase, the hydrophobic tails of DMSO molecules may still have affinity to the hydrophobic membrane walls and parts of DMSO may be attached on the membrane surface during the collision, and thus slowing down the transport to the permeate side. As a result, the DMSO rejection in the VMD process could exceed the estimated value. The extent of transcendence would be even higher if the tortuosity of the membrane pores was considered.

4.3.2.2 Effects of feed temperature and membrane structure

To explore the impact of the feed temperature on the membrane performance, VMD tests were carried out with a 50 wt% DMSO feed solution at temperature ranging from 30 to 60 °C. Three different types of membranes: 200-mASY, 200-mSYM and 20-mASY were tested and the effects of membrane pore size and structure were also studied. As shown in

Figure 4.11(a), the permeation fluxes of all three membranes improved consistently with the increasing temperature. The 20-mASY exhibited the highest permeation flux among them, where the flux increased from 1.5 kg m⁻² h⁻¹ at 30 °C to 6.9 kg m⁻² h⁻¹ at 60 °C. The increase of permeation flux could be explained by the higher vapour pressure generated at high temperature, subsequently rendering a higher driving force of mass transfer. At the same time, all three membranes maintained a high rejection (>98%) of DMSO, with a separation factor higher than 105. As discussed in the previous section, the rejection of DMSO highly depends on the vapour pressure of both water and DMSO at the vapour-liquid interface. For 50 wt% liquid mixture, the partial pressure of DMSO increases from 0.003 to 0.02 kPa, while the partial pressure of water increases from 1.5 to 7 kPa when the temperature rises from 30 to 60 °C. Though the percentage of increase in vapour pressure of DMSO was higher than water, the vapour pressure was still much lower than water and therefore a high rejection of DMSO could still be maintained.

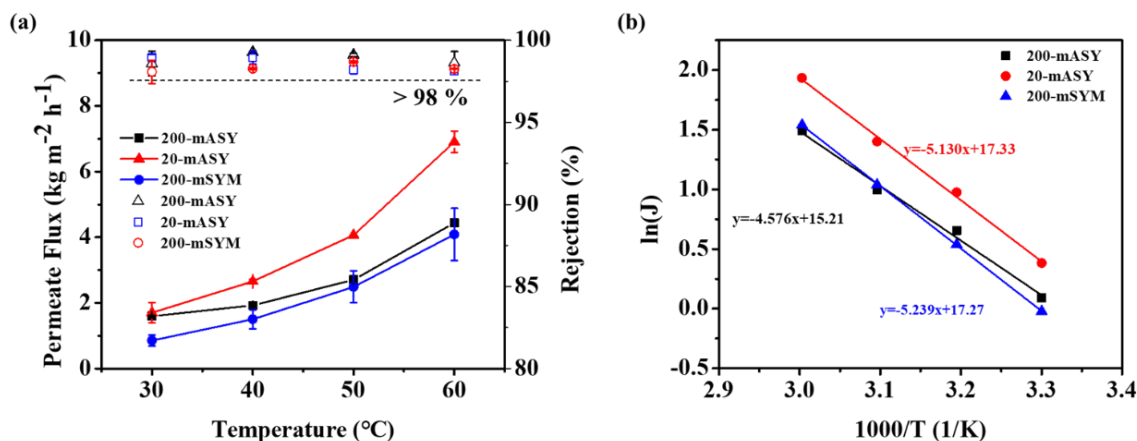


Figure 4.11 Effect of feed solution temperature on the VMD permeate flux of the 200-mASY, 200-mSYM and 20-mASY membranes ($C_f=50$ wt%, $P=5$ kPa, $Q_f=170$ ml min⁻¹).

To further understand the effect of temperature, $\ln(J)$ versus T^{-1} was plotted in Figure 4.11(b). The linear relationship indicates that the permeation fluxes increase exponentially with increasing temperature, following the Arrhenius-type equation. The activation energy can be calculated and it ranges from 38.0-43.6 kJ mol⁻¹. The activation

energy is a combination of the enthalpy of vaporization and energy of diffusion (Huang et al. 2014). Water is the main component in the vapour phase at the VLE, as shown in the rejection data where the concentration of DMSO was less than 1 wt% in the permeate. The enthalpy of vaporization was mainly contributed by water and the heat of evaporation of water was 42.48-43.78 kJ mol⁻¹ in this temperature range (Lide 2004). The similar value between the enthalpy of vaporization and activation energy may suggest the predominant effect of the evaporation step in affecting the permeation flux.

There is no significant difference between the performances of the 200-mASY and 200-mSYM membranes even though their matrix structures are different. The 200-mSYM has a similar pore structure across the membrane while the 200-mASY consists of two layers: a top layer with similar structure as the 200-mSYM and the support layer with a larger pore size. The asymmetric structure of 200-mASY did not enhance the permeation flux and the reason could be laid on the fact that the evaporation step near the vapour-liquid interface presented the predominant impact on the permeation rate.

On the other hand, it was found that the 20-mASY membrane exhibited a higher permeation flux compared to the 200-mASY and 200-mSYM membranes, despite its smaller pore size. This can be explained by the higher surface porosity and smaller membrane thickness of the 20-mASY membrane. As the evaporation step had a strong effect on the permeation flux, the total surface area of the vapour-liquid interface may directly affect the total permeation flux. As illustrated in Figure 4.12, the inner surface porosity of the 20-ASY membrane is 21.6%, which is higher than the 200-SYM and 200-ASY membranes, allowing a larger vapour-liquid interface for vapour evaporation. Also, the 20-ASY membranes (thickness of 0.75 mm) were 17% thinner than the 200-SYM

membranes (thickness of 0.9 mm), which could in turn posed a lower mass transfer resistance to the permeation flux.

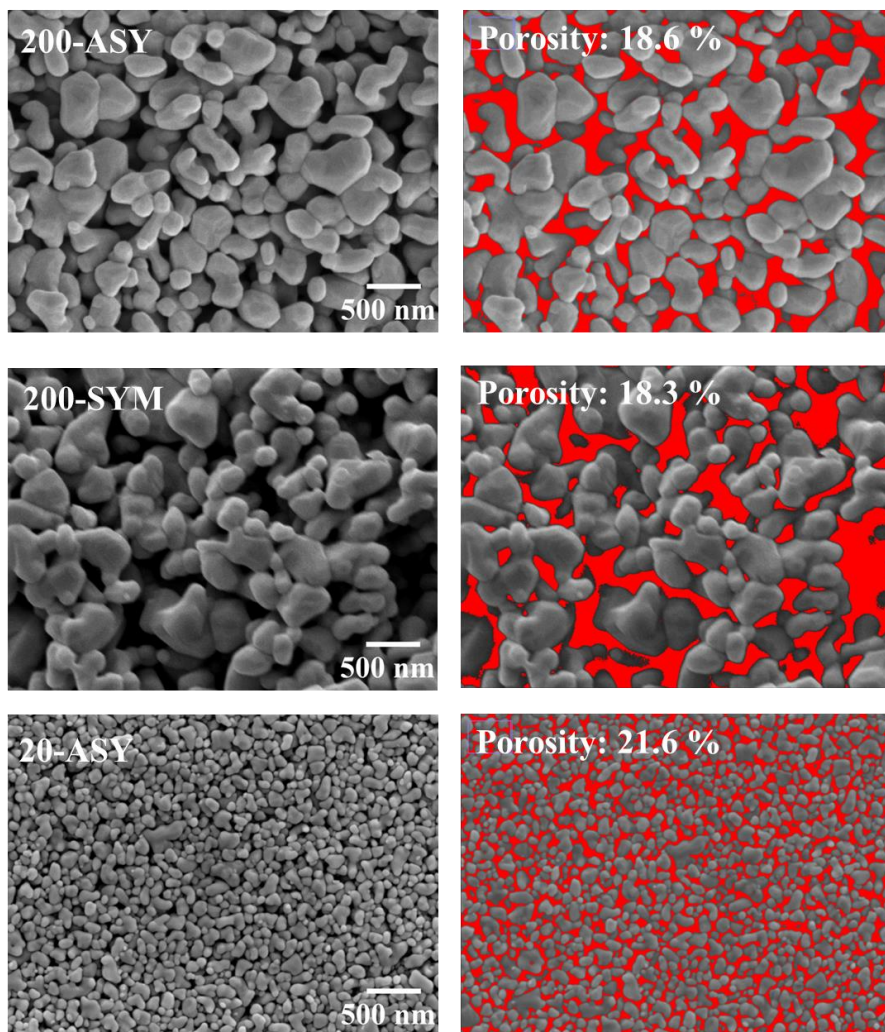


Figure 4.12 Surface porosity of the inner surface of 200-ASY, 200-SYM and 20-ASY membranes (pore area is indicated in red colour).

4.3.2.3 24-hour performance in water-DMSO feed solution

24-hour VMD tests were conducted to study the stability of the membranes in solvent-containing system. The hydrophobic ceramic membranes were prepared through surface functionalization and their stability in MD was highly dependent on the stability of the functionalization layer. As shown in section 3.1, the WCA and SCA of the membranes remained high values even after immersing in DMSO for a month. Besides that, the

membranes are more likely to suffer from membrane wetting in VMD compared to direct contact MD because of the pressure gradient across the membranes (Rezaei et al. 2018). If the membranes were wetted by the feed solution, the arc-shaped interface at the pore entrance will no longer be maintained. The liquid would start to permeate through the membranes via a viscous flow and the DMSO rejection would subsequently deteriorate.

During the experiments, the 200-mSYM membranes were fed with 20-75 wt% DMSO and the VMD process was run for 24 hours for each concentration. As shown in Figure 4.13, the membrane presented consistent performance with no sign of wetting. Though there were some minor fluctuations, the modified membranes were able to maintain an average rejection at higher than 95%. The high rejection reflected that the membrane pores survived from wetting by the feed stream even when the DMSO concentration in the feed was as high as 75 wt%. Also, the permeate flux kept reasonably stable in the whole experiment period, which was in accordance with the results of previous tests. When the DMSO concentrations were lower than 50 wt%, the average flux was higher than $4.7 \text{ kg m}^{-2} \text{ h}^{-1}$.

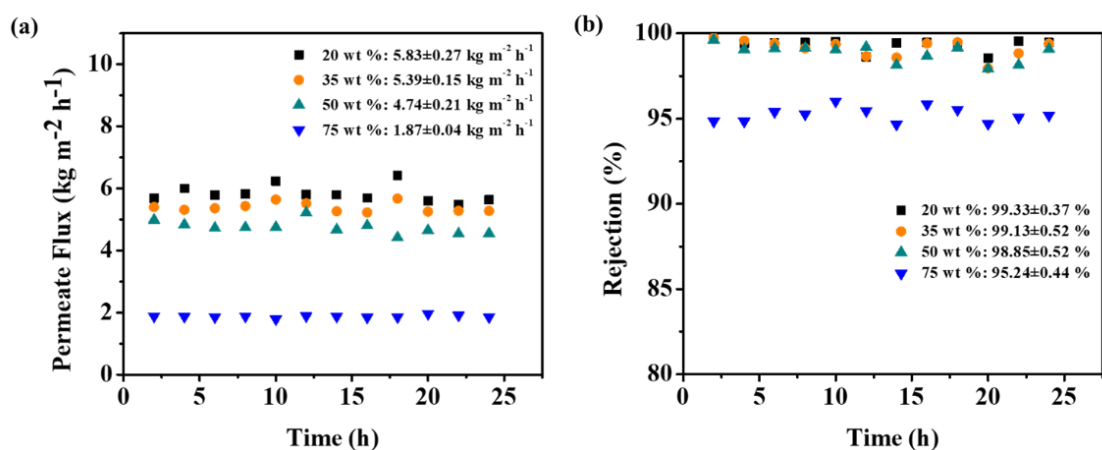


Figure 4.13 (a) Permeate flux and (b) DMSO rejection of the 200-mSYM membranes in 20-75 wt% DMSO/water feed stream ($T_f=60 \text{ }^\circ\text{C}$, $P=5 \text{ kPa}$, $Q_f=170 \text{ ml min}^{-1}$).

4.3.3 Separation performance of other types of membranes

Currently there are limited types of membranes that can be used for SR-MD due to the lack of solvent resistance of most polymeric membranes. Commonly used MD membranes such as PVDF membrane fabricated by phase inversion method cannot withstand strong solvents such as DMSO and NMP (Tan and Rodrigue 2019a). Meanwhile, the PP and PTFE membranes mainly fabricated by melt-spinning, cold-stretching or thermally induced phase separation methods (Tan and Rodrigue 2019b) can be potentially used for SR-MD because they have both high hydrophobicity and excellent chemical resistance. In this study, we also used commercial PTFE hollow fibres for water-DMSO separation to compare with the modified ceramic membranes. This kind of PTFE membrane was selected because of the relatively small pore size and similar composition with the coating layer on the FAS-modified ceramic membranes. The results are shown in Figure 4.14. The membrane showed a much lower permeation flux ($2.6 \text{ kg m}^{-2} \text{ h}^{-1}$) compared to the modified ceramic membranes at feed concentration of 50 wt%. Although it had a pore size larger than 20 nm, its flux was still lower than the 20-mASY membrane because of the lower surface porosity of 12.3% as shown in Figure 4.14(b). Furthermore, it started to wet when the feed DMSO concentration was increased to 85 wt%. The fast wetting of PTFE membranes could be due to its lower WCA, large PSD and pore geometry resulting from the stretching method used in the membrane fabrication (Tan and Rodrigue 2019b).

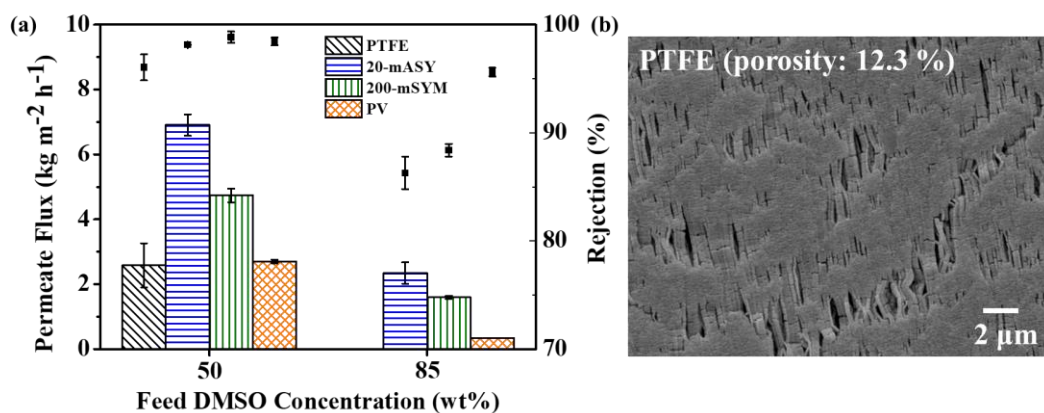


Figure 4.14 (a) Comparison of the separation performance of 20-mASY, 200-mSYM and other membranes. (b) Surface morphology of PTFE membrane.

In this study, we also tested the commercial hybrid silica HybSi[®] AR membrane used in the PV process to compare the efficiency of VMD and PV in separating water-DMSO mixtures. As shown in Figure 4.14, VMD membranes showed great superiority in permeate flux, which was 156% and 588% higher than that of PV process when treating 50 and 85 wt% DMSO with the 20-mASY membrane, respectively. The DMSO rejection of VMD was as great as PV (>98%) when the feed DMSO concentration was 50 wt%. However, when the feed concentration was 85 wt%, the rejection of the 20-mASY and 200-mSYM membranes dropped to 86.3 and 88.4%, respectively, while the rejection of PV remained high at 95.6%. PV is hardly restricted by the VLE at the interface, and the more selective sorption step contributed to the high DMSO rejection at high feed concentration (Guo et al. 2004). However, the permeation flux was significantly lower as diffusion through the dense PV membranes was much slower than Knudsen diffusion. Similar observations have been reported in a study using the hybrid silica membrane to dehydrate aqueous solutions containing 50 wt% of DMAc, DMF or NMP at 50°C, the author reported the permeate flux level is in the range of 2.2-2.3 $\text{kg m}^{-2} \text{h}^{-1}$ (Sarialp 2012).

In summary, SR-MD has been demonstrated to be a promising separation process

to separate water-DMSO effectively. The modified ceramic membranes exhibited a high permeation flux for a wide range of DMSO feed concentrations, and they also showed rejection higher than 90% when the feed concentration was lower than 85 wt%. Water with low organic content can be produced on the permeate side and it can then undergo a simple secondary purification process for further processing before reuse or discharge. For example, DMSO content in the permeate is smaller than the bioreactor limit (0.1-0.15 wt%) when the DMSO concentration in the SR-MD feed stream is lower than 20 wt%. The permeate product can be sent directly to the bioreactor where DMSO will be degraded completely. At the same time, the SR-MD process can dehydrate and concentrate DMSO in a diluted feed stream, making it more viable for reuse in manufacturing. The application of SR-MD is not limited to water-DMSO separation but can potentially be used to treat wastewater containing other organic solvents that have a high boiling point (>150 °C) like NMP, and some typical degradation-resistant solvents, such as DMF and DMAc (Kong et al. 2019, Peng et al. 2018). To give an example, the 20-mASY membrane was tested with a 50 wt% NMP feed stream at 60 °C and showed excellent rejection of $96.4 \pm 0.3\%$ and separation factor of 53.9 ± 4.2 , with high flux of 7.3 ± 0.2 kg m⁻² h⁻¹. Therefore, the treatment strategy involving SR-MD can be extended to treat more complicated industrial feeds containing various organic solvents.

4.4 Conclusions

Hydrophilic ceramic membranes were successfully transformed into hydrophobic ones by chemical grafting of FAS-F17, and the analysis showed that the hydrophobic modification was stable even after immersing in pure DMSO over 30 days. The modified ceramic membranes were subsequently used in SR-MD to separate water-DMSO mixtures. The membranes kept unwetted and showed excellent performance in VMD tests using feed

streams with a wide range of DMSO concentrations (3.5-85 wt%). Especially, the separation factor was as high as 284 at feed concentration of 3.5 wt% DMSO and stayed constant at about 170 at feed concentration of 20-65 wt% DMSO.

In comparison, the commercial PTFE MD membranes failed to resist the penetration of feed containing 85 wt% DMSO. Additionally, all the modified ceramic membranes could maintain a rejection higher than 98% when treating 50 wt% DMSO solution, which was at the same level as the commercial PV membrane tested. The permeation flux of 20-mASY membranes was also much higher, 156% and 588% higher than that of PV process when treating 50 and 85 wt% of DMSO, respectively. The separation performance of SR-MD was found strongly dependent on the VLE near the interface, and the permeation flux was predominantly affected by the evaporation step. This study demonstrates that SR-MD can be a promising technique to treat complex wastewater containing organic solvents.

This page is intentionally left blank

Chapter 5 Hydrophobic Ceramic Membranes Fabricated via Fatty Acid Chloride Modification for Solvent Resistant Membrane Distillation³

5.1 Introduction

In Chapter 4, we prepared ceramic membranes modified by FAS and demonstrated that the separation of water-DMSO could achieve a high separation factor >170 in the SR-MD process when the DMSO content in feed was <65 wt%. SR-MD can potentially be used to treat industrial organic wastes and to dehydrate or concentrate diluted solvents for reuse. This process offers a more energy-efficient alternative in separating water-solvent mixture compared to conventional processes such as distillation. However, silanes are expensive chemicals, especially fluoroalkylsilanes. For instance, the commonly used octadecyltrimethoxysilane and 1H,1H,2H,2H-perfluorodecyltriethoxysilane can cost S\$15/ml and S\$28–40/g, respectively (Sigma-Aldrich 2021a, c). Furthermore, fluorinated silanes may produce per/polyfluoroalkyl substances that have a strong persistence in the environment and may pose a negative ecological impact (Ji et al. 2020, McCarthy et al. 2017).

Alternatively, fatty acids as naturally occurring compounds can be a cost-effective and more environmentally friendly candidate for hydrophobic modification. The carboxylic groups of the fatty acids can form chemical bonds with the ceramic surface, while the long carbon chains will contribute to the hydrophobic properties. Previous studies have applied fatty acids to modify the ZnO surface to enhance hydrophobicity (Gurav et

³ This chapter has been published as Zhang, Y., Chong, J.Y., Xu, R. and Wang, R. (2022) Hydrophobic ceramic membranes fabricated via fatty acid chloride modification for solvent resistant membrane distillation (SR-MD). *Journal of Membrane Science*, 120715. Permission has been granted by the licensed content publisher “Elsevier” to use the published content as a chapter in this thesis.

al. 2014, Wang et al. 2012). However, it was unclear if the fatty acid formed a strong covalent bond with the surface. This is particularly important for SR-MD application as the formation of a strong covalent bond is highly desirable to ensure the long-term stability of the hydrophobic modification. Esterification was proposed as the modification mechanism, but this reaction may not occur readily and strong acids are normally used as the catalyst for esterification (Kastner et al. 2012). Fatty acids are likely to form a thin coating layer on the ceramic surface, attaching with a weaker hydrogen bonding. On the other hand, FACs are more reactive compounds that are more likely to form stronger ester bonds with the ceramic surface. The acyl chloride group of FAC can react with the functional groups on ceramic membranes more easily as the chloride ion is a better leaving group than the hydroxyl group (Willberg-Keyriläinen and Ropponen 2019). FAC has previously been studied to modify materials with rich –OH groups such as cellulose fibre, starch, chitosan, cotton, wood and paper to improve their dispersion ability, photostability or hydrophobicity (Carvalho et al. 2005, Geissler et al. 2014, Moo-Tun et al. 2019, Prakash and Mahadevan 2008, Wang et al. 2019b, Xin et al. 2013). However, FAC has yet been used to modify ceramic membranes. We hypothesized it can be a feasible surface modifier for ceramic membranes as they are also rich in –OH functional groups. Additionally, FAC can be a cost-effective substitute to the commonly used silanes for hydrophobic ceramic fabrication as FAC such as stearyl chloride only costs about S\$1.1–1.6/ml (Sigma-Aldrich 2021b).

In this chapter, we developed a simple surface modification method to prepare hydrophobic ceramic membranes by using FAC. Two different FACs, palmitoyl chloride (PC) and stearyl chloride (SC), were studied because of their long alkyl-chains that can decrease surface energy (Chen et al. 2021). In addition, the optimum conditions for the grafting reaction were investigated. XPS scanning was conducted to examine the formation of ester bonds on the ceramic membrane surface. Meanwhile, the membrane morphologies,

hydrophobic properties and the stability of the modified membranes were studied with a series of characterisations. After that, the hydrophobic ceramic membranes synthesized were tested for SR-MD application to separate water from the water/DMSO mixture. The performance of the FAC-modified membranes was also compared with hydrophobic membranes modified with fatty acid and silane agent, to assess the effectiveness of the FAC modification method. This is the first study to demonstrate that FAC can be grafted on ceramic membranes, and it provides a cost-effective method to produce hydrophobic ceramic membranes for SR-MD and potentially other applications that require the use of porous hydrophobic membranes.

5.2 Experimental

5.2.1 Materials

SC ($C_{18}H_{35}OCl$, $\geq 90\%$), PC ($C_{16}H_{31}OCl$, 98%), stearic acid ($C_{18}H_{36}O_2$, 95%) (SA), octadecyltrimethoxysilane ($C_{21}H_{46}O_3Si$, $\geq 90\%$) (OTMS), DMF (C_3H_7NO , 99.8%), ethanol (C_2H_5OH , 99.8%), triethylamine ($C_6H_{15}N$, $\geq 99\%$) (TEA), sodium dodecyl sulfate ($NaC_{12}H_{25}SO_4$, $\geq 99.0\%$) (SDS) were bought from Sigma-Aldrich (Singapore). DMSO was purchased from Merck Millipore (Singapore). All chemicals were used as received. Aluminium oxide ceramic tubular membranes with an inner diameter of 3 mm and outer diameter of 4.8 mm were supplied by Coorstek B.V. (Netherlands). The ceramic membranes had a nominated pore size of 200 nm and a symmetrical matrix structure. Deionized water was produced by a Milli-Q[®] system of Merck Millipore (USA).

5.2.2 Hydrophobic grafting of ceramic membranes

The reaction mechanism and grafting procedure of FAC onto the ceramic membranes is illustrated in Figure 5.1. The modification was done by the esterification

between the acyl chloride groups on FAC compounds and the hydroxyl groups on the ceramic membranes. TEA was employed as HCl remover which allowed the reaction to completion (Heinze and Liebert 2012). During the grafting, Solution A was first prepared by dissolving a certain amount of FAC in DMF, while Solution B was prepared by adding a fixed proportion of TEA in DMF. The two solutions were heated separately to 60 °C in a water bath and then the ceramic membrane was immersed in Solution A for an hour to ensure enough contact of the membrane surface with the reagent. After that, Solution B was added dropwise into solution A under strong stirring. The reaction bottle was then sealed tightly and placed in an oven at 60 °C for certain hours. After the reaction, the membrane was washed with pure ethanol for several times and then dried in a vacuum oven at 40 °C overnight.

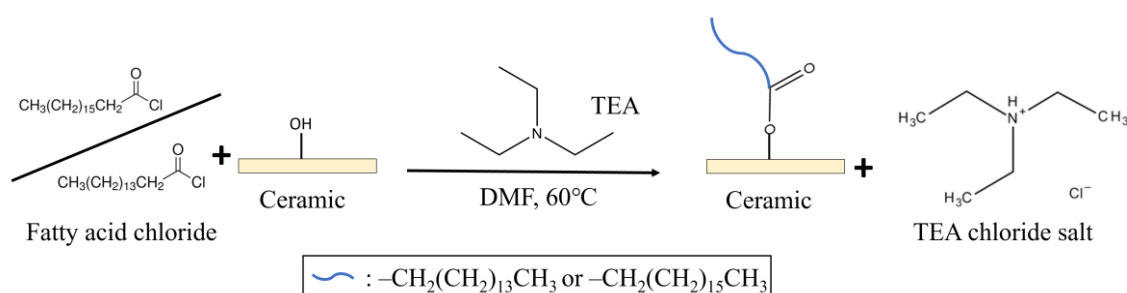


Figure 5.1 Mechanism of FAC modification on the surface of ceramic membranes.

Hydrophobic ceramic membranes modified with fatty acid (using SA as a representative) and through silanization (using OTMS as a representative) were also prepared to compare the effectiveness of the hydrophobic modification among different approaches. The SA-modified membrane was prepared by immersing the pristine membrane in 1 wt% SA/ethanol solution under 60 °C for 24 hours (Gurav et al. 2014). The OTMS-modified membrane was prepared by immersing with the membrane in 2 wt% OTMS/ethanol solution for 24 hour at room temperature (Hubadillah et al. 2019a). Similarly, the membranes were washed with alcohol thoroughly for several times and then dried in an oven at 100 °C overnight.

5.2.3 Membrane characterisations

The characterisation methods of surface morphologies, porosity, average pore size, PSD, WCA, SCA, roughness, LEP_w , LEP_s and chemical bonds can refer to section 3.2.3 and section 4.2.3. In addition to water (surface tension $\gamma \approx 72.1 \text{ mN m}^{-1}$) and DMSO ($\gamma \approx 43.5 \text{ mN m}^{-1}$), the contact angle tests were also carried out to DMF ($\gamma \approx 37.1 \text{ mN m}^{-1}$), ethanol (20 wt%, $\gamma \approx 43.7 \text{ mN m}^{-1}$), water with SDS (1.5 mM, $\gamma \approx 61.0 \text{ mN m}^{-1}$; and 4 mM, $\gamma \approx 50.0 \text{ mN m}^{-1}$).

Gas permeation test was conducted to inspect the gas permeance, which could give a good indication of whether the grafting has changed the membrane porosity. The gas permeance was measured in a dead-end mode where one end of the tubular membrane was sealed with epoxy while the other end was connected to a pressure control valve linked to the nitrogen gas cylinder. During the test, N_2 was supplied to the membrane at a certain pressure, and the permeated gas would flow into a portable gas flow meter (FlowMark™ Flowmeter, PerkinElmer, USA), where the real-time gas flowrate was measured. The gas permeance ($N, \text{ cm s}^{-1} \text{ Pa}^{-1}$) is calculated as equation (5-1)

$$N = \frac{V}{A \cdot P} \quad (5-1)$$

where V is the flowrate of the gas permeate ($\text{m}^3 \text{ s}^{-1}$), A is the effective membrane area (cm^2), P is the applied pressure (Pa).

5.2.4 VMD test and separation performance tests in water/DMSO solution

The SR-MD performance of the membranes for the separation of water-DMSO solution was tested with the similar method in section 4.2.4. Each tested module had one modified membrane with an effective area of 7.065 cm^2 . The analysis of separation performance can be referred to section 4.2.5.

5.3. Results and discussion

5.3.1 Hydrophobic modification of ceramic membranes by grafting of FAC

The FAC grafting on ceramic membrane was conducted through esterification and TEA was added to consume the HCl produced during the grafting reaction by forming chloride salt, which will push the reaction towards the right side (Figure 5.1). The effect of TEA on the grafting was first studied by using different reactant molar ratios (PC: TEA) with the PC concentration fixed at 0.07 M (Figure 5.2(a)). The effectiveness of the grafting was evaluated by measuring the hydrophobicity of the modified membranes, where the WCA and SCA were compared. Without the addition of TEA, the WCA and SCA of the grafted ceramic membranes were 136 ± 1.1 and $105.5 \pm 2.9^\circ$, respectively. The WCA and SCA improved to 141.0 ± 0.3 and $108.0 \pm 2.9^\circ$, respectively when the PC:TEA molar ratio was 1:1. However, a higher TEA concentration did not further improve the hydrophobicity as the a non-uniform grafting may be caused by the excessive concentrated TEA and the over-quick reaction rate. Then, the effect of FAC concentration was studied with the ratio of PC to TEA fixed at 1:1. As shown in Figure 5.2(b), the WCA improved when the PC concentration increased from 0.035 to 0.07 M but decreased when the concentration was increased to 0.14 M, though all samples had a WCA $>130^\circ$. The higher PC concentration improved the grafting reaction, but when the PC concentration was too high at 0.14 M, some solid precipitation was observed in the grafting solution due to saturation. This might reduce the contact between the reactants with the membrane surface, resulting in a less effective grafting. Besides that, the effect of reaction time on the surface modification was studied by varying the reaction time from 8 to 16 and 24 hours, as shown in Figure 5.2(c). Although increasing the reaction time improved the hydrophobicity, the improvement was not remarkable when the reaction time was increased from 16 to 24 hours, as both the membranes had WCA and SCA higher than 139 and 108° , respectively. Thus, the selected procedure to graft FAC was using 0.07 M FAC and 0.07 M TEA to react for 16 hours. In

the subsequent sections, all the FAC modified membranes were prepared using this optimal condition. Two kinds of FAC of SC and PC with different carbon chain lengths were also adopted to modify the ceramic membranes.

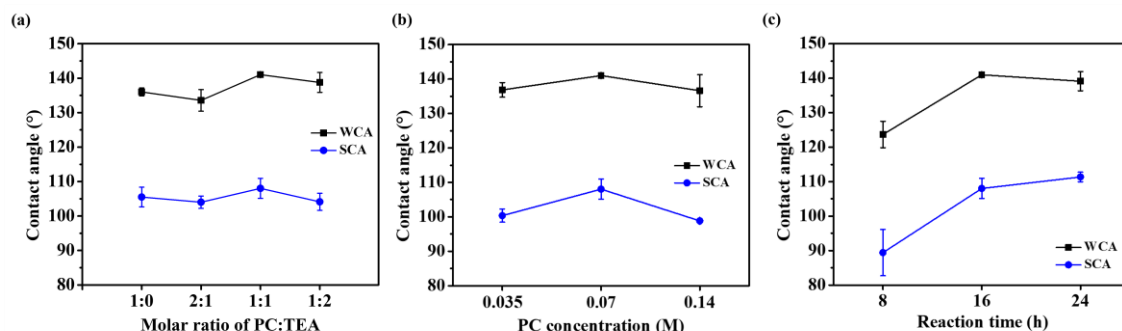


Figure 5.2 WCA and SCA of the hydrophobic ceramic membranes prepared under different conditions.

The hydrophobicity of the FAC-modified membranes was compared with the membranes modified using SA and OTMS, and their WCA and SCA are summarized in Figure 5.3(a). The SC and OTMS-modified membranes showed similar contact angles of about 140° , the highest among these 4 types of membranes. Though with different bonds formed with the ceramic surface, the similar contact angles between the SC and OTMS-modified membranes were contributed by the same carbon chain length grafted. The WCA and SCA of the PC-modified membranes were slightly lower than the SC-modified membranes, which could be due to the shorter carbon chain length. However, the SA-modified membranes had the lowest WCA and SCA, and the largest variation of the contact angles. Though with the similar 18-carbon chain, the surface modification may not be as effective as the SA may only adsorb on the ceramic membrane surface. The carboxylic groups of SA may not form covalent bonds with the ceramic surface but only weaker hydrogen bonds, as illustrated in Figure 5.3(b).

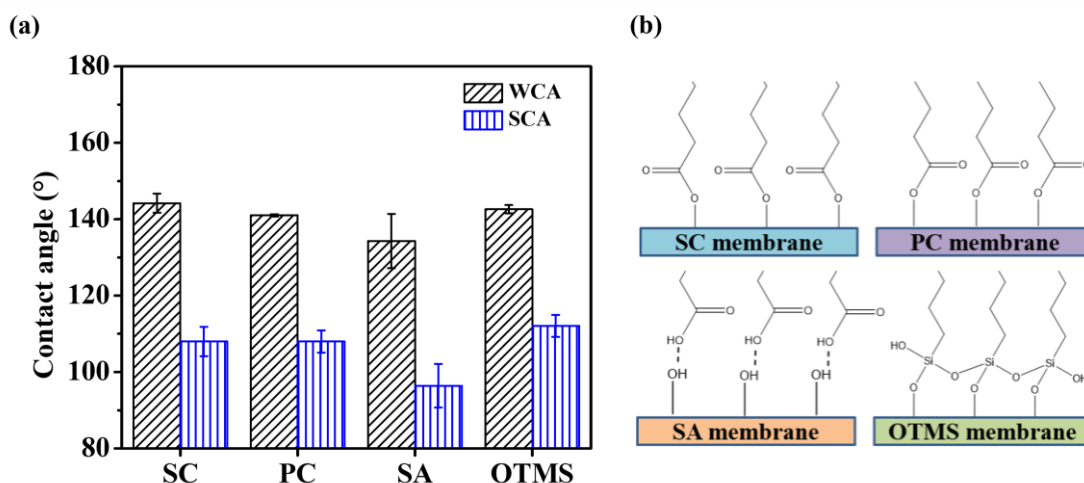


Figure 5.3 (a) Contact angles of SC, PC, SA and OTMS modified membranes; (b) Bonds formed between different modifiers and ceramic membranes.

To confirm the hypothesis, the bonds formed by FAC and SA on the ceramic membrane surface were studied via XPS scans carried out on the pristine, SC-modified and SA-modified membranes. Figure 5.4(a) shows the wide scan spectra, the C peak of the two modified membranes became much higher than the pristine membrane after the introduction of long carbon chains on the ceramic surface. Besides that, the Al peak was still observed after the surface modification as only a very thin grafting layer was formed. The proportion of Al of the SA-modified membranes (33%) was lower than the SC-modified membranes (37%). This may indicate that the SA modification was likely to form a thicker coating layer on the ceramic surface. Figures 5.4(b) and (c) show the O1s signal of the SC-modified and SA-modified membranes. The deconvolution of SC-modified membrane had an extra sub-peak of Al–O–(C=O), which corresponded to the ester bonds formed between the ceramic membrane and FAC. However, the sub-peak was not observed in the SA-modified membrane as covalent bonds did not form during the surface modification.

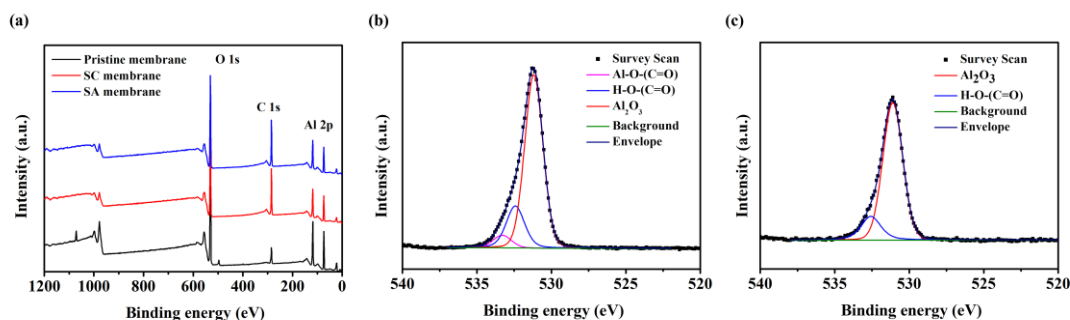


Figure 5.4 (a) XPS spectra of pristine, SC and SA-modified membranes, (b) O signal of SC modified membrane and (c) O signal of SA membrane.

Table 5.1 lists the literatures on the hydrophobic grafting of ceramic membranes with different modifiers. To have a fair comparison on the effects of the grafting agents, studies using nanoparticles to enhance surface roughness to further improve the WCA were not included here. Most of the reported membranes are prepared through silanization. Overall, ceramic membranes modified with the perfluoroalkyl chain have a higher WCA, which could reach as high as 179° . The fluorinated compounds have a lower surface energy compared to the pure carbon chains but their use may carry an environmental cost. For membranes modified with non-fluorinated silanes, their WCA generally ranged from 120° to 140° . The WCA of the FAC-modified membranes in this work is comparable or better than some membranes grafted with silanes, with a $WCA > 140^\circ$. Therefore, FAC is an attractive alternative to silanes for hydrophobic modification as it is more cost effective and eco-friendly. There are also many types FAC with different lengths that can be applied to fine tune the hydrophobicity.

Table 5.1 Ceramic membranes grafted with different modifier and their water contact angles.

Modifier type	Carbon/perfluoroalkyl chain length	Grafting agents	WCA	Ref
Fluorinated silanes	C8	1H,1H,2H,2H-perfluorodecyltriethoxysilane	140-179°	(Hubadillah et al. 2019b, Khemakhem et al. 2013, Khemakhem and Amar 2011, Picard et al. 2001, Zhang et al. 2021b)
	C6	1H,1H,2H,2H-perfluorooctyltriethoxysilane	130-137°	(Fang et al. 2012, Ko et al. 2018, Kujawa et al. 2013)
Non-fluorinated silanes	C16	hexadecyltrimethoxysilane	132.7-158°	(Chen et al. 2018b, Ding et al. 2018, Guo et al. 2022)
	C8	n-octyltriethoxysilane	134.2-140.5°	(Bartels et al. 2019, Kujawa et al. 2017, Wei et al. 2020)
	C6	octyltriethoxysilane	135.9-140°	(Bartels et al. 2019, Kujawa et al. 2020)
	C1	methyltrichlorosilane	120-145°	(Pagliero et al. 2020)
FAC	C16	SC	144.2°	This work
	C18	PC	141°	

5.3.2 Characterisations of hydrophobic ceramic membranes

The properties of the modified hydrophobic ceramic membranes were studied to explore their feasibility in SR-MD application. Figure 5.5 shows the inner surface morphology of the pristine, PC-modified and SC-modified membranes, and no noticeable change was observed after the surface modification. This observation is similar to the silane grafting on ceramic membranes in previous studies, and the FAC grafting was likely to only introduce a molecular layer of hydrophobic chains to the ceramic particle surface (Zhang et al. 2021b). From the membrane pore size measurement using the porometry method (Table 5.2), the mean pore size did not change and remained at about 185 nm after the modification. This further supports that the FAC was molecularly grafted on the ceramic surface without affecting the membrane morphology. The membrane porosity after the modification was also studied by measuring the gas permeation of the membranes (Table 5.2). The gas permeation did not have any significant changes after the modification as the membranes still retained a high porosity after the grafting reaction. The high membrane porosity is particularly important to ensure the fast vapour permeation during the MD process.

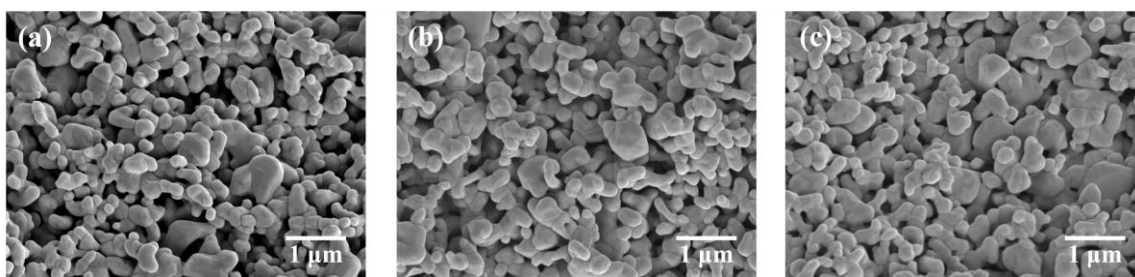


Figure 5.5 FESEM images of the inner surface morphologies of the (a) pristine, (b) PC-modified and (c) SC-modified membranes.

Table 5.2 Properties of pristine and modified membranes.

Membranes	Mean pore size (nm)	N ₂ permeation (cm s ⁻¹ Pa ⁻¹)	LEP _w (kPa)	LEP _s (kPa)
Pristine	185 ± 3	537 ± 2	/	/
PC-modified	188 ± 3	538 ± 13	306.8 ± 19.3	122.7 ± 15.9
SC-modified	184 ± 5	520 ± 22	388.2 ± 11.0	143.4 ± 25.5

A high liquid entry pressure for water and pure DMSO is a prerequisite for SR-MD with the water/DMSO feed stream. This is to ensure the feed solution will not enter the membrane pores and wet the membranes during the membrane process. Both the PC and SC-modified membranes had a high LEP_w >306 and LEP_s >122 kPa, which was ascribed to the high contact angles after the modification. The LEP_s were higher than the pressure difference across the membrane in the VMD experiments, where vacuum will be applied on the permeate side. The SC-modified membranes also had higher LEP_s than the PC-modified membranes, which could be due to the higher contact angles contributed by the longer carbon chain of SC.

The anti-wetting property of the hydrophobic modified membranes was further evaluated by measuring the contact angles for liquids with surface tension ranging from 37.1 to 67.1 mN/m (Figure 5.6(a)). The contact angles decreased with lower liquid surface tension but were still higher than 90° for all the liquids tested, demonstrating good repellence of the membranes to a wide range of liquid. To further evaluate the wetting resistance of modified membrane, a modified Zisman graph is plotted (Figure 5.6(b)) to determine the critical surface tension, which is defined as the surface tension of liquid whose contact angle is zero and wet the surface completely (Bera et al. 2018). It could be calculated that the critical surface tension of the PC-modified membrane was 22.5 mN/m. This is comparable to the 16-22 mN/m of PTFE and 25 mN/m of PVDF membranes with similar pore size (Keurentjes et al. 1989). Besides that, the long-term stability of the surface

modification was ascertained by testing the WCA and SCA of the modified membranes after being immersed in pure DMSO for 0, 7 and 30 days. As depicted in Figure 5.6(c), the modified membranes had a stable contact angle even after 30 days and the decrement was smaller than 4° for WCA and 1° for SCA. This result was good evidence that the grafting agents were strongly bonded to the ceramic membranes and the chemical bonds formed were stable in the solvent solution.

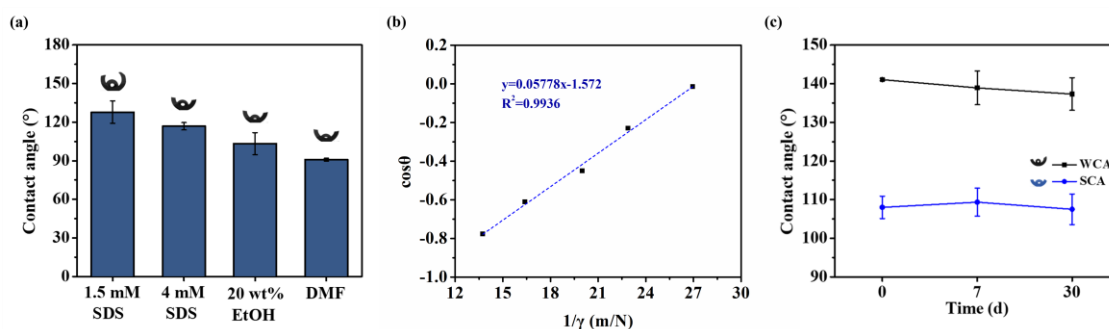


Figure 5.6 (a) Contact angles of 1.5 mM SDS (61 mN m^{-1}), 4 mM SDS (50 mN m^{-1}), 20 wt% ethanol (43.7 mN m^{-1}) and DMF (37.1 mN m^{-1}) on the surface of the PC-modified membrane. (b) Modified Zisman plot: cosine of contact angles of different liquids (1.5 mM SDS, 4 mM SDS, 20 wt% ethanol, DMF and water) versus the inverse of surface tension of the corresponding liquid. (c) WCA and SCA of the PC-modified membrane after immersing in pure DMSO for 7 and 30 days.

5.3.3 SR-MD performance for water-DMSO separation

The hydrophobic PC-modified and SC-modified membranes synthesized were applied for the separation of water/DMSO mixture in the VMD configuration. As shown in Figure 5.7, the PC-modified membranes had a permeation flux of 5.8 and $3.2 \text{ kg m}^{-2} \text{ h}^{-1}$ when treating the feed with a DMSO concentration of 20 and 50 wt%, respectively, at 60°C . The membranes also demonstrated a high DMSO rejection of $>98\%$ and separating factor >110 . During the MD separation, a vapour-liquid interface was formed near the membrane surface and the permeation was driven by the vapour pressure difference across the membranes. Water with a higher vapour pressure permeates through the membrane faster, resulting in an effective separation of water and DMSO. However, when the DMSO

concentration increased in the feed, the lower water composition resulted in a decrease in the total vapour pressure at the liquid-vapour interface, and this subsequently reduced the permeation flux through the membrane. On the other hand, the SC-modified membrane had a flux of 4.5 and 2.8 kg m⁻² h⁻¹, for DMSO feed solution of 20 and 50 wt%, respectively. The membrane also showed an excellent DMSO rejection of >98%, separating factor >110 for both the DMSO feed concentrations. The relatively lower flux of the SC-modified membrane could be due to the higher hydrophobicity compared to the PC-modified membrane. The more hydrophobic membrane surface had a stronger repulsion to the feed solution. The vapour-liquid interface on the feed side may be prevented from intruding into membrane pores, resulting in a longer vapour transport path (Li et al. 2020a). The performance of the FAC-modified membranes actually have transcended the commercial PTFE hollow fibre membranes tested in our previous study, which only had a flux of 2.58 kg m⁻² h⁻¹ and a rejection of 96.05% when treating 20 wt% DMSO and was wetted by 50 wt% DMSO solution (Zhang et al. 2021b). The better performance of the FAC-modified membranes could be contributed by the higher surface porosity and the narrower PSD of the ceramic membranes.

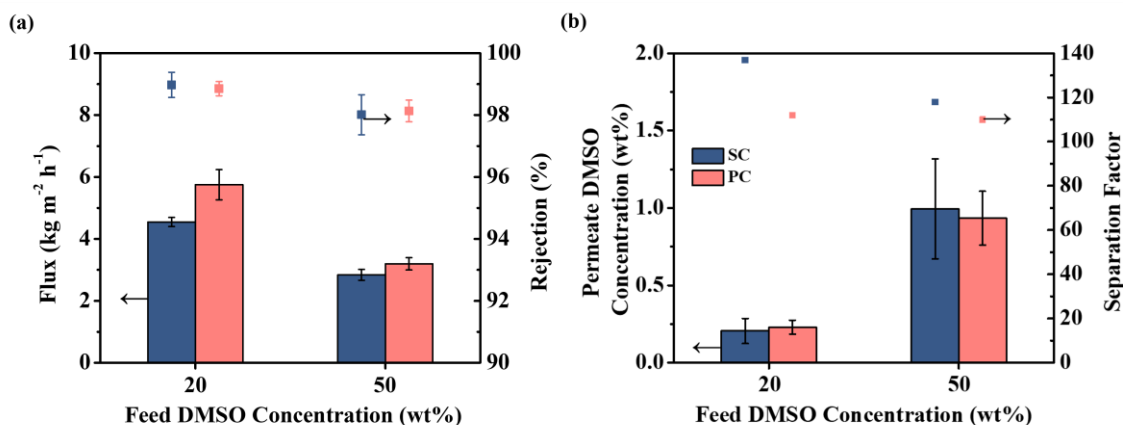


Figure 5.7 SR-MD performance of the PC-modified and SC-modified membranes in the 20 and 50 wt% DMSO feed solution at 60 °C ($T_f=60$ °C, $P_p=5$ kPa, $Q_f=170$ ml min⁻¹)

It is worth noting that when feed concentration was 20 wt%, the DMSO rejection of FAC-modified membranes was slightly lower than the theoretical rejection (99.99%). However, both FAC-modified membranes showed better rejection in treating 50 wt% DMSO solution, where the theoretical rejection was estimated as 97.93%. The better separating performance at higher concentration could be due to the Knudsen diffusion step in the membrane pores where the DMSO molecules may have a lower transport rate as a result of the hydrophobic interaction with the pore channels. Besides that, the DMSO concentration in the permeate collected was very low, only around 0.2% when the feed DMSO concentration was 20% (Figure 5.7b). With such a low solvent content, a simple secondary purification step can be carried out to further process the water stream for reuse or discharge.

Figure 5.8(a) depicts the effects of feed temperature on the performance of the PC-modified and SC-modified membranes in the separation of 50 wt% water/DMSO. Conspicuously, the membranes showed a high DMSO rejection, >96 and >98% for the PC-modified and SC-modified membranes, respectively, at all the temperature tested. With the temperature increased from 40 to 70 °C, the water partial pressure increased from 2.60 to 10.97 kPa while the DMSO partial pressure increased from 0.005 to 0.03 kPa. The water vapour pressure was still much higher than DMSO in this temperature range, enabling the DMSO rejection to maintain high. However, the slight decrease in the DMSO rejection at a higher temperature was due to higher increase rate of the DMSO vapour pressure at increasing temperature. Meanwhile, the higher total vapour pressure at higher temperature also resulted in the increase in the total flux as more vapour flew through the pores. The highest flux of the PC and SC-modified membranes were obtained at 70 °C as 4.53 and 3.81 kg m⁻² h⁻¹, respectively. Besides, the permeation flux at different temperatures was plotted as ln(J) versus T⁻¹ in Figure 5.8(b). According to the Arrhenius-type equation, the activation energy was calculated to be 40.9 and 35.9 kJ mol⁻¹ for the SC-modified and PC-

modified membranes, respectively. The higher energy barrier of SC-modified membrane could be owing to its higher hydrophobicity, which may pose a higher mass transfer resistance to the permeate flux (Kujawa et al. 2017).

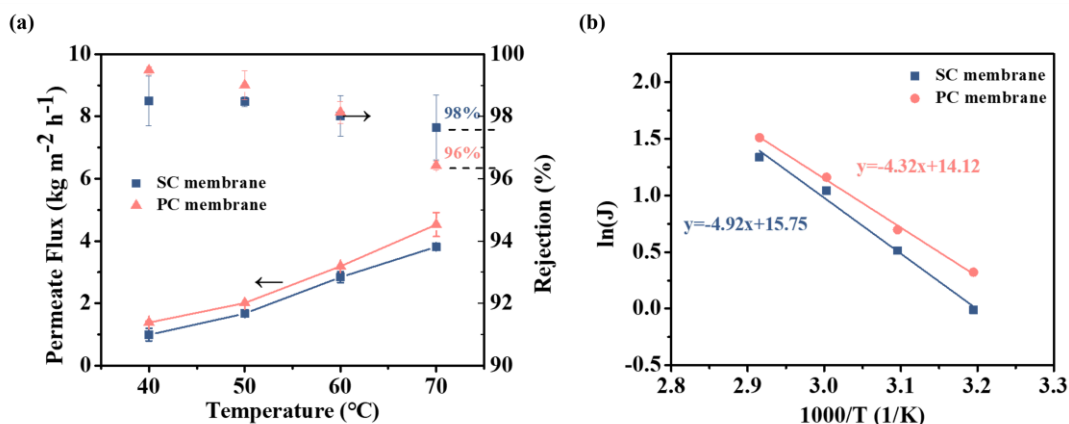


Figure 5.8 Effect of feed solution temperature on the SR-MD permeate flux and DMSO rejection of the PC-modified and SC-modified membranes. ($C_f=50$ wt%, $P=5$ kPa, $Q_f=170$ ml min⁻¹).

The SR-MD performance of the FAC-modified membranes were tested for 24 hours to study their performance stability over a longer period (Figure 5.9). We also included the OTMS-modified membranes in this long-term study to compare the SR-MD performance with membranes prepared via silanization. When tested with the feed solution containing 50 wt% of DMSO, the SC-modified and OTMS-modified membranes had similar average flux of 2.8 kg m⁻² h⁻¹ while the PC modified membrane had a slightly higher average flux of 3.2 kg m⁻² h⁻¹. As discussed earlier, the higher flux of the PC-modified membranes could be caused by the slightly lower membrane hydrophobicity. Meanwhile the similar flux of the SC and OTMS-modified membranes could be due to their similar hydrophobicity or water contact angle, as shown in Figure 5.3(a), which was contributed by the same 18-carbon chains grafted on the membranes. As depicted in Figure 5.9(b), the average DMSO rejections across the three membranes were at a high level of ~98% though displayed slight fluctuations. The small decrement in rejection from the initial value of ~99 to 98% may be attributed to the gradually increased feed DMSO concentration in the feed tank over time.

Another contribution for the observed decrease in rejection rate during the initial hours of operation could be attributed to the reduced contact angles of the membranes in the solvent environment. As shown in Figure 5.6(c), the WCA and surface contact angle (SCA) of the membranes exhibited a slight decline, which may have been caused by the desorption of some residual modifiers that were still adhering to the membrane surface. The SR-MD performance of the FAC grafted membranes were comparable to the membranes grafted with nonfluorinated silane. The Al–O–C=O bonds showed good stability similar to the Al–O–Si bonds, and the FAC-grafted membranes demonstrated great potential for applications involving environment with high temperature and high solvent content.

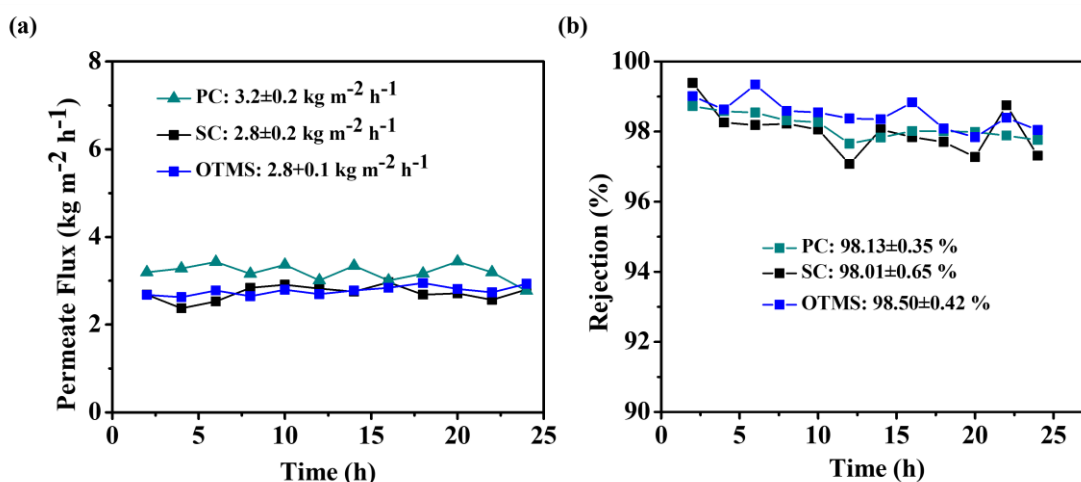


Figure 5.9 (a) Permeate flux and (b) DMSO rejection of the pristine, PC-modified and SC-modified membranes in 50 wt% DMSO/water feed stream ($T_f=60$ °C, $P=5$ kPa, $Q_f=170$ ml min^{-1}).

SR-MD also provides a cost-effective solution to reclaim water and to dehydrate solvent-containing waste streams without the need for high temperature and expensive installation. After the SR-MD treatment, the water product with a little amount of organic solvent content will be easier to handle by conventional biological treatment method, while the concentrated solvent feed stream can potentially be reused and recirculated in the production process.

5.4 Conclusions

This study demonstrates a facile hydrophobic modification on ceramic membranes with FAC. Both PC and SC with different carbon chain lengths were successfully grafted on the surface of ceramic membranes, forming strong covalent bonds. The hydrophobic FAC-modified membranes had high WCA >141° and SCA >108°, which were higher than the membranes prepared with fatty acid modification and comparable to the hydrophobic ceramic membranes prepared through silanization. Moreover, the synthesized membranes demonstrated outstanding properties required for SR-MD application: strong solvent-resistance and the good liquid repellence to prevent pore wetting. In a series of SR-MD experiments, the PC-modified membrane showed a competitive performance comparing with other membranes made of PTFE or modified with silane agent, with an average DMSO rejection >98% and stable flux >3.2 kg m⁻² h⁻¹ over 24 hours when treating 50 wt% DMSO. This facile hydrophobic modification method deserves further investigation as it demonstrates the possibility of a cost-effective and environmental-friendly approach to synthesize MD membranes with high performance. Specifically, pretreatment techniques and alternative organic bases may be investigated to strengthen the chemical bonds formed by FAC and ceramic membranes to enhance the hydrophobicity. Moreover, it is suggested to further investigate the durability of FAC grafting under prolonged exposure to organic solvents.

Chapter 6 Conclusions and Recommendations

6.1 Overall conclusions

This thesis presents several hydrophobic modification methods conducted on hydrophilic polymeric membranes and ceramic membranes to prepare robust MD membranes for treating challenging streams with high-salinity and organic solvents, respectively. Currently, there are still limited MD studies related with these two particular waste streams owing to the fact that there is a lack of applicable membranes with easy fabrication and high performance. In the treatment of highly salty water, the commercial membranes have limited flux while most methods reported in the literature are complex with multi-steps.

Thus, a novel modification using LF-200 is first developed, which has advantages of time-saving, simple handling, effectiveness and versatility to different substrates. Different concentration of coating solution was studied in order to optimize the membrane hydrophobicity. The modified membranes were tested in the separation of water and salt ranging from 3.5-10 wt%. In the next step, we targeted a more challenging feed stream with a high concentration of organic solvent with high boiling points. Ceramic membranes modified by common FAS grafting were particularly chosen to treat the water-DMSO mixture and the potential of SR-MD is fully elucidated. And the influence of membrane pore size, membrane structures, feed concentrations and operating conditions were studied. Then, the danger of the modifier (FAS) was noticed and another modification method that is greener and cheaper was developed using fatty acid chloride grafting. The modified ceramic membranes were also challenged by concentrated water-DMSO mixtures.

The major findings of this thesis are summarized as follows:

From Chapter 3:

- A facile hydrophobic modification method that could transform the originally hydrophilic NC and nylon membranes into hydrophobic membranes was developed using a novel copolymer LF-200.
- This method is facile and effective as it only requires dip-coating followed by crosslinking at low temperature to increase the membranes' WCA to $\sim 130^\circ$, without significantly changing membranes' pore structures.
- The modified-NC membranes showed good performance in treating high-salinity water. The 12LF-NC membrane showed an excellent flux of $10.1 \text{ kg m}^{-2} \text{ h}^{-1}$ in the treatment of 10 wt% salt water, which is 31% higher than the commercial PVDF membrane. The permeate conductivity was stable over 120 h.
- The method was successfully carried out on nylon membranes as well and produced usable MD membranes for desalination. It suggested that the LF-200 coating has wide versatility on different substrates, including but not limited to nylon and NC membranes.

From Chapter 4:

- SR-MD is a novel and effective alternative for separating water from solvents with high boiling points. Hydrophobic ceramic membranes with different sizes and structures were obtained through chemical grafting of FAS-F17 and used in the separation of water-DMSO mixture via VMD.

- The modified membranes performed excellently in feed DMSO concentrations ranging from 3.5-85 wt%. Rejection >98% can be achieved for a feed containing <65 wt% DMSO and the permeate product can be sent to bioreactor (upper limit at 0.1-0.15 wt%) if the feed DMSO concentration is <20 wt%.
- The membranes with smaller pore size obtained higher permeate flux than the membranes with larger pore size due to the higher surface porosity. The membranes with similar pore size but different structures (asymmetric and symmetric) presented similar MD performance. It suggested that the separation performance of SR-MD is strongly dependent on the VLE near the interface, and the permeation flux was predominantly affected by the evaporation step.
- Compared to PV, SR-MD showed 156% and 588% higher fluxes than that of PV process when treating 50 and 85 wt% of DMSO, respectively. Compared to commercial PTFE membrane, the grafted ceramic membranes have better anti-wetting ability and permeability.
- In addition to DMSO, SR-MD can be promoted to the separation of water with other organic solvents with a high boiling point, such as DMF (153 °C), DMAc (165 °C), and NMP (202 °C), as they have a lower vapour pressure compared to water.

From Chapter 5:

- This study presents a greener and cheaper surface modification chemistry to synthesize hydrophobic ceramic membranes through fatty acid chloride grafting.
- Two types of fatty acid chloride (PC and SC) with different carbon chain lengths were

successfully grafted on the surface of ceramic membranes. The acyl chloride groups formed strong ester bonds on the ceramic surface and the modified membranes had high hydrophobicity.

- The modified ceramic membrane showed a flux of $3.2 \text{ kg m}^{-2} \text{ h}^{-1}$, rejection $>98\%$ and separation factor >110 can be achieved when treating 50 wt% DMSO in SR-MD. The performance is comparable to the ceramic membranes prepared through silanization.
- The FAC modification method is a cost-effective and environmental-friendly approach to synthesize hydrophobic ceramic membranes. It is meaningful for extended SR-MD applications.

6.2 Recommendations for future research

Based on the findings in this thesis, there are some recommendations for future studies in the following aspects.

While this thesis has tried to harness the unique advantages of MD in challenging wastewater treatment with high concentration of NaCl or DMSO, the compositions of the synthetic feed solutions are still different from the real feed. For example, real brine water may consist of other inorganic ions such as Mg^{2+} , Ca^{2+} and SO_4^{2-} , which can cause scaling easily; and the real industrial organic waste streams may contain metal ions or organics matters together with organic solvents. Further studies are required to explore whether the modified MD membranes are stable and effective in these real feeds. In addition, the long-term stability of the modified membranes needs further investigation, in which case the pretreatment of the feed solutions or cleaning procedure of MD membranes may be beneficial to prolong their lifetime to months or even years. (Chapter 3, 4, 5)

Considering the low cost and easy operation of the LF-200 coating method, it is worth exploring its adaptability on other hydrophilic substrates that resist to non-polar solvent (xylene), such as PVA, polyimide and polyethylene. In addition, applying this hydrophobic coating on electrospun membranes with high porosity and roughness is a possible solution to obtain MD membranes with higher permeate flux, better wetting resistance and fouling resistance. To test the practical application value of this coating method, the scale-up production of coated membranes should also be conducted to evaluate the material cost. Similarly, the ceramic modification method utilized FAC also requires a prolonged MD study and scale-up production to test the viability and stability of the grafted membranes. (Chapter 3, 5)

In terms of SR-MD, though it shows a higher flux than PV method, its long-term performance needs further exploration. In fact, the commercial hybrid silica PV membranes have been challenged with long-term tests for up to 1000 days. To prove the SR-MD is a good alternative method to PV in the separation of water-solvent mixtures, the comparison of their performance for a longer period is necessary. Moreover, only two organic solvents (DMSO and NMP) are considered in this thesis. It is suggested to continue exploring the viability of SR-MD in other aggressive organic solvents. Since the separation performance is highly dependent on the partial vapour pressure difference of feed components, it is suggested to select solvents with boiling points >150 °C, such as DMF and combine the VLE theory to deduce the feasibility of SR-MD. By testing the performances with different organic solvents and comparing them with other technologies, a strategy can be developed to identify the optimal technique for organic solvent recovery under different conditions, such as solvent's boiling point, concentration and temperature. Furthermore, the superiority of ceramic membranes and the importance of surface porosity has been shown in this thesis, presenting DMSO rejection higher than the estimated value in high solvent concentrations.

To figure out the reasons behind, further studies can be done to analyze the interactions between the feed components and membranes and develop a better model to fit the experimental data under high DMSO feed concentration. (Chapter 4)

References

Global Industry Analysts. (2023) Global Dimethyl Sulfoxide (DMSO) Industry. Report number 5817800, USA.

A Shirazi, M.M., Kargari, A., Bastani, D., Soleimani, M. and Fatehi, L. (2020) Study on commercial membranes and sweeping gas membrane distillation for concentrating of glucose syrup. *Journal of Membrane Science and Research* 6(1), 47-57.

Abd Aziz, M.H., Pauzan, M.A.B., Mohd Hisam, N.A.S., Othman, M.H.D., Adam, M.R., Iwamoto, Y., Hafiz Puteh, M., Rahman, M.A., Jaafar, J., Fauzi Ismail, A., Agustiono Kurniawan, T. and Abu Bakar, S. (2022) Superhydrophobic ball clay based ceramic hollow fibre membrane via universal spray coating method for membrane distillation. *Separation and Purification Technology* 288, 120574.

Adnan, S., Hoang, M., Wang, H. and Xie, Z. (2012) Commercial PTFE membranes for membrane distillation application: Effect of microstructure and support material. *Desalination* 284, 297-308.

Agirre, I., Güemez, M.B., van Veen, H.M., Motelica, A., Vente, J.F. and Arias, P.L. (2011) Acetalization reaction of ethanol with butyraldehyde coupled with pervaporation. Semi-batch pervaporation studies and resistance of HybSi® membranes to catalyst impacts. *Journal of Membrane Science* 371(1), 179-188.

Ahmad, A.L., Ramli, W.K.W., Fernando, W.J.N. and Daud, W.R.W. (2012) Effect of ethanol concentration in water coagulation bath on pore geometry of PVDF membrane for Membrane Gas Absorption application in CO₂ removal. *Separation and Purification Technology* 88, 11-18.

Ajdar, M., Azdarpour, A., Mansourizadeh, A. and Honarvar, B. (2020) Improvement of porous polyvinylidene fluoride-co-hexafluoropropylene hollow fiber membranes for sweeping gas membrane distillation of ethylene glycol solution. *Chinese Journal of Chemical Engineering* 28(12), 3002-3010.

Alder, C.M., Hayler, J.D., Henderson, R.K., Redman, A.M., Shukla, L., Shuster, L.E. and Sneddon, H.F. (2016) Updating and further expanding GSK's solvent sustainability guide. *Green Chemistry* 18(13), 3879-3890.

Alftessi, S.A., Othman, M.H.D., Adam, M.R., Farag, T.M., Mustafa, A., Matsuura, T., Jaafar, J., Rahman, M.A. and Ismail, A.F. (2022) Omniphobic surface modification of silica sand ceramic hollow fiber membrane for desalination via direct contact membrane distillation. *Desalination* 532, 115705.

Alkhudhiri, A., Darwish, N. and Hilal, N. (2012a) Membrane distillation: A comprehensive review. *Desalination* 287, 2-18.

Alkhudhiri, A., Darwish, N. and Hilal, N. (2012b) Treatment of high salinity solutions: Application of air gap membrane distillation. *Desalination* 287, 55-60.

AlMarzooqi, F.A., Bilad, M.R. and Arafat, H.A. (2016) Development of PVDF membranes for membrane distillation via vapour induced crystallisation. *European Polymer Journal* 77, 164-173.

Aloulou, H., Aloulou, W., Daramola, M.O. and Ben Amar, R. (2021) Silane-grafted sand membrane for the treatment of oily wastewater via air gap membrane distillation: Study of the efficiency in comparison with microfiltration and ultrafiltration ceramic membranes. *Materials Chemistry and Physics* 261, 124186.

Alsaadi, A.S., Alpatova, A., Lee, J.-G., Francis, L. and Ghaffour, N. (2018) Flashed-feed VMD configuration as a novel method for eliminating temperature polarization effect and enhancing water vapor flux. *Journal of Membrane Science* 563, 175-182.

Ameen, N.A.M., Ibrahim, S.S., Alsahy, Q.F. and Figoli, A. (2020) Highly Saline Water Desalination Using Direct Contact Membrane Distillation (DCMD): Experimental and Simulation Study. *Water* 12(6).

Anvari, A., Azimi Yancheshme, A., Kekre, K.M. and Ronen, A. (2020) State-of-the-art methods for overcoming temperature polarization in membrane distillation process: A review. *Journal of Membrane Science* 616, 118413.

Anvari, A., Kekre, K.M., Azimi Yancheshme, A., Yao, Y. and Ronen, A. (2019) Membrane distillation of high salinity water by induction heated thermally conducting membranes. *Journal of Membrane Science* 589, 117253.

Ashoor, B.B., Mansour, S., Giwa, A., Dufour, V. and Hasan, S.W. (2016) Principles and applications of direct contact membrane distillation (DCMD): A comprehensive review. *Desalination* 398, 222-246.

Baker, R.W. (2004) Overview of membrane science and technology. *Membrane technology and applications* 3, 1-14.

Bartels, J., Batista, A.G., Kroll, S., Maas, M. and Rezwan, K. (2019) Hydrophobic ceramic capillary membranes for versatile virus filtration. *Journal of Membrane Science* 570-571, 85-92.

Basile, A. and Napporn, T.W. (2020) Current trends and future developments on (bio-) membranes: membrane systems for hydrogen production.

Bera, B., Carrier, O., Backus, E.H., Bonn, M., Shahidzadeh, N. and Bonn, D. (2018) Counteracting interfacial energetics for wetting of hydrophobic surfaces in the presence of surfactants. *Langmuir* 34(41), 12344-12349.

Bindels, M. and Nelemans, B. (2021) Theoretical analysis of heat pump assisted air gap membrane distillation. *Desalination* 518, 115282.

- Bonyadi, S. and Chung, T.S. (2007) Flux enhancement in membrane distillation by fabrication of dual layer hydrophilic–hydrophobic hollow fiber membranes. *Journal of Membrane Science* 306(1), 134-146.
- Boretti, A. and Rosa, L. (2019) Reassessing the projections of the World Water Development Report. *npj Clean Water* 2(1), 15.
- Bouchrit, R., Boubakri, A., Hafiane, A. and Bouguecha, S.A.-T. (2015) Direct contact membrane distillation: Capability to treat hyper-saline solution. *Desalination* 376, 117-129.
- Camacho, L., Dumée, L., Zhang, J., Li, J.-d., Duke, M., Gomez, J. and Gray, S. (2013) Advances in Membrane Distillation for Water Desalination and Purification Applications. *Water* 5(1), 94-196.
- Capizzano, S., Frappa, M., Macedonio, F. and Drioli, E. (2022) A review on membrane distillation in process engineering: design and exergy equations, materials and wetting problems. *Frontiers of Chemical Science and Engineering* 16(5), 592-613.
- Carvalho, A.J.F., Curvelo, A.A.S. and Gandini, A. (2005) Surface chemical modification of thermoplastic starch: reactions with isocyanates, epoxy functions and stearyl chloride. *Industrial Crops and Products* 21(3), 331-336.
- Chandra Bhoumick, M., Paul, S., Roy, S. and Mitra, S. (2023) Selective Recovery of Ethyl Acetate by Air-Sparged Membrane Distillation Using Carbon Nanotube-Immobilized Membranes and Process Optimization via a Response Surface Approach. *Industrial & Engineering Chemistry Research*.
- Chandra Bhoumick, M., Roy, S. and Mitra, S. (2021) Enrichment of 1, 4-dioxane from water by sweep gas membrane distillation on nano-carbon immobilized membranes. *Separation and Purification Technology* 276, 119360.
- Chen, L.-H., Huang, A., Chen, Y.-R., Chen, C.-H., Hsu, C.-C., Tsai, F.-Y. and Tung, K.-L. (2018a) Omniphobic membranes for direct contact membrane distillation: Effective deposition of zinc oxide nanoparticles. *Desalination* 428, 255-263.
- Chen, Q., Muhammad, B., Akhtar, F.H., Ybyraiymkul, D., Muhammad, W.S., Li, Y. and Ng, K.C. (2020a) Thermo-economic analysis and optimization of a vacuum multi-effect membrane distillation system. *Desalination* 483, 114413.
- Chen, W., Karde, V., Cheng, T.N.H., Ramli, S.S. and Heng, J.Y.Y. (2021) Surface hydrophobicity: effect of alkyl chain length and network homogeneity. *Frontiers of Chemical Science and Engineering* 15(1), 90-98.
- Chen, X., Boo, C. and Yip, N.Y. (2020b) Transport and structural properties of osmotic membranes in high-salinity desalination using cascading osmotically mediated reverse osmosis. *Desalination* 479, 114335.
- Chen, X., Chen, T., Li, J., Qiu, M., Fu, K., Cui, Z., Fan, Y. and Drioli, E. (2019) Ceramic nanofiltration and membrane distillation hybrid membrane processes for the purification

and recycling of boric acid from simulative radioactive waste water. *Journal of Membrane Science* 579, 294-301.

Chen, X., Gao, X., Fu, K., Qiu, M., Xiong, F., Ding, D., Cui, Z., Wang, Z., Fan, Y. and Drioli, E. (2018b) Tubular hydrophobic ceramic membrane with asymmetric structure for water desalination via vacuum membrane distillation process. *Desalination* 443, 212-220.

Chen, Y., Wang, Z., Jennings, G.K. and Lin, S. (2017) Probing pore wetting in membrane distillation using impedance: early detection and mechanism of surfactant-induced wetting. *Environmental Science & Technology Letters* 4(11), 505-510.

Cheng, H.-H., Liu, C.-B., Lei, Y.-Y., Chiu, Y.-C., Mangalindan, J., Wu, C.-H., Wu, Y.-J. and Whang, L.-M. (2019) Biological treatment of DMSO-containing wastewater from semiconductor industry under aerobic and methanogenic conditions. *Chemosphere* 236, 124291.

Cheng, L., Zhao, Y., Li, P., Li, W. and Wang, F. (2018) Comparative study of air gap and permeate gap membrane distillation using internal heat recovery hollow fiber membrane module. *Desalination* 426, 42-49.

Cheng, X., Wodarczyk, M., Lendzinski, R., Peterkin, E. and Burlingame, G.A. (2009) Control of DMSO in wastewater to prevent DMS nuisance odors. *Water Research* 43(12), 2989-2998.

Chew, N.G.P., Zhang, Y., Goh, K., Ho, J.S., Xu, R. and Wang, R. (2019a) Hierarchically structured Janus membrane surfaces for enhanced membrane distillation performance. *ACS Applied Materials & Interfaces* 11(28), 25524-25534.

Chew, N.G.P., Zhao, S., Loh, C.H., Permogorov, N. and Wang, R. (2017) Surfactant effects on water recovery from produced water via direct-contact membrane distillation. *Journal of Membrane Science* 528, 126-134.

Chew, N.G.P., Zhao, S. and Wang, R. (2019b) Recent advances in membrane development for treating surfactant- and oil-containing feed streams via membrane distillation. *Adv Colloid Interface Sci* 273, 102022.

Chong, J.Y. and Wang, R. (2019) From micro to nano: Polyamide thin film on microfiltration ceramic tubular membranes for nanofiltration. *Journal of Membrane Science* 587.

Choudhury, M.R., Anwar, N., Jassby, D. and Rahaman, M.S. (2019) Fouling and wetting in the membrane distillation driven wastewater reclamation process – A review. *Advances in Colloid and Interface Science* 269, 370-399.

Chul Woo, Y., Chen, Y., Tijing, L.D., Phuntsho, S., He, T., Choi, J.-S., Kim, S.-H. and Kyong Shon, H. (2017) CF₄ plasma-modified omniphobic electrospun nanofiber membrane for produced water brine treatment by membrane distillation. *Journal of Membrane Science* 529, 234-242.

- Ciora, R. and Liu, P.K. (2003) Ceramic membranes for environmental related applications. *Fluid/Particle Separation Journal* 15(1), 51-60.
- Cong, S., Liu, X. and Guo, F. (2019) Membrane distillation using surface modified multi-layer porous ceramics. *International Journal of Heat and Mass Transfer* 129, 764-772.
- Cui, Z., Pan, J., Wang, Z., Frappa, M., Drioli, E. and Macedonio, F. (2020) Hyflon/PVDF membranes prepared by NIPS and TIPS: Comparison in MD performance. *Separation and Purification Technology* 247, 116992.
- Dai, X., Wei, Q., Wang, Y., Li, Q., Cui, S. and Nie, Z. (2022) A novel strategy to enhance the desalination stability of FAS (fluoroalkylsilane)-modified ceramic membranes via constructing a porous SiO₂@PDMS (polydimethylsiloxane) protective layer on their top. *Chemical Engineering Journal* 435, 134757.
- Dao, T.D., Laborie, S. and Cabassud, C. (2016) Direct As (III) removal from brackish groundwater by vacuum membrane distillation: effect of organic matter and salts on membrane fouling. *Separation and Purification Technology* 157, 35-44.
- Ding, D., Mao, H., Chen, X., Qiu, M. and Fan, Y. (2018) Underwater superoleophobic-underoil superhydrophobic Janus ceramic membrane with its switchable separation in oil/water emulsions. *Journal of Membrane Science* 565, 303-310.
- Dong, Y., Ma, L., Tang, C.Y., Yang, F., Quan, X., Jassby, D., Zaworotko, M.J. and Guiver, M.D. (2018) Stable Superhydrophobic Ceramic-Based Carbon Nanotube Composite Desalination Membranes. *Nano Letters* 18(9), 5514-5521.
- Dong, Z.-Q., Wang, B.-J., Ma, X.-h., Wei, Y.-M. and Xu, Z.-L. (2015) FAS Grafted Electrospun Poly(vinyl alcohol) Nanofiber Membranes with Robust Superhydrophobicity for Membrane Distillation. *ACS Applied Materials & Interfaces* 7(40), 22652-22659.
- Du, Y., Wang, D., Wang, W., Fu, J., Chen, X., Wang, L., Yang, W. and Zhang, X. (2019) Electrospun Nanofibrous Polyphenylene Oxide Membranes for High-Salinity Water Desalination by Direct Contact Membrane Distillation. *ACS Sustainable Chemistry & Engineering* 7(24), 20060-20069.
- El-Bourawi, M.S., Ding, Z., Ma, R. and Khayet, M. (2006) A framework for better understanding membrane distillation separation process. *Journal of Membrane Science* 285(1), 4-29.
- Eryildiz, B., Yuksekdog, A., Korkut, S., Zeytuncu, B., Pasaoglu, M.E. and Koyuncu, I. (2020) Effect of operating parameters on removal of boron from wastewater containing high boron concentration by vacuum assisted air gap membrane distillation. *Journal of Water Process Engineering* 38, 101579.
- Eykens, L., De Sitter, K., Dotremont, C., Pinoy, L. and Van der Bruggen, B. (2016a) How To Optimize the Membrane Properties for Membrane Distillation: A Review. *Industrial & Engineering Chemistry Research* 55(35), 9333-9343.

Eykens, L., Reyns, T., De Sitter, K., Dotremont, C., Pinoy, L. and Van der Bruggen, B. (2016b) How to select a membrane distillation configuration? Process conditions and membrane influence unraveled. *Desalination* 399, 105-115.

Fadhil, S., Marino, T., Makki, H.F., Alsahy, Q.F., Blefari, S., Macedonio, F., Nicolò, E.D., Giorno, L., Drioli, E. and Figoli, A. (2016) Novel PVDF-HFP flat sheet membranes prepared by triethyl phosphate (TEP) solvent for direct contact membrane distillation. *Chemical Engineering and Processing: Process Intensification* 102, 16-26.

Fahmey, M.S., El-Aassar, A.-H.M., M.Abo-Elfadel, M., Orabi, A.S. and Das, R. (2019) Comparative performance evaluations of nanomaterials mixed polysulfone: A scale-up approach through vacuum enhanced direct contact membrane distillation for water desalination. *Desalination* 451, 111-116.

Fan, T., Li, Z., Cheng, B. and Li, J. (2018) Preparation, characterization of PPS microporous membranes and their excellent performance in vacuum membrane distillation. *Journal of Membrane Science* 556, 107-117.

Fane, A.G., Schofield, R. and Fell, C.J.D. (1987) The efficient use of energy in membrane distillation. *Desalination* 64, 231-243.

Fane, A.G., Tang, C.Y. and Wang, R. (2011) *Treatise on Water Science*. Wilderer, P. (ed), pp. 301-335, Elsevier, Oxford.

Fang, C., Garcia-Rodriguez, O., Shang, C., Imbrogno, J., Swenson, T.M., Lefebvre, O. and Zhang, S. (2023) An omniphobic membrane with macro-corrugation for the treatment of real pharmaceutical wastewater via membrane distillation. *Journal of Membrane Science*, 121582.

Fang, H., Gao, J., Wang, H. and Chen, C. (2012) Hydrophobic porous alumina hollow fiber for water desalination via membrane distillation process. *Journal of Membrane Science* 403, 41-46.

Farid, M.U., Kharraz, J.A., Lee, C.-H., Fang, J.K.-H., St-Hilaire, S. and An, A.K. (2022) Nanobubble-assisted scaling inhibition in membrane distillation for the treatment of high-salinity brine. *Water Research* 209, 117954.

Feng, S., Zhong, Z., Wang, Y., Xing, W. and Drioli, E. (2018) Progress and perspectives in PTFE membrane: Preparation, modification, and applications. *Journal of Membrane Science* 549, 332-349.

Figoli, A., Ursino, C., Galiano, F., Di Nicolò, E., Campanelli, P., Carnevale, M.C. and Criscuoli, A. (2017) Innovative hydrophobic coating of perfluoropolyether (PFPE) on commercial hydrophilic membranes for DCMD application. *Journal of Membrane Science* 522, 192-201.

Francis, L., Ahmed, F.E. and Hilal, N. (2022a) Advances in Membrane Distillation Module Configurations. *Membranes* 12(1), 81.

- Francis, L., Ahmed, F.E. and Hilal, N. (2022b) Electrospun membranes for membrane distillation: The state of play and recent advances. *Desalination* 526, 115511.
- Francis, L., Ghaffour, N., Al-Saadi, A.S. and Amy, G.L. (2015) Submerged membrane distillation for seawater desalination. *Desalination and Water Treatment* 55(10), 2741-2746.
- Francis, L., Ghaffour, N., Alsaadi, A.A. and Amy, G.L. (2013) Material gap membrane distillation: A new design for water vapor flux enhancement. *Journal of Membrane Science* 448, 240-247.
- Fukuda, Y., Miyamae, K. and Sasanuma, Y. (2017) Computational design of polymers: poly (ester amide) and polyurethane. *RSC Advances* 7(61), 38387-38398.
- García-Fernández, L., Wang, B., García-Payo, M.C., Li, K. and Khayet, M. (2017) Morphological design of alumina hollow fiber membranes for desalination by air gap membrane distillation. *Desalination* 420, 226-240.
- Geissler, A., Loyal, F., Biesalski, M. and Zhang, K. (2014) Thermo-responsive superhydrophobic paper using nanostructured cellulose stearoyl ester. *Cellulose* 21(1), 357-366.
- Ghaffour, N., Soukane, S., Lee, J.G., Kim, Y. and Alpatova, A. (2019) Membrane distillation hybrids for water production and energy efficiency enhancement: A critical review. *Applied Energy* 254, 113698.
- Gholamzadeh, N., Peyravi, M., Jahanshahi, M., Hoseinpour, H. and Rad, A.S. (2017) Developing PES membrane by modified Co₃O₄-OA nanoparticles for direct contact membrane distillation process. *Asia - Pacific Journal of Chemical Engineering* 12(4), 582-594.
- Ghorabi, S., Ashtiani, F.Z., Karimi, M., Fouladitajar, A., Yousefi, B. and Dorkalam, F. (2021) Development of a novel dual-bioinspired method for synthesis of a hydrophobic/hydrophilic polyethersulfone coated membrane for membrane distillation. *Desalination* 517, 115242.
- Giannetti, E. (2001) Semi - crystalline fluorinated polymers. *Polymer international* 50(1), 10-26.
- González, D., Amigo, J. and Suárez, F. (2017) Membrane distillation: Perspectives for sustainable and improved desalination. *Renewable and Sustainable Energy Reviews* 80, 238-259.
- Gryta, M. (2016) The study of performance of polyethylene chlorinetrifluoroethylene membranes used for brine desalination by membrane distillation. *Desalination* 398, 52-63.
- Gunka, S., Verbych, S., Bryk, M. and Hilal, N. (2006) Concentration of apple juice using direct contact membrane distillation. *Desalination* 190(1-3), 117-124.

Guo, F., Servi, A., Liu, A., Gleason, K.K. and Rutledge, G.C. (2015) Desalination by Membrane Distillation using Electrospun Polyamide Fiber Membranes with Surface Fluorination by Chemical Vapor Deposition. *ACS Applied Materials & Interfaces* 7(15), 8225-8232.

Guo, W.F., Chung, T.S., Matsuura, T., Wang, R. and Liu, Y. (2004) Pervaporation study of water and tert - butanol mixtures. *Journal of Applied Polymer Science* 91(6), 4082-4090.

Guo, Y., Qi, W., Fu, K., Chen, X., Qiu, M. and Fan, Y. (2022) Permeability and Stability of Hydrophobic Tubular Ceramic Membrane Contactor for CO₂ Desorption from MEA Solution. *Membranes* 12(1), 8.

Gupta, O., Roy, S. and Mitra, S. (2018) Enhanced membrane distillation of organic solvents from their aqueous mixtures using a carbon nanotube immobilized membrane. *Journal of Membrane Science* 568, 134-140.

Gurav, A.B., Latthe, S.S., Vhatkar, R.S., Lee, J.-G., Kim, D.-Y., Park, J.-J. and Yoon, S.S. (2014) Superhydrophobic surface decorated with vertical ZnO nanorods modified by stearic acid. *Ceramics International* 40(5), 7151-7160.

He, S.-Y., Lin, Y.-H., Hou, K.-Y. and Hwang, S.-C.J. (2011) Degradation of dimethylsulfoxide-containing wastewater using airlift bioreactor by polyvinyl-alcohol-immobilized cell beads. *Bioresource Technology* 102(10), 5609-5616.

Hebbar, R.S., Isloor, A.M. and Ismail, A.F. (2017) Membrane Characterization. Hilal, N., Ismail, A.F., Matsuura, T. and Oatley-Radcliffe, D. (eds), pp. 219-255, Elsevier.

Heinze, T. and Liebert, T. (2012) Polymer Science: A Comprehensive Reference. Matyjaszewski, K. and Möller, M. (eds), pp. 83-152, Elsevier, Amsterdam.

Hendren, Z.D., Brant, J. and Wiesner, M.R. (2009) Surface modification of nanostructured ceramic membranes for direct contact membrane distillation. *Journal of Membrane Science* 331(1), 1-10.

Horváth, D., Matolcsy, K., Szita, K. and Zajáros, A. (2017) Life Cycle Sustainability Assessment of DMSO Solvent Recovery from Hazardous Waste Water. *Periodica Polytechnica Chemical Engineering* 62(3), 305-309.

Hosseini, M. and Ameri, E. (2017) Pervaporation characteristics of a PDMS/PMHS membrane for removal of dimethyl sulfoxide from aqueous solutions. *Vacuum* 141, 288-295.

Hou, D., Wang, J., Qu, D., Luan, Z. and Ren, X. (2009) Fabrication and characterization of hydrophobic PVDF hollow fiber membranes for desalination through direct contact membrane distillation. *Separation and Purification Technology* 69(1), 78-86.

Huang, K., Liu, G., Lou, Y., Dong, Z., Shen, J. and Jin, W. (2014) A graphene oxide membrane with highly selective molecular separation of aqueous organic solution. *Angew Chem Int Ed Engl* 53(27), 6929-6932.

Huang, Y., Huang, Q.-L., Liu, H., Zhang, C.-X., You, Y.-W., Li, N.-N. and Xiao, C.-F. (2017) Preparation, characterization, and applications of electrospun ultrafine fibrous PTFE porous membranes. *Journal of Membrane Science* 523, 317-326.

Hubadillah, S.K., Othman, M.H.D., Ismail, A.F., Rahman, M.A. and Jaafar, J. (2019a) A low cost hydrophobic kaolin hollow fiber membrane (h-KHFM) for arsenic removal from aqueous solution via direct contact membrane distillation. *Separation and Purification Technology* 214, 31-39.

Hubadillah, S.K., Othman, M.H.D., Kadir, S.H.S.A., Jamalludin, M.R., Harun, Z., Abd Aziz, M.H., Rahman, M.A., Jaafar, J., Nomura, M. and Honda, S. (2019b) Removal of As (III) and As (V) from water using green, silica-based ceramic hollow fibre membranes via direct contact membrane distillation. *RSC Advances* 9(6), 3367-3376.

Hussain, A., Janson, A., Matar, J.M. and Adham, S. (2022) Membrane distillation: recent technological developments and advancements in membrane materials. *Emergent Materials* 5(2), 347-367.

Hussein, S.S., Ibrahim, S.S., Toma, M.A., Alsahy, Q.F. and Drioli, E. (2020) Novel chemical modification of polyvinyl chloride membrane by free radical graft copolymerization for direct contact membrane distillation (DCMD) application. *Journal of Membrane Science* 611, 118266.

Hwang, S., Lin, Y., Chang, Y. and He, S. (2012) Effect of microbial activity on dimethyl sulfoxide degradation in an air-lift bioreactor. *WIT Transactions on Ecology and the Environment* 163, 403-413.

Jafari, A., Kebria, M.R.S., Rahimpour, A. and Bakeri, G. (2018) Graphene quantum dots modified polyvinylidene fluoride (PVDF) nanofibrous membranes with enhanced performance for air Gap membrane distillation. *Chemical Engineering and Processing - Process Intensification* 126, 222-231.

Janajreh, I., El Kadi, K., Hashaikeh, R. and Ahmed, R. (2017) Numerical investigation of air gap membrane distillation (AGMD): Seeking optimal performance. *Desalination* 424, 122-130.

Javier, L., Pulido-Beltran, L., Vrouwenvelder, J.S. and Farhat, N.M. (2022) Permeation Increases Biofilm Development in Nanofiltration Membranes Operated with Varying Feed Water Phosphorous Concentrations. *Membranes* 12(3), 335.

Ji, B., Kang, P., Wei, T. and Zhao, Y. (2020) Challenges of aqueous per- and polyfluoroalkyl substances (PFASs) and their foreseeable removal strategies. *Chemosphere* 250, 126316.

Ji, H., Zhang, G., Teng, L., Xing, J., Jia, X., Luo, H., Shen, S., Zhou, X., Liu, D. and Wyman, I. (2021) Fabrication of aramid-coated asymmetric PVDF membranes towards acidic and alkaline solutions concentration via direct contact membrane distillation. *Applied Surface Science* 562, 150185.

Jia, F., Yin, Y. and Wang, J. (2018) Removal of cobalt ions from simulated radioactive wastewater by vacuum membrane distillation. *Progress in Nuclear Energy* 103, 20-27.

Jones, E., Qadir, M., van Vliet, M.T.H., Smakhtin, V. and Kang, S.-m. (2019) The state of desalination and brine production: A global outlook. *Science of The Total Environment* 657, 1343-1356.

Jones, E.R., Van Vliet, M.T., Qadir, M. and Bierkens, M.F. (2021) Country-level and gridded estimates of wastewater production, collection, treatment and reuse. *Earth System Science Data* 13(2), 237-254.

Ju, J., Li, Z., Lv, Y., Liu, M., Fejjari, K., Kang, W. and Liao, Y. (2020) Electrospun PTFE/PI bi-component membranes with robust 3D superhydrophobicity and high water permeability for membrane distillation. *Journal of Membrane Science* 611, 118420.

Kalla, S., Upadhyaya, S. and Singh, K. (2019) Principles and advancements of air gap membrane distillation. *Reviews in Chemical Engineering* 35(7), 817-859.

Kastner, J.R., Miller, J., Geller, D.P., Locklin, J., Keith, L.H. and Johnson, T. (2012) Catalytic esterification of fatty acids using solid acid catalysts generated from biochar and activated carbon. *Catalysis Today* 190(1), 122-132.

Kebria, M.R.S. and Rahimpour, A. (2020) Membrane distillation: basics, advances, and applications. *Advances in membrane technologies*.

Keurentjes, J., Harbrecht, J., Brinkman, D., Hanemaaijer, J., Stuart, M.C. and Van't Riet, K. (1989) Hydrophobicity measurements of microfiltration and ultrafiltration membranes. *Journal of Membrane Science* 47(3), 333-344.

Khaisri, S., deMontigny, D., Tontiwachwuthikul, P. and Jiraratananon, R. (2009) Comparing membrane resistance and absorption performance of three different membranes in a gas absorption membrane contactor. *Separation and Purification Technology* 65(3), 290-297.

Khayet, M. (2011) Membranes and theoretical modeling of membrane distillation: A review. *Advances in Colloid and Interface Science* 164(1), 56-88.

Khayet, M. (2013) Treatment of radioactive wastewater solutions by direct contact membrane distillation using surface modified membranes. *Desalination* 321, 60-66.

Khayet, M., García-Payo, C. and Matsuura, T. (2019) Superhydrophobic nanofibers electrospun by surface segregating fluorinated amphiphilic additive for membrane distillation. *Journal of Membrane Science* 588, 117215.

Khayet, M. and Matsuura, T. (2001) Preparation and Characterization of Polyvinylidene Fluoride Membranes for Membrane Distillation. *Industrial & Engineering Chemistry Research* 40(24), 5710-5718.

Khayet, M. and Matsuura, T. (2011) Membrane Distillation. Khayet, M. and Matsuura, T. (eds), pp. 1-16, Elsevier, Amsterdam.

Khayet, M., Suk, D., Narbaitz, R., Santerre, J. and Matsuura, T. (2003) Study on surface modification by surface - modifying macromolecules and its applications in membrane - separation processes. *Journal of Applied Polymer Science* 89(11), 2902-2916.

Khayet, M. and Wang, R. (2018) Mixed Matrix Polytetrafluoroethylene/Polysulfone Electrospun Nanofibrous Membranes for Water Desalination by Membrane Distillation. *ACS Applied Materials & Interfaces* 10(28), 24275-24287.

Khemakhem, M., Khemakhem, S. and Amar, R.B. (2013) Emulsion separation using hydrophobic grafted ceramic membranes by. *Colloids and Surfaces A: Physicochemical and Engineering Aspects* 436, 402-407.

Khemakhem, S. and Amar, R.B. (2011) Grafting of fluoroalkylsilanes on microfiltration Tunisian clay membrane. *Ceramics International* 37(8), 3323-3328.

Klinov, A.V., Akberov, R.R., Fazlyev, A.R. and Farakhov, M.I. (2017) Experimental investigation and modeling through using the solution-diffusion concept of pervaporation dehydration of ethanol and isopropanol by ceramic membranes HybSi. *Journal of Membrane Science* 524, 321-333.

Ko, C.-C., Ali, A., Drioli, E., Tung, K.-L., Chen, C.-H., Chen, Y.-R. and Macedonio, F. (2018) Performance of ceramic membrane in vacuum membrane distillation and in vacuum membrane crystallization. *Desalination* 440, 48-58.

Kolesnichenko, I.V., Goloverda, G.Z. and Kolesnichenko, V.L. (2019) A Versatile Method of Ambient-Temperature Solvent Removal. *Organic Process Research & Development* 24(1), 25-31.

Kong, Z., Li, L., Xue, Y., Yang, M. and Li, Y.-Y. (2019) Challenges and prospects for the anaerobic treatment of chemical-industrial organic wastewater: A review. *Journal of Cleaner Production* 231, 913-927.

Koonaphapdeelert, S. and Li, K. (2007) Preparation and characterization of hydrophobic ceramic hollow fibre membrane. *Journal of Membrane Science* 291(1-2), 70-76.

Kujawa, J., Al-Gharabli, S., Kujawski, W. and Knozowska, K. (2017) Molecular Grafting of Fluorinated and Nonfluorinated Alkylsiloxanes on Various Ceramic Membrane Surfaces for the Removal of Volatile Organic Compounds Applying Vacuum Membrane Distillation. *ACS Applied Materials & Interfaces* 9(7), 6571-6590.

- Kujawa, J., Kujawski, W., Cerneaux, S., Li, G. and Al-Gharabli, S. (2020) Zirconium dioxide membranes decorated by silanes based-modifiers for membrane distillation–Material chemistry approach. *Journal of Membrane Science* 596, 117597.
- Kujawa, J., Kujawski, W., Koter, S., Jarzynka, K., Rozicka, A., Bajda, K., Cerneaux, S., Persin, M. and Larbot, A. (2013) Membrane distillation properties of TiO₂ ceramic membranes modified by perfluoroalkylsilanes. *Desalination and Water Treatment* 51(7-9), 1352-1361.
- Kujawski, W., Krajewska, S., Kujawski, M., Gazagnes, L., Larbot, A. and Persin, M. (2007) Pervaporation properties of fluoroalkylsilane (FAS) grafted ceramic membranes. *Desalination* 205(1), 75-86.
- Kujawski, W., Kujawa, J., Wierzbowska, E., Cerneaux, S., Bryjak, M. and Kujawski, J. (2016) Influence of hydrophobization conditions and ceramic membranes pore size on their properties in vacuum membrane distillation of water–organic solvent mixtures. *Journal of Membrane Science* 499, 442-451.
- Laganà, F., Barbieri, G. and Drioli, E. (2000) Direct contact membrane distillation: modelling and concentration experiments. *Journal of Membrane Science* 166(1), 1-11.
- Lalia, B.S., Guillen-Burrieza, E., Arafat, H.A. and Hashaikeh, R. (2013) Fabrication and characterization of polyvinylidene fluoride-co-hexafluoropropylene (PVDF-HFP) electrospun membranes for direct contact membrane distillation. *Journal of Membrane Science* 428, 104-115.
- Law, K.-Y. (2014) Definitions for Hydrophilicity, Hydrophobicity, and Superhydrophobicity: Getting the Basics Right. *The Journal of Physical Chemistry Letters* 5(4), 686-688.
- Le, N.L. and Nunes, S.P. (2016) Materials and membrane technologies for water and energy sustainability. *Sustainable Materials and Technologies* 7, 1-28.
- Leeper, S., Abdel-Karim, A., Gad-Allah, T.A. and Gorgojo, P. (2019) Air-gap membrane distillation as a one-step process for textile wastewater treatment. *Chemical Engineering Journal* 360, 1330-1340.
- Lee, T., Min, C., Naidu, G., Huang, Y., Shon, H.K. and Kim, S.-H. (2022) Optimizing the performance of sweeping gas membrane distillation for treating naturally heated saline groundwater. *Desalination* 532, 115736.
- Li, C., Li, X., Du, X., Zhang, Y., Wang, W., Tong, T., Kota, A.K. and Lee, J. (2020a) Elucidating the Trade-off between Membrane Wetting Resistance and Water Vapor Flux in Membrane Distillation. *Environmental Science & Technology* 54(16), 10333-10341.
- Li, G. (2010) Thermal stability of DMSO and vapor liquid equilibrium of DMSO aqueous solution, Beijing University of Chemical Technology.

- Li, H., Shi, W., Zeng, X., Huang, S., Zhang, H. and Qin, X. (2020b) Improved desalination properties of hydrophobic GO-incorporated PVDF electrospun nanofibrous composites for vacuum membrane distillation. *Separation and Purification Technology* 230, 115889.
- Li, W., Estager, J., Monbaliu, J.C.M., Debecker, D.P. and Luis, P. (2020c) Separation of bio - based chemicals using pervaporation. *Journal of Chemical Technology & Biotechnology* 95(9), 2311-2334.
- Li, X., Shan, H., Cao, M. and Li, B. (2019) Facile fabrication of omniphobic PVDF composite membrane via a waterborne coating for anti-wetting and anti-fouling membrane distillation. *Journal of Membrane Science* 589, 117262.
- Liao, Y., Wang, R., Tian, M., Qiu, C. and Fane, A.G. (2013a) Fabrication of polyvinylidene fluoride (PVDF) nanofiber membranes by electro-spinning for direct contact membrane distillation. *Journal of Membrane Science* 425-426, 30-39.
- Liao, Y., Wang, R., Tian, M., Qiu, C.Q. and Fane, A.G. (2013b) Fabrication of polyvinylidene fluoride (PVDF) nanofiber membranes by electro-spinning for direct contact membrane distillation. *Journal of Membrane Science* 425, 30-39.
- Lide, D.R. (2004) *CRC handbook of chemistry and physics*, CRC press.
- Lim, Y.J., Goh, K., Kurihara, M. and Wang, R. (2021) Seawater desalination by reverse osmosis: Current development and future challenges in membrane fabrication – A review. *Journal of Membrane Science* 629, 119292.
- Liu, L., Shen, F., Chen, X., Luo, J., Su, Y., Wu, H. and Wan, Y. (2016a) A novel plasma-induced surface hydrophobization strategy for membrane distillation: Etching, dipping and grafting. *Journal of Membrane Science* 499, 544-554.
- Liu, L., Shen, F., Zhang, B., Jiang, H., Li, J., Luo, J., Wu, H., Khan, R. and Wan, Y. (2016b) Fabrication of PES-based membranes with a high and stable desalination performance for membrane distillation. *RSC advances* 6(109), 107840-107850.
- Lu, K.J., Chen, Y. and Chung, T.-S. (2019) Design of omniphobic interfaces for membrane distillation – A review. *Water Research* 162, 64-77.
- Luo, Q., Ren, T., Shen, H., Zhang, J. and Liang, D. (2018) The thermal properties of nitrocellulose: from thermal decomposition to thermal explosion. *Combustion Science and Technology* 190(4), 579-590.
- Marchetti, P., Jimenez Solomon, M.F., Szekely, G. and Livingston, A.G. (2014) Molecular separation with organic solvent nanofiltration: a critical review. *Chemical reviews* 114(21), 10735-10806.
- Marni Sandid, A., Bassyouni, M., Nehari, D. and Elhenawy, Y. (2021) Experimental and simulation study of multichannel air gap membrane distillation process with two types of solar collectors. *Energy Conversion and Management* 243, 114431.

- McCarthy, C., Kappleman, W. and DiGuisseppi, W. (2017) Ecological Considerations of Per- and Polyfluoroalkyl Substances (PFAS). *Current Pollution Reports* 3(4), 289-301.
- Meng, S., Hsu, Y.-C., Ye, Y. and Chen, V. (2015) Submerged membrane distillation for inland desalination applications. *Desalination* 361, 72-80.
- Mohamed, E.S., Boutikos, P., Mathioulakis, E. and Belessiotis, V. (2017) Experimental evaluation of the performance and energy efficiency of a Vacuum Multi-Effect Membrane Distillation system. *Desalination* 408, 70-80.
- Moo-Tun, N.M., Valadez-Gonzalez, A. and Uribe-Calderon, J.A. (2019) Thermo-Oxidative Aging of LDPE/Stearoyl Chloride-Grafted Cellulose Nanocrystals Blown Films. *Journal of Polymers and the Environment* 27(6), 1226-1239.
- Mountford, P. (2010) *Green Chemistry in the Pharmaceutical Industry*. Dunn, PJ, 145-160.
- Mousavi, S.A., Arab Aboosadi, Z., Mansourizadeh, A. and Honarvar, B. (2021) Surface modified porous polyetherimide hollow fiber membrane for sweeping gas membrane distillation of dyeing wastewater. *Colloids and Surfaces A: Physicochemical and Engineering Aspects* 610, 125439.
- Munirasu, S., Banat, F., Durrani, A.A. and Haija, M.A. (2017) Intrinsically superhydrophobic PVDF membrane by phase inversion for membrane distillation. *Desalination* 417, 77-86.
- Nagy, E. (2019) *Basic Equations of Mass Transport Through a Membrane Layer (Second Edition)*. Nagy, E. (ed), pp. 483-496, Elsevier.
- Nguyen, H.T., Bui, H.M., Wang, Y.-F. and You, S.-J. (2022) Non-fluoroalkyl functionalized hydrophobic surface modifications used in membrane distillation for cheaper and more environmentally friendly applications: A mini-review. *Sustainable Chemistry and Pharmacy* 28, 100714.
- Nishimura, M., Nakayama, M. and Yano, T. (1972) Vapor pressure of pure DMSO and vapor-liquid equilibria in DMSO-H₂O system under isobaric conditions. *Journal of Chemical Engineering of Japan* 5(3), 223-226.
- Ozbey-Unal, B., Imer, D.Y., Keskinler, B. and Koyuncu, I. (2018) Boron removal from geothermal water by air gap membrane distillation. *Desalination* 433, 141-150.
- Pagliero, M., Bottino, A., Comite, A. and Costa, C. (2020) Silanization of tubular ceramic membranes for application in membrane distillation. *Journal of Membrane Science* 601, 117911.
- Pan, J., Xiao, C., Huang, Q., Liu, H. and Hu, J. (2015) ECTFE porous membranes with conveniently controlled microstructures for vacuum membrane distillation. *Journal of Materials Chemistry A* 3(46), 23549-23559.

- Peng, J., Yan, J., Chen, Q., Jiang, X., Yao, G. and Lai, B. (2018) Natural mackinawite catalytic ozonation for N, N-dimethylacetamide (DMAC) degradation in aqueous solution: Kinetic, performance, biotoxicity and mechanism. *Chemosphere* 210, 831-842.
- Peng, Y., Dong, Y., Fan, H., Chen, P., Li, Z. and Jiang, Q. (2013) Preparation of polysulfone membranes via vapor-induced phase separation and simulation of direct-contact membrane distillation by measuring hydrophobic layer thickness. *Desalination* 316, 53-66.
- Peng, Y., Fan, H., Dong, Y., Song, Y. and Han, H. (2012) Effects of exposure time on variations in the structure and hydrophobicity of polyvinylidene fluoride membranes prepared via vapor-induced phase separation. *Applied Surface Science* 258(20), 7872-7881.
- Picard, C., Larbot, A., Guida-Pietrasanta, F., Boutevin, B. and Ratsimihety, A. (2001) Grafting of ceramic membranes by fluorinated silanes: hydrophobic features. *Separation and Purification Technology* 25(1), 65-69.
- Prakash, G.K. and Mahadevan, K.M. (2008) Enhancing the properties of wood through chemical modification with palmitoyl chloride. *Applied Surface Science* 254(6), 1751-1756.
- Pruett, D. and Felker, L. (1985) Densities and apparent molar volumes in the binary system dimethyl sulfoxide-water at 25, 40, 60, and 65. degree. C. *Journal of Chemical and Engineering Data* 30(4), 452-455.
- Qaiser, A.A. and Hyland, M.M. (2010) X-ray photoelectron spectroscopy characterization of polyaniline-cellulose ester composite membranes, pp. 35-45, *Trans Tech Publ.*
- Qtaishat, M., Khayet, M. and Matsuura, T. (2009a) Novel porous composite hydrophobic/hydrophilic polysulfone membranes for desalination by direct contact membrane distillation. *Journal of Membrane Science* 341(1), 139-148.
- Qtaishat, M., Matsuura, T., Khayet, M. and Khulbe, K. (2009b) Comparing the desalination performance of SMM blended polyethersulfone to SMM blended polyetherimide membranes by direct contact membrane distillation. *Desalination and Water Treatment* 5(1-3), 91-98.
- Rastegarpanah, A. and Mortaheb, H.R. (2016) Surface treatment of polyethersulfone membranes for applying in desalination by direct contact membrane distillation. *Desalination* 377, 99-107.
- Ravi, J., Othman, M.H.D., Matsuura, T., Ro'il Bilad, M., El-badawy, T.H., Aziz, F., Ismail, A.F., Rahman, M.A. and Jaafar, J. (2020) Polymeric membranes for desalination using membrane distillation: A review. *Desalination* 490, 114530.
- Ravikumar, Y.V.L., Sridhar, S. and Satyanarayana, S.V. (2013) Development of an electro dialysis–distillation integrated process for separation of hazardous sodium azide to

recover valuable DMSO solvent from pharmaceutical effluent. *Separation and Purification Technology* 110, 20-30.

Ren, J., Li, Z. and Wong, F.-S. (2006) A new method for the prediction of pore size distribution and MWCO of ultrafiltration membranes. *Journal of Membrane Science* 279(1-2), 558-569.

Rezaei, M., Warsinger, D.M., Lienhard, V.J., Duke, M.C., Matsuura, T. and Samhaber, W.M. (2018) Wetting phenomena in membrane distillation: Mechanisms, reversal, and prevention. *Water Res* 139, 329-352.

Rezaei, M., Warsinger, D.M. and Samhaber, W.M. (2017) Wetting prevention in membrane distillation through superhydrophobicity and recharging an air layer on the membrane surface. *Journal of Membrane Science* 530, 42-52.

Roy, S. and Ragunath, S. (2018) Emerging Membrane Technologies for Water and Energy Sustainability: Future Prospects, Constraints and Challenges. *Energies* 11(11), 2997.

Ryu, S., Naidu, G., Johir, M.A.H., Choi, Y., Jeong, S. and Vigneswaran, S. (2019) Acid mine drainage treatment by integrated submerged membrane distillation–sorption system. *Chemosphere* 218, 955-965.

Said, I.A., Chomiak, T., Floyd, J. and Li, Q. (2020) Sweeping gas membrane distillation (SGMD) for wastewater treatment, concentration, and desalination: A comprehensive review. *Chemical Engineering and Processing-Process Intensification* 153, 107960.

Sarialp, G. (2012) Dehydration of aqueous aprotic solvent mixtures by pervaporation, Middle East Technical University.

Schofield, R.W., Fane, A.G. and Fell, C.J.D. (1990) Gas and vapour transport through microporous membranes. I. Knudsen-Poiseuille transition. *Journal of Membrane Science* 53(1), 159-171.

Servi, A.T., Kharraz, J., Klee, D., Notarangelo, K., Eyob, B., Guillen-Burrieza, E., Liu, A., Arafat, H.A. and Gleason, K.K. (2016) A systematic study of the impact of hydrophobicity on the wetting of MD membranes. *Journal of Membrane Science* 520, 850-859.

Shah, K.M., Billinge, I.H., Chen, X., Fan, H., Huang, Y., Winton, R.K. and Yip, N.Y. (2022) Drivers, challenges, and emerging technologies for desalination of high-salinity brines: A critical review. *Desalination* 538, 115827.

Shahu, V.T. and Thombre, S. (2019) Air gap membrane distillation: A review. *Journal of Renewable and Sustainable Energy* 11(4), 045901.

Shao, F., Hao, C., Ni, L., Zhang, Y., Du, R., Meng, J., Liu, Z. and Xiao, C. (2014) Experimental and theoretical research on N-methyl-2-pyrrolidone concentration by vacuum membrane distillation using polypropylene hollow fiber membrane. *Journal of Membrane Science* 452, 157-164.

Shi, W., Li, T., Fan, M., Li, H., Zhang, H. and Qin, X. (2022) Construction of rough and porous surface of hydrophobic PTFE powder-embedded PVDF hollow fiber composite membrane for accelerated water mass transfer of membrane distillation. *Journal of Industrial and Engineering Chemistry* 108, 328-343.

Shon, H., Phuntsho, S., Chaudhary, D., Vigneswaran, S. and Cho, J. (2013) Nanofiltration for water and wastewater treatment—a mini review. *Drinking Water Engineering and Science* 6(1), 47-53.

Sigma-Aldrich (2021a) 1H,1H,2H,2H-Perfluorodecyltriethoxysilane.

Sigma-Aldrich (2021b) Stearoyl chloride.

Sigma-Aldrich (2021c) Trimethoxy(octadecyl)silane.

Smallwood, I.M. (2002) *Solvent recovery handbook*, CRC Press.

Souhaimi, M.K. and Matsuura, T. (2011) *Membrane distillation: principles and applications*.

Srisurichan, S., Jiraratananon, R. and Fane, A.G. (2006) Mass transfer mechanisms and transport resistances in direct contact membrane distillation process. *Journal of Membrane Science* 277(1), 186-194.

Štirn, Ž., Čolović, M., Vasiljević, J., Šobak, M., Žitko, G., Čelan Korošin, N., Simončič, B. and Jerman, I. (2022) Effect of bridged DOPO/polyurethane nanocomposites on solar absorber coatings with reduced flammability. *Solar Energy* 231, 104-114.

Su, C., Li, Y., Cao, H., Lu, C., Li, Y., Chang, J. and Duan, F. (2019) Novel PTFE hollow fiber membrane fabricated by emulsion electrospinning and sintering for membrane distillation. *Journal of Membrane Science* 583, 200-208.

Suk, D.E., Chowdhury, G., Matsuura, T., Narbaitz, R.M., Santerre, P., Pleizier, G. and Deslandes, Y. (2002) Study on the Kinetics of Surface Migration of Surface Modifying Macromolecules in Membrane Preparation. *Macromolecules* 35(8), 3017-3021.

Suk, D.E., Matsuura, T., Park, H.B. and Lee, Y.M. (2010) Development of novel surface modified phase inversion membranes having hydrophobic surface-modifying macromolecule (nSMM) for vacuum membrane distillation. *Desalination* 261(3), 300-312.

Swaminathan, J., Chung, H.W., Warsinger, D.M., AlMarzooqi, F.A. and Arafat, H.A. (2016) Energy efficiency of permeate gap and novel conductive gap membrane distillation. *Journal of Membrane Science* 502, 171-178.

Tai, Z.S., Abd Aziz, M.H., Othman, M.H.D., Mohamed Dzahir, M.I.H., Hashim, N.A., Koo, K.N., Hubadillah, S.K., Ismail, A.F., A Rahman, M. and Jaafar, J. (2019) Ceramic Membrane Distillation for Desalination. *Separation & Purification Reviews*, 1-40.

Tai, Z.S., Abd Aziz, M.H., Othman, M.H.D., Mohamed Dzahir, M.I.H., Hashim, N.A., Koo, K.N., Hubadillah, S.K., Ismail, A.F., A Rahman, M. and Jaafar, J. (2020) Ceramic membrane distillation for desalination. *Separation & Purification Reviews* 49(4), 317-356.

Tai, Z.S., Othman, M.H.D., Mustafa, A., Ravi, J., Wong, K.C., Koo, K.N., Hubadillah, S.K., Azali, M.A., Alias, N.H., Ng, B.C., Mohamed Dzahir, M.I.H., Ismail, A.F., Rahman, M.A. and Jaafar, J. (2021) Development of hydrophobic polymethylhydrosiloxane/tetraethylorthosilicate (PMHS/TEOS) hybrid coating on ceramic membrane for desalination via membrane distillation. *Journal of Membrane Science* 637, 119609.

Tan, X. and Rodrigue, D. (2019a) A Review on Porous Polymeric Membrane Preparation. Part I: Production Techniques with Polysulfone and Poly (Vinylidene Fluoride). *Polymers* 11(7).

Tan, X. and Rodrigue, D. (2019b) A Review on Porous Polymeric Membrane Preparation. Part II: Production Techniques with Polyethylene, Polydimethylsiloxane, Polypropylene, Polyimide, and Polytetrafluoroethylene. *Polymers (Basel)* 11(8).

Tan, Y.Z., Chew, J.W. and Krantz, W.B. (2016) Effect of humic-acid fouling on membrane distillation. *Journal of Membrane Science* 504, 263-273.

Tang, J. and Sirkar, K.K. (2012) Perfluoropolymer membrane behaves like a zeolite membrane in dehydration of aprotic solvents. *Journal of Membrane Science* 421-422, 211-216.

Tang, N., Jia, Q., Zhang, H., Li, J. and Cao, S. (2010) Preparation and morphological characterization of narrow pore size distributed polypropylene hydrophobic membranes for vacuum membrane distillation via thermally induced phase separation. *Desalination* 256(1), 27-36.

Thakur, A.K., Hsieh, I.M., Islam, M.R., Lin, B., Chen, C.-C. and Malmali, M. (2020) Performance of sweeping gas membrane distillation for treating produced water: Modeling and experiments. *Desalination* 492, 114597.

Tian, M., Yin, Y., Yang, C., Zhao, B., Song, J., Liu, J., Li, X.-M. and He, T. (2015) CF₄ plasma modified highly interconnective porous polysulfone membranes for direct contact membrane distillation (DCMD). *Desalination* 369, 105-114.

Tian, M., Zhu, J., Yuan, S., Zhang, Y. and Van der Bruggen, B. (2021) A co-casting route enables the formation of skinless, hydrophobic poly (vinylidene fluoride) membranes for DCMD. *Journal of Membrane Science* 630, 119299.

Tong, T. and Elimelech, M. (2016) The Global Rise of Zero Liquid Discharge for Wastewater Management: Drivers, Technologies, and Future Directions. *Environmental Science & Technology* 50(13), 6846-6855.

Tortajada, C. (2020) Contributions of recycled wastewater to clean water and sanitation Sustainable Development Goals. *npj Clean Water* 3(1), 22.

Twibi, M.F., Othman, M.H.D., Hubadillah, S.K., Alftessi, S.A., Adam, M.R.B., Ismail, A.F., Rahman, M.A., Jaafar, J., Raji, Y.O., Abd Aziz, M.H., Sokri, M.N.B.M., Abdullah, H. and Naim, R. (2021) Hydrophobic mullite ceramic hollow fibre membrane (Hy-MHFM) for seawater desalination via direct contact membrane distillation (DCMD). *Journal of the European Ceramic Society* 41(13), 6578-6585.

Van der Bruggen, B., Vandecasteele, C., Van Gestel, T., Doyen, W. and Leysen, R. (2003) A review of pressure - driven membrane processes in wastewater treatment and drinking water production. *Environmental progress* 22(1), 46-56.

Van Ness, H.C., Smith, J.M. and Abbott, M.M. (1996) *Introduction to chemical engineering thermodynamics*, McGraw-Hill New York.

van Veen, H.M., Rietkerk, M.D.A., Shanahan, D.P., van Tuel, M.M.A., Kreiter, R., Castricum, H.L., ten Elshof, J.E. and Vente, J.F. (2011) Pushing membrane stability boundaries with HybSi® pervaporation membranes. *Journal of Membrane Science* 380(1), 124-131.

Vieira, T., Carvalho Silva, J., Botelho do Rego, A.M., Borges, J.P. and Henriques, C. (2019) Electrospun biodegradable chitosan based-poly(urethane urea) scaffolds for soft tissue engineering. *Materials Science and Engineering: C* 103, 109819.

Villalobos Garcia, J., Dow, N., Milne, N., Zhang, J., Naidoo, L., Gray, S. and Duke, M. (2018) Membrane Distillation Trial on Textile Wastewater Containing Surfactants Using Hydrophobic and Hydrophilic-Coated Polytetrafluoroethylene (PTFE) Membranes. *Membranes (Basel)* 8(2).

Wang, D.-M. and Lai, J.-Y. (2013) Recent advances in preparation and morphology control of polymeric membranes formed by nonsolvent induced phase separation. *Current Opinion in Chemical Engineering* 2(2), 229-237.

Wang, J., Zheng, L., Wu, Z., Zhang, Y. and Zhang, X. (2016) Fabrication of hydrophobic flat sheet and hollow fiber membranes from PVDF and PVDF-CTFE for membrane distillation. *Journal of Membrane Science* 497, 183-193.

Wang, P. and Chung, T.-S. (2015) Recent advances in membrane distillation processes: Membrane development, configuration design and application exploring. *Journal of Membrane Science* 474, 39-56.

Wang, W., Du, X., Vahabi, H., Zhao, S., Yin, Y., Kota, A.K. and Tong, T. (2019a) Trade-off in membrane distillation with monolithic omniphobic membranes. *Nature Communications* 10(1), 3220.

Wang, W., Shi, Y., Zhang, C., Li, R., Wu, M., Zhuo, S., Aleid, S. and Wang, P. (2021) Solar Seawater Distillation by Flexible and Fully Passive Multistage Membrane Distillation. *Nano Letters* 21(12), 5068-5074.

Wang, X., Xiao, C., Liu, H., Huang, Q. and Fu, H. (2018) Fabrication and properties of PVDF and PVDF - HFP microfiltration membranes. *Journal of Applied Polymer Science* 135(40), 46711.

Wang, X., Yu, P., Zhang, K., Wu, M., Wu, Q., Liu, J., Yang, J. and Zhang, J. (2019b) Superhydrophobic/Superoleophilic Cotton for Efficient Oil–Water Separation Based on the Combined Octadecanoyl Chain Bonding and Polymer Grafting via Surface-Initiated ATRP. *ACS Applied Polymer Materials* 1(11), 2875-2882.

Wang, Y., Li, B. and Xu, C. (2012) Fabrication of superhydrophobic surface of hierarchical ZnO thin films by using stearic acid. *Superlattices and Microstructures* 51(1), 128-134.

Water, U. (2020) UN World Water Development Report 2020. United Nation: New York, NY, USA.

Wei, C.C. and Li, K. (2009) Preparation and Characterization of a Robust and Hydrophobic Ceramic Membrane via an Improved Surface Grafting Technique. *Industrial & Engineering Chemistry Research* 48(7), 3446-3452.

Wei, X., Zhao, B., Li, X.-M., Wang, Z., He, B.-Q., He, T. and Jiang, B. (2012) CF₄ plasma surface modification of asymmetric hydrophilic polyethersulfone membranes for direct contact membrane distillation. *Journal of Membrane Science* 407-408, 164-175.

Wei, Y., Xie, Z. and Qi, H. (2020) Superhydrophobic-superoleophilic SiC membranes with micro-nano hierarchical structures for high-efficient water-in-oil emulsion separation. *Journal of Membrane Science* 601, 117842.

Wenzel, R.N. (1936) RESISTANCE OF SOLID SURFACES TO WETTING BY WATER. *Industrial & Engineering Chemistry* 28(8), 988-994.

Willberg-Keyriläinen, P. and Ropponen, J. (2019) Evaluation of esterification routes for long chain cellulose esters. *Heliyon* 5(11), e02898.

Wu, H., Shen, F., Su, Y., Chen, X. and Wan, Y. (2018) Modification of polyacrylonitrile membranes via plasma treatment followed by polydimethylsiloxane coating for recovery of ethyl acetate from aqueous solution through vacuum membrane distillation. *Separation and Purification Technology* 197, 178-188.

Wu, Y., Kong, Y., Lin, X., Liu, W. and Xu, J. (1992) Surface-modified hydrophilic membranes in membrane distillation. *Journal of Membrane Science* 72(2), 189-196.

Xiang, J.-C., Gao, Q.-H. and Wu, A.-X. (2017) The Applications of DMSO. *Solvents as Reagents in Organic Synthesis: Reactions and Applications*, 315-353.

Xin, Z., Hou, J., Ding, J., Yang, Z., Yan, S. and Liu, C. (2013) Surface functionalization of polyethylene via covalent immobilization of O-stearoyl-chitosan. *Applied Surface Science* 279, 424-431.

Xu, K., Cai, Y., Hassankiadeh, N.T., Cheng, Y., Li, X., Wang, X., Wang, Z., Drioli, E. and Cui, Z. (2019) ECTFE membrane fabrication via TIPS method using ATBC diluent for vacuum membrane distillation. *Desalination* 456, 13-22.

Yang, P.Y. and Myint, T.T. (2003) Integrating entrapped mixed microbial cell (EMMC) technology for treatment of wastewater containing dimethyl sulfoxide (DMSO) for reuse in semiconductor industries. *Clean Technologies and Environmental Policy* 6(1), 43-50.

Yang, S., Abdalkareem Jasim, S., Bokov, D., Chupradit, S., Nakhjiri, A.T. and El-Shafay, A.S. (2022) Membrane distillation technology for molecular separation: A review on the fouling, wetting and transport phenomena. *Journal of Molecular Liquids* 349, 118115.

Yang, Y., Liu, Q., Wang, H., Ding, F., Jin, G., Li, C. and Meng, H. (2017) Superhydrophobic modification of ceramic membranes for vacuum membrane distillation. *Chinese Journal of Chemical Engineering* 25(10), 1395-1401.

Yao, M., Tijing, L.D., Naidu, G., Kim, S.-H., Matsuyama, H., Fane, A.G. and Shon, H.K. (2020) A review of membrane wettability for the treatment of saline water deploying membrane distillation. *Desalination* 479, 114312.

Yıldırım, E., Yıldırım, İ. and Yurtsever, E. (2002) Hydrogen bonding and polyurethane morphology. I. Quantum mechanical calculations of hydrogen bond energies and vibrational spectroscopy of model compounds. *Polymer* 43(24), 6551-6559.

Yoshihara, K. and Tanaka, A. (2002) Interlaboratory study on the degradation of poly (vinyl chloride), nitrocellulose and poly (tetrafluoroethylene) by x - rays in XPS. *Surface and Interface Analysis: An International Journal devoted to the development and application of techniques for the analysis of surfaces, interfaces and thin films* 33(3), 252-258.

You, X., Chong, J.Y., Goh, K.S., Tian, M., Chew, J.W. and Wang, R. (2021) Electrospun polyimide-based thin-film composite membranes for organic solvent nanofiltration. *Journal of Membrane Science* 640, 119825.

Zakrzewska-Trznadel, G., Harasimowicz, M. and Chmielewski, A.G. (1999) Concentration of radioactive components in liquid low-level radioactive waste by membrane distillation. *Journal of Membrane Science* 163(2), 257-264.

Zaragoza, G., Andrés-Mañas, J.A. and Ruiz-Aguirre, A. (2018) Commercial scale membrane distillation for solar desalination. *npj Clean Water* 1(1), 20.

Zare, S. and Kargari, A. (2018) *Emerging Technologies for Sustainable Desalination Handbook*, pp. 107-156, Elsevier.

Zarebska, A., Nieto, D.R., Christensen, K.V. and Norddahl, B. (2014) Ammonia recovery from agricultural wastes by membrane distillation: Fouling characterization and mechanism. *Water Research* 56, 1-10.

- Zhang, R., Tang, W., Gao, H., Wu, C., Gray, S. and Lu, X. (2021a) In-situ construction of superhydrophobic PVDF membrane via NaCl-H₂O induced polymer incipient gelation for membrane distillation. *Separation and Purification Technology* 274, 117762.
- Zhang, Y., Chong, J.Y., Xu, R. and Wang, R. (2021b) Effective separation of water-DMSO through solvent resistant membrane distillation (SR-MD). *Water Research* 197, 117103.
- Zhang, Y., Chong, J.Y., Xu, R. and Wang, R. (2022) Hydrophobic ceramic membranes fabricated via fatty acid chloride modification for solvent resistant membrane distillation (SR-MD). *Journal of Membrane Science*, 120715.
- Zhang, Y., Peng, Y., Ji, S., Li, Z. and Chen, P. (2015) Review of thermal efficiency and heat recycling in membrane distillation processes. *Desalination* 367, 223-239.
- Zhang, Y., Wang, R., Zhang, L. and Fane, A.G. (2012) Novel single-step hydrophobic modification of polymeric hollow fiber membranes containing imide groups: Its potential for membrane contactor application. *Separation and Purification Technology* 101, 76-84.
- Zhani, K., Zarzoum, K., Ben Bacha, H., Koschikowski, J. and Pfeifle, D. (2016) Autonomous solar powered membrane distillation systems: state of the art. *Desalination and Water Treatment* 57(48-49), 23038-23051.
- Zhao, K., Heinzl, W., Wenzel, M., Büttner, S., Bollen, F., Lange, G., Heinzl, S. and Sarda, N. (2013) Experimental study of the memsys vacuum-multi-effect-membrane-distillation (V-MEMD) module. *Desalination* 323, 150-160.
- Zhao, L., Wu, C., Lu, X., Ng, D., Truong, Y.B., Zhang, J. and Xie, Z. (2020) Theoretical guidance for fabricating higher flux hydrophobic/hydrophilic dual-layer membranes for direct contact membrane distillation. *Journal of Membrane Science* 596, 117608.
- Zhong, W., Hou, J., Yang, H.-C. and Chen, V. (2017) Superhydrophobic membranes via facile bio-inspired mineralization for vacuum membrane distillation. *Journal of Membrane Science* 540, 98-107.
- Zhou, T., Yao, Y., Xiang, R. and Wu, Y. (2014) Formation and characterization of polytetrafluoroethylene nanofiber membranes for vacuum membrane distillation. *Journal of Membrane Science* 453, 402-408.
- Zhu, Z., Zhong, L., Horseman, T., Liu, Z., Zeng, G., Li, Z., Lin, S. and Wang, W. (2021) Superhydrophobic-omniphobic membrane with anti-deformable pores for membrane distillation with excellent wetting resistance. *Journal of Membrane Science* 620, 118768.
- Zou, L., Gusnawan, P., Zhang, G. and Yu, J. (2020) Study of the effective thickness of the water-intrudable hydrophilic layer in dual-layer hydrophilic-hydrophobic hollow fiber membranes for direct contact membrane distillation. *Journal of Membrane Science* 615, 118552.